Chapter 2
In-Cylinder Pressure Measurement in Reciprocating Engines

Abbreviations and Symbols

ATDC	After top dead center
AEAP	Average exhaust absolute pressure
ANN	Artificial neural networks
ARMA	Autoregressive moving average
ASE	Average signal envelope
BDC	Bottom dead center
BTDC	Before top dead center
CA	Crank angle
CA_{50}	Combustion phasing 50% heat release
CI	Compression ignition
COV	Coefficient of variation
ECU	Electronic control unit
EGR	Exhaust gas recirculation
EMS	Engine management systems
EVC	Exhaust valve closing
EVO	Exhaust valve opening
FSO	Full-scale output
$GaPO_4$	Gallium phosphate
GDI	Gasoline direct injection
HCCI	Homogeneous charge compression ignition
IEPE	Integrated electronics piezoelectric
IMEP	Indicated mean effective pressure
IVC	Inlet valve closing
IVO	Inlet valve opening
$LiNbO_3$	Lithium niobate
LP	Low pass
LSE	Lower signal envelope

LTD	Long-term drift
NO	Nitric oxide
$PbTiO_3$	Lead titanate
PC	Personal computer
PE	Piezoelectric
P_{max}	Peak cylinder pressure
RPM	Revolution per minute
RTV	Room temperature vulcanizing
SI	Spark ignition
SiO_2	Silicon dioxide
TDC	Top dead center
USE	Upper signal envelope
WOT	Wide open throttle
L	Length of the air duct
Q	Calculation of charge output
R	Gain adjustment resistance
Δt	Time interval
a_b	Mounting base or reference acceleration
a_o	Output acceleration
D_i	Vector of electric flow density
$d_{i\mu}$	Tensor of piezoelectric coefficients
f_n	Undamped natural frequency
G_A	Charge amplifier gain
G_s	Piezoelectric pressure transducer sensitivity
L_T	Length of tube
T_μ	Tensor of mechanical stress
V_A	Amplifier output voltage
V_c	Clearance volume
V_{cv}	Volume of the cavity in front of the pressure sensor
V_{dead}	Dead volume of measuring bore
V_{disp}	Displacement volume
V_P	Passage volume
φ	Equivalence ratio

2.1   In-Cylinder Pressure Measurement Setup

Combustion pressure measurement was a topic of interest for researchers since the advent of reciprocating engines [1]. The mechanical work produced by reciprocating engines results from the action of gas pressure on the piston. The cylinder (combustion chamber) pressure is directly related to engine power output and the fuel conversion efficiency. The data of cylinder pressure development versus crank angle is used to calculate heat release rates and to analyze the progress of combustion

process in the cycle. In engine development process, combustion diagnostics is always used when the unexploited potential in comparison to thermodynamically possible targets is determined during the measurement of fuel consumption, output, and emissions. Thermodynamic combustion analysis by in-cylinder pressure measurement is a fixed element in the development sequence of modern engines due to high-performance targets [2]. Currently, most of the combustion parameter required for the industrial application can be derived from cylinder pressure measurement. The measurement of cylinder pressure in reciprocating engines poses one of the most challenging tasks for instrument manufacturers. Pressure transducers not only need to be compact and stable with the very fast response as well as good dynamic range, but these characteristics must be realized and withstand explosive and intense transient thermal conditions of the combustion chamber. High accuracy of cylinder pressure measurement is required for combustion work and thermodynamic calculations such as determination of IMEP, efficiency, and friction losses. Typically, high repeatability of cylinder pressure measurement is required for engine calibration and component testing. Various types of pressure transducers were used including variable resistance, variable inductance, balanced disk type, and piezoelectric, with different levels of robustness and accuracy [3].

Early in-cylinder pressure measurements of reciprocating engines were conducted using several configurations of mechanical indicators [4, 5]. The term "indicating" is used to designate the measurement and depiction of the cylinder pressure plot with crank angle position or time [2]. With the development of high operating speed engines, the frequency response of mechanical indicators was found to be insufficient for in-cylinder pressure measurement. Thus, mechanical indicators become outdated in the mid-1960s [5]. To meet the demand of in-cylinder pressure measurement in high speed engines, electronic transducers were used to convert the deflection of a low inertia diaphragm into an electrical signal. Early versions of electrical pressure transducers were built using extensometers and piezoelectric crystals as sensing element, and these devices had sufficient frequency response to the combustion process in the engine cylinder. Toward the end of the 1960s, the complex analog systems having the potential of completely electronic pressure signal processing became available, which were used for indicated work calculation and study of knock and misfire. In the mid-1970s, analog-to-digital converters were included, and the signal from transducer amplifier was digitized and stored in the computer, which can be further post-processed [5]. Hence, flexibility in data analysis and higher storage capacity were achieved while maintaining the adequate level of accuracy.

Figure 2.1 schematically illustrates the typical in-cylinder pressure measurement setup using piezoelectric transducer along with supplementary measurements for combustion diagnosis in a diesel engine. Typically, piezoelectric transducers are used for in-cylinder pressure measurements in modern engine tests due to their small size, light weight, the potential of high-frequency response, and low sensitivity to environmental conditions. Cylinder pressure measurements are augmented with various measured variables which define the working fluid state and component functions. Such "indicated data," which are typically recorded on cycle-to-cycle
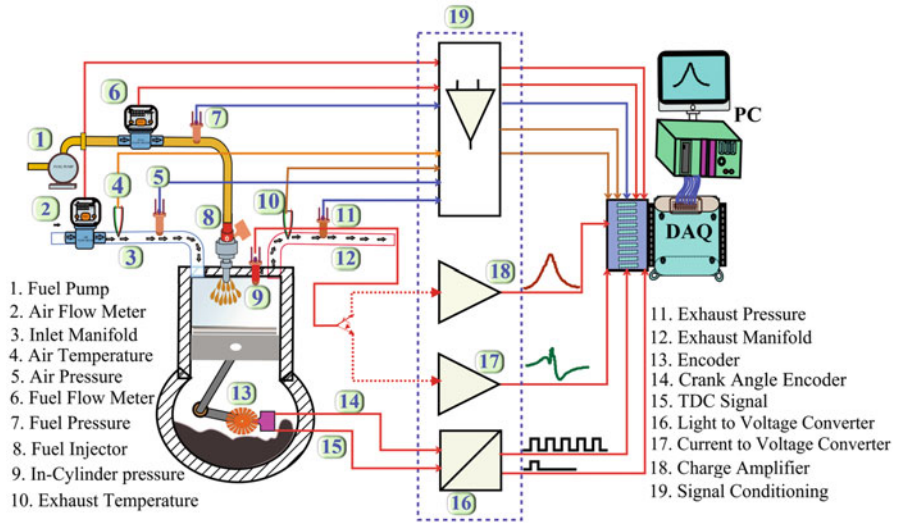
Fig. 2.1 Schematic diagram of typical in-cylinder pressure measurement setup using piezoelectric transducer (adapted from [5, 6])

basis or crank angle basis (depending on the test), form the basis for thermodynamic evaluation of combustion and the optimization of the adjustment parameters of the engine [2]. Thus, data logging of supplementary characteristic variables, such as measurement of air and fuel flow rates, measurement of the injection characteristics (injection pressure, needle lift), manifold pressures, ignition current, and thermal variables (intake and exhaust temperatures), proceeds as a natural progression from cylinder pressure indicating (Fig. 2.1).

High-pressure measurement in the engine cylinder is mostly used for combustion analysis. In addition to cylinder pressure measurement, low-pressure indicating on the intake and exhaust manifold constitutes the precondition for the gas exchange analysis and the estimation of intake gas mass used for combustion. Piezoresistive and piezoelectric pressure sensors are typically used for low-pressure indicating in reciprocating engines. The measured pressure traces in the intake and exhaust manifold form the basis for analyzing the gas exchange, which involves intake and exhaust duct design, controls design (cam profiles and control times), gas exchange work estimation, and mass flow analysis (charge, residual gas, reverse flows) [1]. Cylinder pressure data are indexed with the crank angle position using angle encoder (discussed in Sect. 2.4), with reference to the compression top dead center (TDC) position (Fig. 2.1). As illustrated in Fig. 2.1, the piezoelectric pressure signal generated can be conditioned for two measurement procedures: (1) in-cylinder pressure is acquired by using a charge amplifier for signal conditioning, and (2) in the second method, a current-to-voltage converter is employed for the measurement of derivative of in-cylinder pressure signal [5, 6].

The main structure of a cylinder pressure measurement system includes a piezoelectric pressure sensor, measuring amplifier, measurement wiring, data acquisition

system, real-time characteristics calculator, system operation, and post-processing of data [2]. The piezoelectric sensor is typically installed either directly by a special boring in the engine cylinder or by special adapters in existing borings, such as those for the spark plugs (SI engines) or glow plug (CI engines). The functional principle of the piezoelectric pressure sensor is that a particular crystal creates a charge under mechanical strain (deformation) and thus, it acts as an active measuring element, where charge generated is proportional to the applied pressure [1]. More detailed discussion on piezoelectric pressure transducer is provided in Sect. 2.2. The low level of charge generated by piezoelectric pressure transducer is amplified and integrated into a voltage signal, which is typically processed for combustion analysis. The magnitude of amplified voltage range needs to ensure the transmission through long cable distance to data acquisition system while maintaining high signal-to-noise ratio. In addition to low-noise amplification, the long-term stability and short-circuit strength are very important for amplifier units [2]. The charge and voltage signals are transferred through measurement wirings. The length of measurement wiring between the pressure transducer and the charge amplifier is always kept as short as possible, to achieve high signal quality. Low noise levels, very high insulating values (10^{14} Ω), robustness, and simple handling are required for both charge amplifier and the measurement wiring [1]. Data acquisition system records the measured data based on crank angle position depending on the resolution of crank angle encoder. Detailed discussion on data acquisition system is presented in Chap. 4. Real-time characteristics calculator generates control signals on the basis of measured pressure progressions compared with reference values predefined as model characteristics for the particular operating conditions. The control signals affect the actuators (injector, ignition, timing settings, valve lift, etc.) through the engine control unit (ECU). Real-time analyses are subjected to continuous modification depending on needs and appropriateness and as a function of computing potentials. Real-time calculation of important combustion parameters is described in Chap. 7. System operation is typically achieved by a special PC software which performs the following functions: (1) parameterizes the entire measuring system and the measurement itself, (2) obtains characteristics data and calculations, (3) defines algorithms for the determination of characteristics data or the calculation of results from the measured data, and (4) displays the measured and calculated data values. Post-processing is applied for the presentation and processing of the measured data. More complex calculations, comparisons of results, and documentation procedures are conducted during post-processing using corresponding graphical and computing aids [2].

2.2   Piezoelectric Pressure Transducer

In general, combustion sensors (such as piezoelectric pressure sensors, ion current sensors, and optical sensors) are used for engine research and development. In modern engines, there is a need for installation of combustion sensors on production vehicles for closed-loop control of engine combustion. Combustion sensors are used for determination of various combustion parameters as well as different engine input

and output parameters. Several design issues with combustion sensors need to be considered for engine applications [7]. Sensor cost, real-time signal processing, and working environment of the sensor are the major factors governing the design of combustion sensor. Signal processing is typically not a problem in an engine test cell as additional hardware performs signal processing. However, in a production vehicle, real-time signal processing is limited by the computational capability of the electronic control unit (ECU) of the engine. The engine compartment of the automotive vehicle is not sensor friendly, and the combustion chamber also has high temperature and pressure. In the laboratory conditions, the life expectancy or recalibration interval of a hundred hours may be acceptable, but on a production vehicle, the operation of combustion sensors is expected for hundreds of millions of cycles with minimal or no servicing requirements. These factors limit the widespread use of combustion sensor on a production vehicle. Ruggedness has an immediate bearing on the packaging. Choice and flexibility of sensor installation are heavily restricted due to space constraints and servicing/replacement requirements. Sensor installation must penetrate the combustion chamber, which is typically surrounded by oil and cooling water circuits. In modern multivalve engines, space is almost always very limited. Sensor installations considered as the best which require no additional access to the engine combustion chamber, and if it also needs to be installed on production vehicle, then awkward or costly modification should be avoided [7]. Ideal combustion sensor should be nonintrusive and non-perturbing. Any protrusion in the combustion chamber can locally distort the flow field of the charge, which affects the combustion characteristics. Thus, flush-mounted or recessed sensor installation is preferred. Electronics and electronic packaging are also important in packaging. In case of the production vehicle, the burden on ECU can be reduced when some aspects of signal conditionings are integrated with the sensor. Electronic package must guard against earth loops and electromagnetic interferences by appropriate shielding. Sensor fouling is another important design aspect to be considered for combustion sensors. Carbon deposition due to soot formation in the combustion chamber can contribute to fouling. A more complete description of design issues can be found in reference [7].

In-cylinder pressure measurement (high-pressure indicating) has been developed into highly sophisticated analytic methods for reciprocating engine combustion optimization and diagnosis. Modern sensors and computer-based high-speed data acquisition systems make indicating technology as an industrial measurement technology and also satisfy the accuracy demands for calculating extensive information from the measured pressure signal. Indicating is widely used because of the following reasons [1]: (1) it is a developmental tool for engine combustion optimization with high quality and speed; (2) it provides huge amount of information about the in-cylinder phenomena and engine operations, which is typically not available with other measurement techniques; and (3) it is a safe, reliable, and repeatable measurement technique and thus used as standard technology on development test beds [8]. Piezoelectric pressure transducers are typically used for combustion pressure measurement by directly installing the sensor into the engine head or installed into the spark or glow plug using adapters.

The main advantages of piezoelectric sensors are extremely wide measuring range (span-to-threshold ratio up to over 108), extremely high rigidity (measuring deflections are typically in the μm range), high natural frequency (up to over 500 kHz), high reproducibility, very high stability, wide operating temperature range, high linearity, and insensitivity to electric and magnetic fields and to radiation [9]. The main demerit of the piezoelectric sensor is that it is inherently not able to measure static signal over a long period of time due to self-discharge as there is no material with infinitely high insulation resistance and no semiconductor is completely free of leakage currents. Ideally, materials suitable for transduction elements in pressure sensors should have the following properties [9]: (1) high piezoelectric sensitivity, (2) high rigidity, (3) high electric insulation resistance, (4) high mechanical strength, (5) linear relationship between mechanical stress and electric polarization, (6) minimal hygroscopicity, (7) high stability of all properties, (8) absence of hysteresis, (9) low-temperature dependence of all properties within a wide temperature range, (10) low anisotropy of mechanical properties, (11) good machinability, and (12) low production cost. Operating principle, design, construction, and the mounting position of a piezoelectric pressure transducer used for engine indicating are discussed in the next subsections.

2.2.1   Functional Principle

Piezoelectric pressure transducers are the most commonly used sensors for combustion measurement, which rely on the piezoelectric effect that refers to the property of particular crystals to exhibit electrical charge under mechanical deformation. Figure 2.2 schematically illustrates the piezoelectric effect using quartz crystal.

Fig. 2.2 Illustration of direct piezoelectric effect (Courtesy of Kistler)
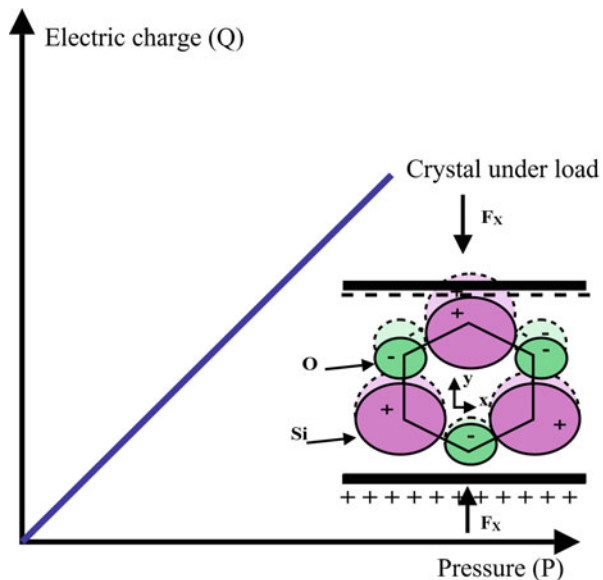
The piezoelectric materials generate positive or negative electrical charges on mechanical loading to their outer surfaces. An electric dipole is formed due to the charge generated by the displacement of positive and negative crystal lattice elements. The electrical charge produced is proportional to the force (pressure) applied to the piezoelectric crystal.

In order to produce a measurable electrical output from a cylinder pressure input, the pressure must first be converted into a proportional mechanical strain, which is transmitted to an electrical transduction element that creates the required electrical signal. Therefore, piezoelectric pressure transducers consist of two key components, i.e., one mechanical (diaphragm of the sensor) and one electrical (piezoelectric crystal). Figure 2.3 illustrates the functional principle of the piezoelectric pressure transducer. The diaphragm of pressure transducer experiences the change in the cylinder pressure (dP/dt) which is transmitted to a piezoelectric crystal through intermediate elements [5]. The rate of pressure change leads to the deformation in the piezoelectric crystal at a strain rate of $d\varepsilon/dt$. Deformation in piezoelectric crystal polarizes charge "q" in the transducer electrode, which generates an electric current "i" that establishes the output signal of pressure transducer as represented by Eq. (2.1) [6].

$$i = -\frac{dq}{dt} = -G_s\frac{dp}{dt} \tag{2.1}$$

where G_s is the sensitivity of piezoelectric pressure transducer.

Figure 2.4 presents a simplified schematic of signal conditioning of piezoelectric pressure transducer that is used to get in-cylinder pressure data in combustion engines. Typically, two methods can be used to obtain the pressure data, i.e., through
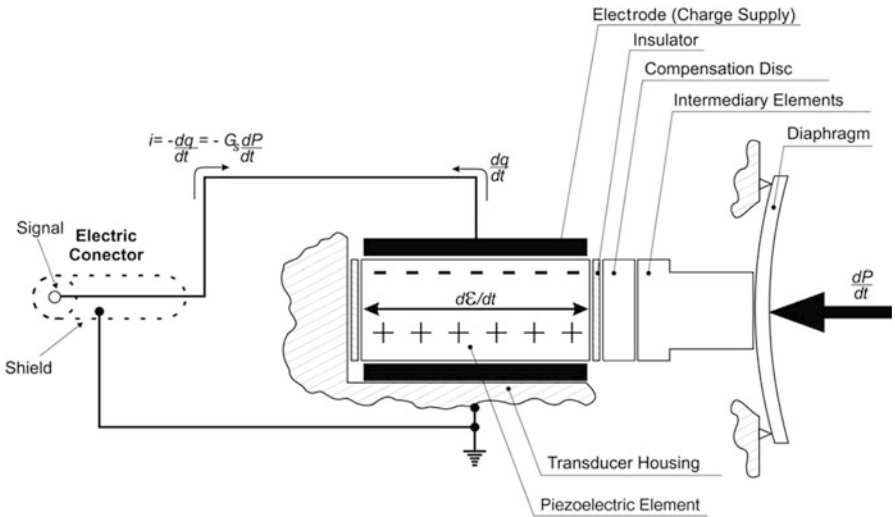
Fig. 2.3 The schematic diagram of piezoelectric pressure transducer [6]
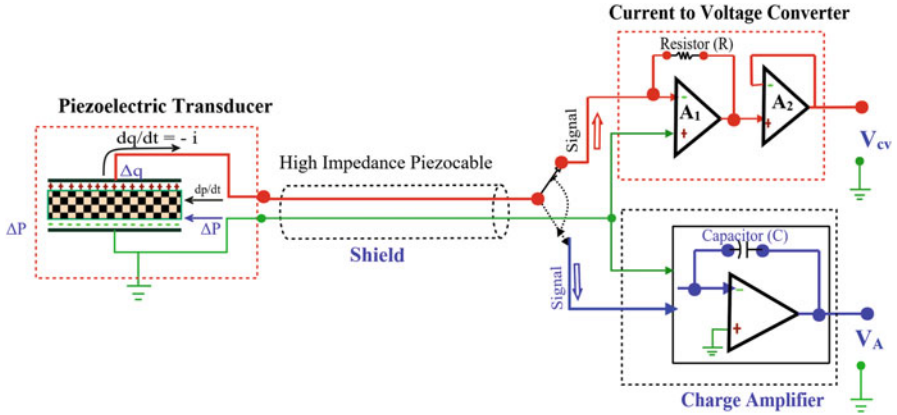
Fig. 2.4 Signal conditioning of piezoelectric pressure transducer by charge amplifier or current-to-voltage converter (adapted from [5, 6])

charge amplifier or current-to-voltage converter (Fig. 2.4). Charge amplifier is most commonly used for getting the pressure data. The charge amplifier-based method is preferred possibly due to the legacy of the mechanical indicators [5]. During early engine development, the mechanical indicators were used for pressure measurement as well as for determination of indicated work from measured pressure data or for evaluating the thermodynamic state of the charge. The charge polarized by piezo-electric pressure transducer is carried to the inlet of the charge amplifier by a shielded cable with high insulation resistance. The charge received from the piezoelectric pressure transducer is converted into a voltage signal in the charge amplifier, which mainly consists of an amplifier and a degenerative feedback capacitor (C) to integrate the charge (Fig. 2.4). The integrator circuit of charge amplifier produces an output voltage proportional to the time integration of the electric current produced by the transducer during a time interval Δt. The time interval is considered between the desired instant of measurement and the instant from which it was started (or reset). The change in measured pressure level during the interval Δt is given by Eq. (2.2) [5].

$$P - P_{\text{ref}} = \frac{V_A G_A}{G_s} \tag{2.2}$$

where G_A is the charge amplifier gain, V_A is amplifier output voltage, and P and P_{ref} are the pressure acting on the diaphragm during time interval Δt.

The charge amplifier has very large internal charge amplification (amplification factor up to about 100,000). The charge received from the piezoelectric pressure transducer is drawn off by the feedback capacitor, and it is not used for charging (i.e., to increase the voltage at the input capacitances). Feedback capacitor has been negatively pre-loaded to accept the charge from the sensor input [1]. The piezoelectric pressure transducer generates very small charge (just tens of picocoulombs per

bar). Therefore, the charge amplifier output is highly sensitive to electronic circuit nonidealities; particularly leakage currents occur by insulation resistance of the measurement system, which slowly and continuously yields lower-voltage output leading to lower-pressure measurement values. In order to reduce this inaccuracy, high input impedance in the charge amplifier is used. The operation of signal conditioning system in the low-humidity environment along with clean electrical contacts also helps in reducing the measurement error. Long-term drift error (load change drift) along with instrumentation nonidealities also leads to instability in the pressure data baseline (up to several bars), which is inherent demerit of charge amplifier system. Therefore, it is mandatory to periodically reset the charge amplifier to avoid saturation during pressure measurement [6].

Another approach to obtaining the cylinder pressure data is through current-to-voltage converter (Fig. 2.4). This circuit fulfills the gain and the frequency response requirements for cylinder pressure measurements. This device has low input impedance, as provided by the ratio of the gain adjustment resistance (R) to the open-loop gain of the operational amplifier A_1, which removes the inaccuracies generated from the inherent capacitance of the sensor. A voltage follower amplifier (A_2) is used to isolate the converter with respect to the impedance of the instrument. The change in pressure rate is estimated by Eq. (2.3).

$$\frac{dP}{dt} = \frac{V_{cv}}{G_s R} \tag{2.3}$$

where V_{cv} is the voltage output of converter and R is the gain-adjusting resistance of the current-to-voltage converter.

The in-cylinder pressure can be obtained by integrating the measured pressure derivative data. The cylinder pressure measurement with this method eliminates the need for special care for insulation resistance and leakage currents because in this case current generated from the transducer flows to the ground unrestrictedly. Additionally, the need of periodically resetting the charge amplifier during measurements is also eliminated [5, 6]. One of the main objectives of cylinder pressure measurement is the determination of heat release for combustion diagnostics [10]. Since pressure derivative is used for computation of heat release, the inaccuracies in the pressure data get amplified and reflected in heat release data. Direct measurement of the pressure derivative data through current-to-voltage converter reduces the noise of pressure derivative data (~70 times) [6]. A similar strategy based on direct pressure derivative measurement for combustion detection is also demonstrated in reference [11].

2.2.2   Transducer Materials and Construction

Materials used for transduction elements in piezoelectric pressure sensors are expected to have good measuring behavior (high output signal, good linearity, high natural frequency), good resistance (high mechanical strength and high

temperature resistance), stability of the measuring properties (against temperature and load variations), and low price (including material cost and easy machining) [8]. Quartz is the most frequently used piezoelectric material in pressure sensors for combustion measurements; however, researchers continue to investigate and develop alternative piezoelectric materials because of their manufacturing advantages over quartz [7], but the alternative materials can compromise the quality of the measurement data for engine combustion measurement application. Alternative piezoelectric materials are polycrystals of lead niobate ($LiNbO_3$) and lead titanate ($PbTiO_3$) and single crystals of gallium phosphate ($GaPO_4$), lithium niobate ($LiNbO_3$), and silicon dioxide (SiO_2) [12]. Thermal tolerance (sensor operating temperature) is one of the major limitations for selection of piezoelectric transduction materials as temperature affects the piezoelectric effect as well as durability of the sensor. Piezoelectric effect vanishes, and the sensor does not respond above a threshold temperature (Curie temperature) [7, 13]. During piezoelectric material selection, thermal tolerance of material is traded with pyroelectricity in which charge is produced due to thermal variations instead of mechanical strain. Pyroelectricity is also a linear function of the first differential of temperature similar to piezoelectricity which is a linear function of the first differential of force [7]. The pyroelectric effect needs to be small (preferably no) in the signal used for obtaining pressure sensor. Temperature effects are significant even with quartz crystals used in pressure sensors. Figure 2.5 depicts the temperature effect on the piezoelectric constant for quartz and gallium orthophosphate material, which are presently used in combustion pressure sensors. The figure illustrates that the maximum operating temperature limit of quartz crystal is around 250 °C. Thus, this simple crystal can be used in combustion pressure measured with the suitable cooling system in a cooled pressure
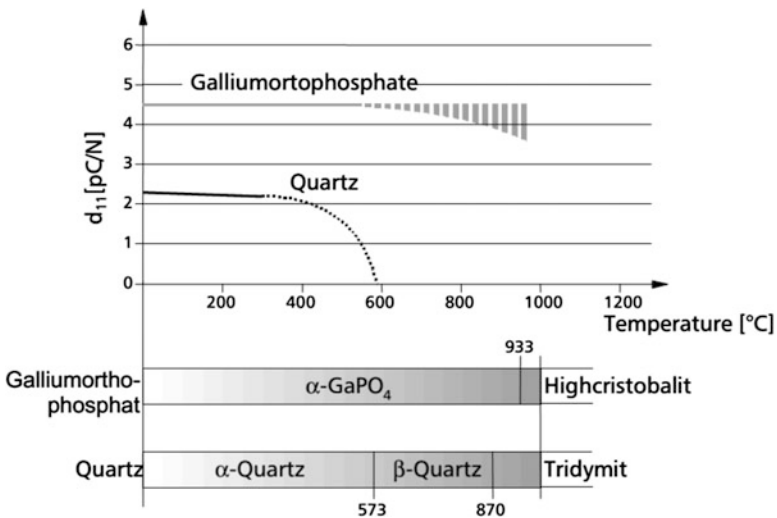
Fig. 2.5 Variations of the piezoelectric constant with operating temperature for gallium orthophosphate and quartz (Courtesy of AVL)

transducer. In typical reciprocating engine environment, the temperature of more than 400 °C can likely occur at transducer locations [1]. Engineered gallium orthophosphate has a typically higher piezoelectric sensitivity (nearly twice of quartz), and it is independent of temperature until much higher than 500 °C (Fig. 2.5). Therefore, gallium orthophosphate is suitable for construction of uncooled miniature pressure transducers for in-cylinder pressure measurement in reciprocating engines.

Piezoelectric pressure transducer is typically protected by enclosing it in sensor housing (due to limited temperature tolerance range), and the transducer indirectly receives the strain from the diaphragm. Thus, high-temperature resistance, small size, and invulnerability to electrical interference are essential requirements for transducers for combustion application. Pyroelectric effects can also be reduced by constructing electrodes that are parallel to polarization axis [14]. The optimization of the orientation of crystal cut can extend the temperature range of piezoelectric crystal (quartz). Three main types of operations can be distinguished as transversal, longitudinal, and shear depending on the way of piezoelectric material cut. Figure 2.6 illustrates the different types of cuts in the piezoelectric material used in sensor technology. Piezoelectric elements with longitudinal or transverse cut are typically used for combustion-measuring applications [15].
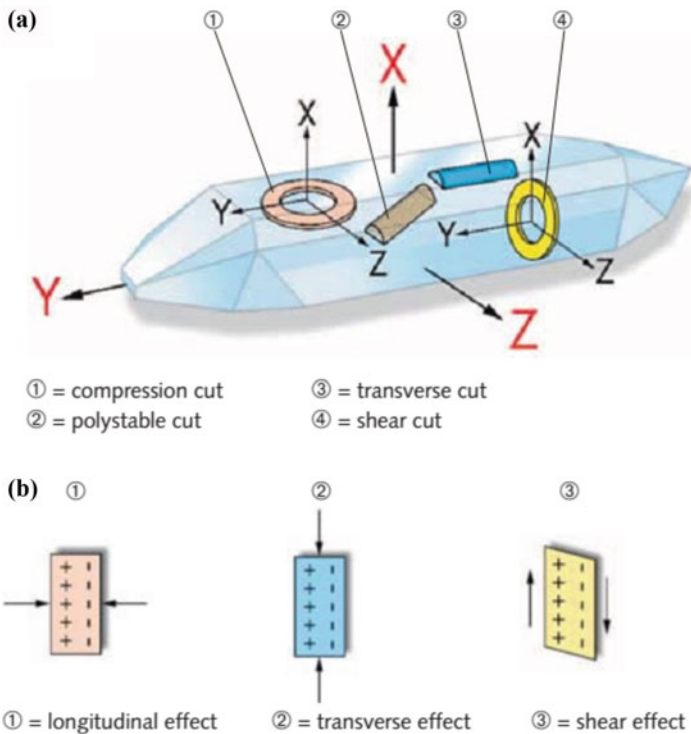
Fig. 2.6 Illustration of different piezoelectric crystal cuts (Courtesy of Kistler)

The piezoelectric effect is differentiated based on the direction of piezoelectric polarization with respect to the direction of mechanically introduced strain. The direct piezoelectric effect can be phenomenologically described using Eq. (2.4) [1].

$$D_i = d_{i\mu} \cdot T_\mu \tag{2.4}$$

where D_i ($i = 1$ to 3) is a vector of electric flow density, $d_{i\mu}$ is the tensor of piezoelectric coefficients, and T_μ ($\mu = 1$ to 6) is the tensor of mechanical stress. The Eq. (2.4) is used for calculation of charge output (Q) using Eq. (2.5).

$$Q = A \cdot D_i \cdot n_i \tag{2.5}$$

where A is the surface area and n_i ($i = 1$ to 3) are components of the normal vector of the face.

In longitudinal piezoelectric effect, the amount of charges generated is strictly proportional to the acting force (mechanical strain), and output is independent of shape and size of the piezoelectric element. However, in transverse piezoelectric effect, the quantity of charge output depends on the geometrical dimensions of the piezoelectric element, and the polarized charge is perpendicular to the line of applied force. Therefore, the crystal elements used in the pressure transducer can be cut to optimize charge output as a function of the force and stresses in the element. A "polystable" cut (Fig. 2.6) is employed by Kistler company for particular sensors, which is optimized to decrease the effect of operating temperature on the piezoelectric sensitivity of the quartz element. This cut enhances the maximum operating range of around 350 °C (piezoelectric behavior remains constant within range), which makes the possibility of using this crystal in uncooled sensors as well [15].

The current trend toward miniaturization and higher operating temperatures leads to the development of new types of crystals having greater sensitivity and higher temperature. The PiezoStar® crystal elements (KI85 and KI91) developed by Kistler are optimized for use in such demanding applications [16]. Figure 2.7 depicts the sensitivity and sensitivity shift as a function of temperature for different piezoelectric crystals. PiezoStar crystal has a very high piezoelectric sensitivity (~3–5 times of quartz), high stability of the properties, no twin formation, no phase transition up to the melting point, and no pyroelectric effect and can be used up to 600 °C temperature. The stated disadvantages of PiezoStar crystal are lower mechanical strength and higher cost than quartz [16]. The major drawbacks of quartz crystal are low sensitivity, twin formation, and phase transition at 573 °C. Peculiarities with different piezoelectric crystals along with their production process and operating temperatures are presented in Table 2.1.

The amount of electrical charge produced by a single crystal element under mechanical strain depends on the piezoelectric material. To fulfill the requirement of high-sensitivity sensor with lower-sensitivity piezoelectric material (such as quartz), several crystal disks are stacked and connected electrically in parallel, which is illustrated in Fig. 2.8.

Fig. 2.7 (**a**) Longitudinal
sensitivity, (**b**) sensitivity
shift with temperature for
different high-temperature
crystals (Courtesy of
Kistler)
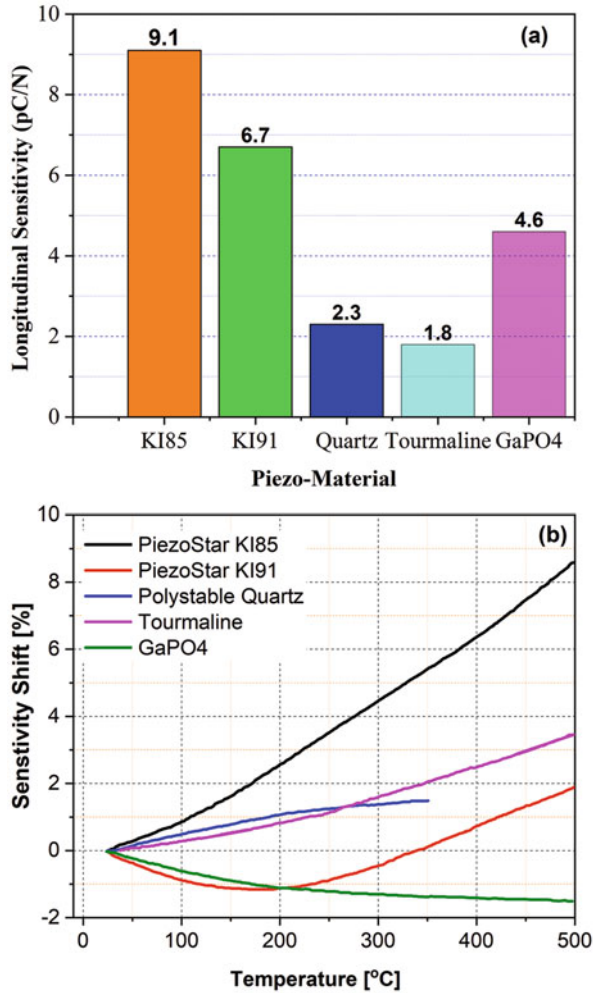
Piezoresistive materials can also be used as pressure-sensing devices [17]. In
engine research application, piezoresistive pressure sensors are used for
low-pressure indicating and only few applications for high-pressure combustion
measurements. The advantages of piezoresistive sensors over piezoelectric sensors
are the ease of signal processing (including temperature compensation) and better
noise rejection due to low output impedance [17]. In the piezoresistive sensors, the
electrical resistivity of sensing material (typically semiconductor) changes when
mechanical strain (force) is applied. The electrical resistance of material varies due
to change in conductivity of mater as well as geometry change.

Table 2.1 Comparison of different high-temperature piezoelectric materials (Courtesy of Kistler)

Crystal	Peculiarity	Pyroelectric effect	T_{max} [a]	Production		
				Process	Volume	Cost
Quartz	High mechanical	No	573 °C	Hydrothermal	Large	Low
KI85	strength	No	T_m	Czochralski	Average	High
KI91	High sensitivity Low-temperature coefficient	No	T_m	Czochralski	Average	High
GaPO4	Low-temperature coefficient	No	970 °C	Hydrothermal	Small	High
Tourmaline	High-tempera-ture stability	Yes	>900 °C	Natural	Small	High
Piezoceramic (PZT)	High sensitivity	Yes	250 °C	Sintering	Large	Low

Tm no transition below the melting point
[a]Phase transition temperature

Fig. 2.8 Arrangement of crystal elements to increase the sensitivity of transducer (Courtesy of Kistler)
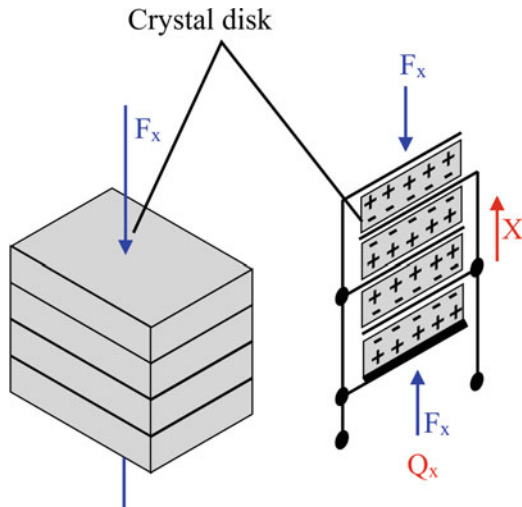
2.2.3   Transducer Design

Piezoelectric pressure sensor for engine combustion application is available in a large number of designs (as illustrated in Fig. 2.9) depending on the complexity of the application. The variety of demands such as temperature stress, installation space, vibrations, mechanical deformation of the location of sensor installation, etc. leads to the development of different designs of pressure sensors. Mostly pressure sensors have a flush-welded diaphragm (eliminating any dead volume) which allows flush mounting of the transducer on the engine cylinder head. Typically, the measuring element is housed inside the transducer body so that installation, sealing, and heat transfer are away from the sensing element. Some of the sensors are

Fig. 2.9 Different types of
piezoelectric pressure
sensors based on their
construction (courtesy of
Kistler)

Type 6052   6054   6056   6055   6061B   6043A

constructed and designated as probe type (6043, 6055, and 6056 in Fig. 2.9), which
are suitable for cylinder pressure measurement in engines with very little space such
as multivalve engines, motorcycles, etc. A basic difference in design of the sensor is
based on with or without mounting threads on the sensor. Pressure sensors with
mounting threads can be directly screwed into the combustion chamber (engine
head) having mounting bore with suitable thread. Pressure sensors without mounting
thread are mounted into bores providing only a sealing shoulder, and sensors are
held by adapters, and mounting nuts or nipples. Both of these types of sensors have
corresponding merit and demerit (discussed in Sect. 2.2.4). A precise mounting bore
on cylinder head is essential along with tight tolerances for surface finish of the
sealing surface, and orthogonality between thread axis and sealing face. The sensor
can be strained during mounting with compromised tolerances, which leads to
variations in sensor characteristics such as sensitivity and linearity. Sensors without
mounting threads are mounted in an adapter that is installed in a corresponding bore
in the engine head. Sensor mounting with adapter sleeve needs more space, but this
method ensures the sensor specifications by well-defined mounting geometry.
Adapters can handle less stringent tolerances in the mounting bore due to their
massiveness and ruggedness [9].

Thermal tolerance is critical constraint in the selection of the piezoelectric
material. Depending on the piezoelectric material, both cooled and uncooled sensors
are developed over a period of time for combustion analysis in reciprocating engines.
Figure 2.10 shows the typical cross section of cooled and uncooled piezoelectric
pressure transducers. Cooled type of piezoelectric pressure transducers is most
widely used for accurate combustion pressure measurement and analysis
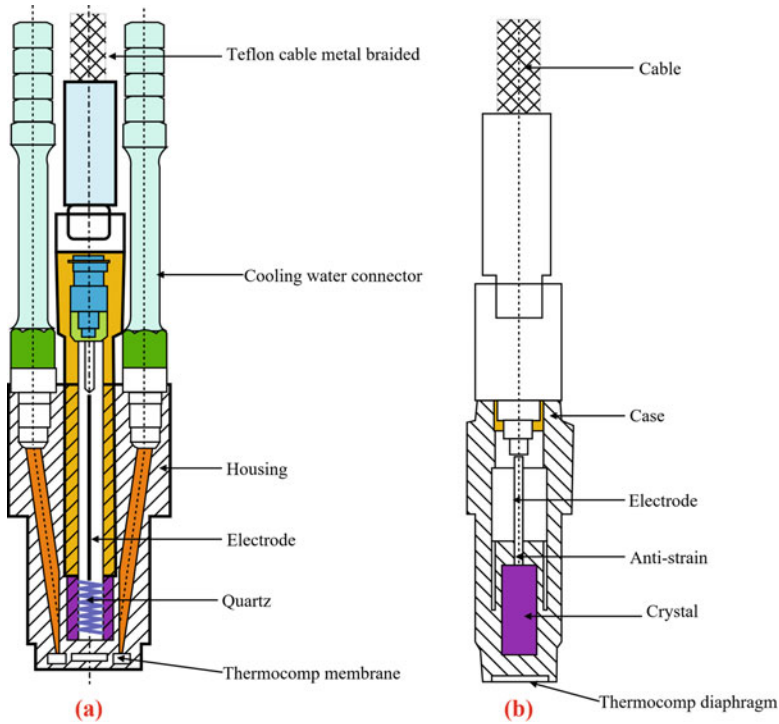
Fig. 2.10 Cross section of (**a**) cooled and (**b**) uncooled piezoelectric pressure sensor (Adapted from and courtesy of Kistler)

[15]. Cooled type of pressure transducer is relatively larger and available in mounting thread size from M8 to M14. Cooled sensors can accommodate relatively larger sensing element because of the relatively large size of the sensor, but the advantage of high sensitivity depends on crystal cut. During the operation of cooled pressure sensor, the sensing element and the membrane are directly cooled by surrounding water jacket, and thus, sensing element is only slightly warmer than the coolant (~10–20 °C) [1].

Water-cooled piezoelectric sensors are used for applications where sufficient mounting space is available and extreme precision is the top priority [18]. In the cooled pressure sensors, engine load change drift is small because the almost constant temperature is maintained using the cooling system by supplying optimal quantity of water at the right pressure. Thus, absolute reproducibility in the measurement can be ensured. The pressure transducer must be cooled using deionized water or a cooling agent-water mixture. Local supply water can lead to deposits that can affect the sensitivity or in worst case block the water lines. Therefore, a closed cooling circuit is typically used and recommended. Pressure pulsations in the water flow should be avoided because it can be picked by sensing elements and superimposed with measured cylinder pressure sensor (cross-talk phenomena) [15].
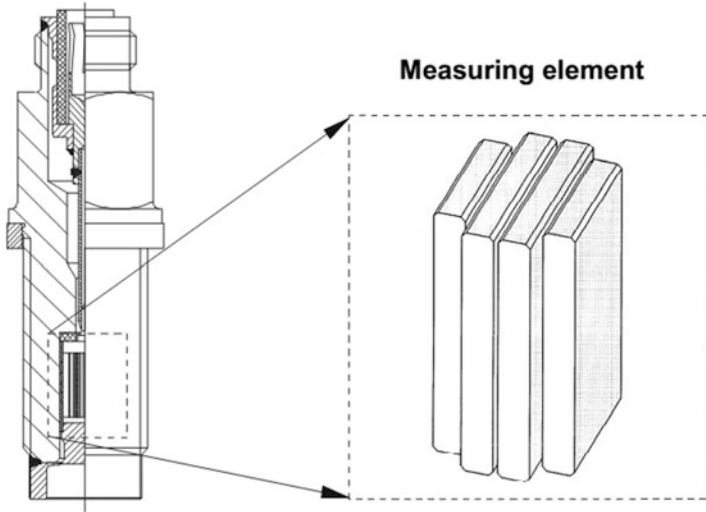
Fig. 2.11 Cutaway view of the uncooled pressure sensor with transverse piezoelectric effect (courtesy of AVL)

Modern reciprocating engines are very compact in terms of construction due to four-valve technology and direct fuel injection, which leads to very less availability of space for installation of pressure sensors for combustion analysis. Thus, miniature piezoelectric pressure sensors are used for such limited space applications. Figure 2.11 shows the cross section of such miniature piezoelectric pressure sensor using transverse crystal cut. This type of sensors is typically uncooled due to their smaller size. The uncooling requirement demands piezomaterials with high-temperature resistance and stability in properties over wide temperature range [1]. Current uncooled pressure sensors have reached to a comparable measurable quality similar to cooled piezoelectric pressure sensors.

ThermoComp$^®$ sensor from Kistler has a double diaphragm to minimize the thermal shock. The cyclical combustion process and heat flow between cylinder charge and cylinder head leads to the different temperatures in the surrounding of the pressure transducer. Thus, the temperature of pressure transducer depends on the engine operating conditions, the mounting position, and the type of sensor used. Figure 2.12 schematically shows the heat flow from the combustion chamber through pressure to the cooled cylinder head. For higher measuring accuracy and a long sensor service life, Kistler uses front sealing which keeps the measuring element at a lower temperature by heat dissipation in the front of the pressure sensor (Fig. 2.12).

AVL uses Double Shell™ design of piezoelectric pressure sensors (illustrated in Fig. 2.13) for combustion analysis which ensures premium signal quality by decoupling the piezoelectric crystals mechanically from the sensor housing. Piezo-electric crystals are susceptible to any kind of mechanical strain due to their high sensitivity. Double shell design of the pressure sensor makes sensing element

Fig. 2.12 Schematic of heat dissipation from the combustion chamber through pressure sensor to the cooled cylinder head (courtesy of Kistler)

Sealing surface
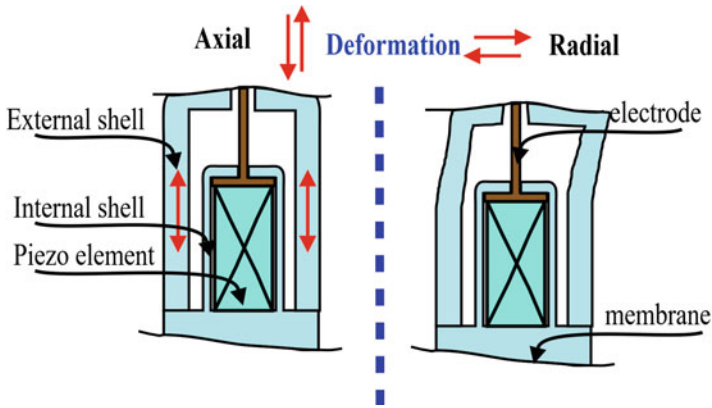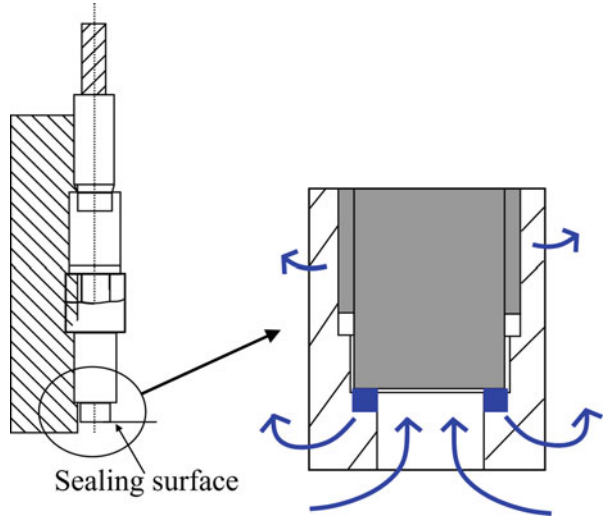
Fig. 2.13 Illustration of Double Shell™ technology in piezoelectric pressure sensors for combustion analysis (courtesy AVL)

isolated from any axial or radial deformation of sensor housing that can occur from different sources such as mechanical stress by sensor mounting, etc. Thus, double shell design helps in ensuring absolute pressure measurement precision.

The output signal of the piezoelectric sensor is transported out to an external connector, which is transmitted to the charge amplifier via a measuring cable. This signal can be ground isolated or ground referenced depending on the sensor construction. Figure 2.14 shows the schematic of piezoelectric pressure sensor without ground isolation and with ground insulation. Most of the sensors are not ground isolated [18]. One terminal of sensing element is connected to the ground of the engine (test stand ground), and the amplifier is connected to the equipment ground, which is also connected to the power system ground. Thus, ground-isolated pressure
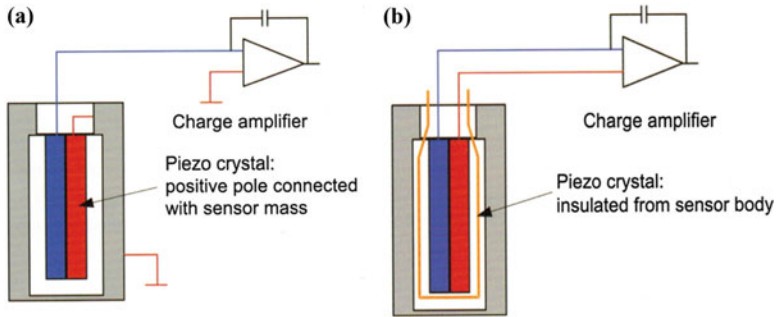
Fig. 2.14 Piezoelectric pressure sensor (**a**) without ground isolation and (**b**) with ground insulation (courtesy of Kistler)

transducers should be used with suitable charge amplifiers. Ground-insulated sensor design avoids problems with ground loops and increases immunity to electrical noise in the test environment.

Piezoelectric pressure transducers are sensitive to acceleration, particularly in the direction of transducer axis. The diaphragm mass and transmitting plates in front of the piezoelectric element act as a seismic mass (similar to acceleration sensor) which leads to acceleration sensitivity in the transducer. Hence, during vibration (acceleration), the output signal of the transducer is superimposed with the actual pressure signal. Typically, the acceleration error is in the order of a few mbar/g [9]. The acceleration error is increased in cooled piezoelectric sensors due to the additional mass of the cooling water present in cooling ducts in front of the sensing element. The acceleration error can be ignored in most applications, but it can be significant when the sensor is subjected to strong vibrations while measuring small pressure. This leads to the development of accelerated sensitivity compensated pressure sensors. Figure 2.15 shows the section through sensor and operation principle for active and passive acceleration sensitivity compensation designs. The Kistler company has developed these two concepts. Two piezoelectric elements of different piezoelectric sensitivities are used for active acceleration compensation techniques. An additional measuring element is used in conjunction with a seismic mass along with the sensing element. The additional element is connected with opposite polarity, and the signal produced by tuned vibration frequency gets canceled. In passive acceleration sensitivity compensation, the additional measuring element is not required, and the sensing element is supported by a sleeve which acts as a dynamic spring-mass system. In this system, the sensing element is tuned to the same natural frequency as the transducer diaphragm. Thus, the piezoelectric sensing element is effectively "sandwiched" between the two spring-mass systems, and both the diaphragm and the mounting support sleeve system respond by oscillating with the same amplitude and direction during acceleration of transducer. In this method, the sensing element does not receive any additional force due to vibration. The passive acceleration sensitivity compensation technique is more suitable for uncooled sensors as it does not require any additional compensating measurement elements.
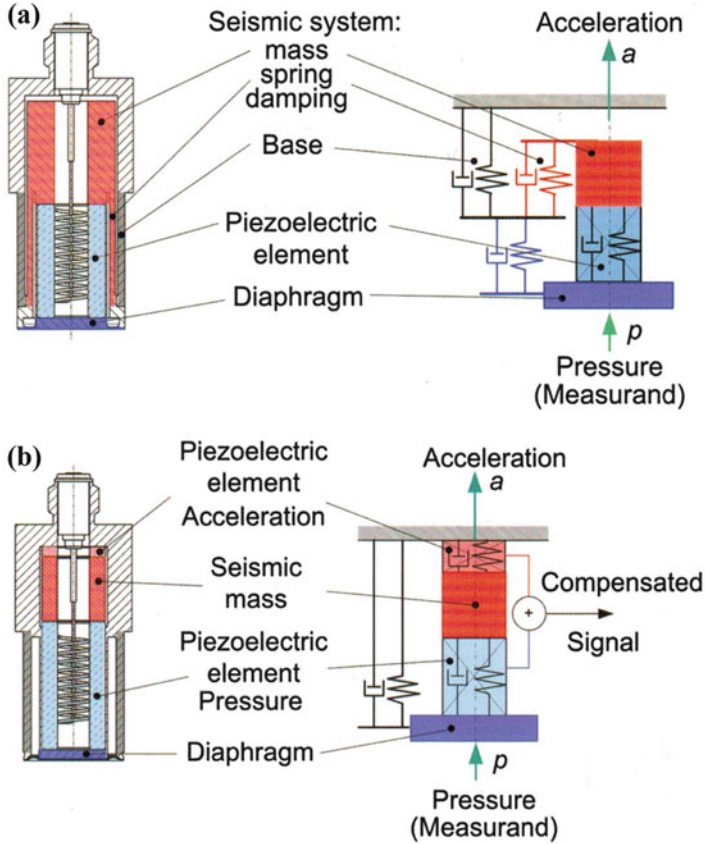
Fig. 2.15 Section through sensor and operation principle for (**a**) active acceleration sensitivity compensation and (**b**) passive acceleration sensitivity compensation (courtesy of Kistler)

The piezoelectric sensor can be divided into two categories based on the output signal. Pressure sensors are available as high impedance or charge output (PE) and low impedance or voltage output (IEPE). In voltage output sensors or integrated electronics piezoelectric (IEPE) sensor, the electronic circuit for converting the charge into a voltage is integrated with sensor body. Kistler company has registered trademark Piezotron® for IEPE sensors. Figure 2.16 illustrates the basic design of charge mode and voltage mode pressure sensor system. The charge output or PE sensors produce a high-impedance charge that needs to be converted into a usable low-impedance voltage signal (that can be recorded by data acquisition system) by the external charge amplifier. For transmitting the charge to amplifier, special low-noise high-impedance cable is required. The standard two-wire coaxial cable can have triboelectric noise generation (charge generation) due to friction between the conductors of the cable [19]. Since the charge produced by the sensor is very small, it is very difficult to differentiate it with charge produced by cable.
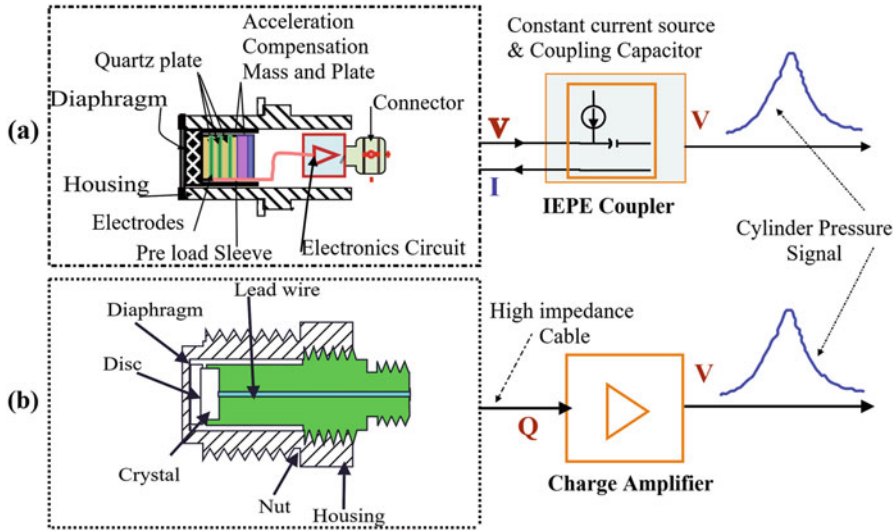
Fig. 2.16 Schematic illustration of pressure sensor system with (**a**) voltage output (IEPE) and (**b**) charge output (PE)

Additionally, environmental contaminants on the connector, such as moisture, dirt, oil, or grease, contribute to reduced insulation that can lead to inconsistency in results as well as signal. Therefore, high insulation resistance of the cables and connections is essential for PE sensors. The PE sensors need not be powered because the charge is generated by piezoelectric element when mechanical pressure is acting on it. The dynamic pressure traces and pressure pulsations can be measured with both PE and IEPE pressure sensors. Typically, high-impedance systems are more versatile than low impedance. The time constant, gain, normalization, and reset parameters are all controlled via an external charge amplifier. Adjustable measuring range can be achieved with one pressure sensor as the range is adjustable in the charge amplifier. Additionally, the time constants are generally longer with high-impedance systems, allowing easy short-term static calibration. Since electronic circuit is not attached to PE sensors, measurement of pressure in extremely low- or very-high-temperature conditions is possible.

Voltage output types (IEPE) of transducers also use the same piezoelectric sensing element and also have an integrated miniaturized electronic circuit for the charge-to-voltage converter (Fig. 2.16a). The IEPE sensors should be connected to a current (IEPE) coupler, which powers the sensor electronics and decouples the voltage signal from the power supply signal. Typically, low-impedance or low-voltage output systems are tailored to a particular application because the transducer has an internally fixed range and time constant.

2.2.4 Transducer Properties and Specifications

The piezoelectric pressure sensor for reciprocating engine combustion measurement has to operate in an extremely harsh environment. Figure 2.17 illustrates the typical working conditions of the piezoelectric in-cylinder pressure sensor, which affects the characteristics of the output signal. The pressure sensor is exposed to very high dynamic gas temperature (up to >2700 °C) in each combustion cycle. The cyclic heat flux exposed can be more than 1000 W/cm^2 during abnormal combustion (e.g., knocking) conditions. However, in normal operating conditions, the mean heat flux is about 50 W/cm^2 [1]. The temperature of the sensor needs to be maintained below the maximum working temperature of the transducer. Pressure transducer also typically faces acceleration of 1000 g due structure-borne vibrations produced by reciprocating engine parts, and the vibrations/acceleration can increase during abnormal combustion conditions (such as knocking/ringing) of engines. Large stress of up to 200 N/mm^2 in the cylinder head material at the transducer mounting
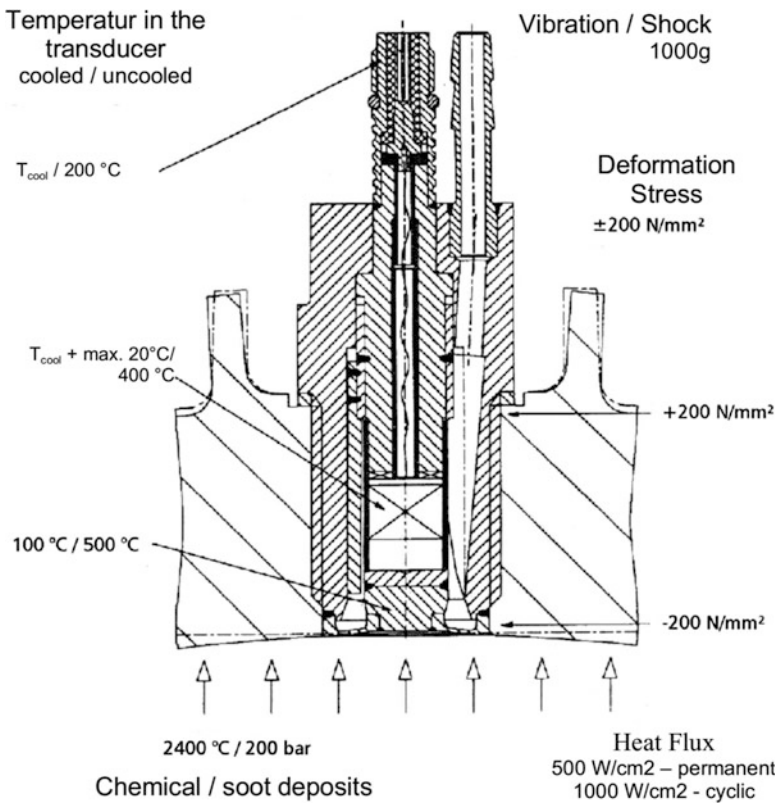
Fig. 2.17 Illustration of typical working conditions of an in-cylinder pressure transducer (Courtesy of AVL)
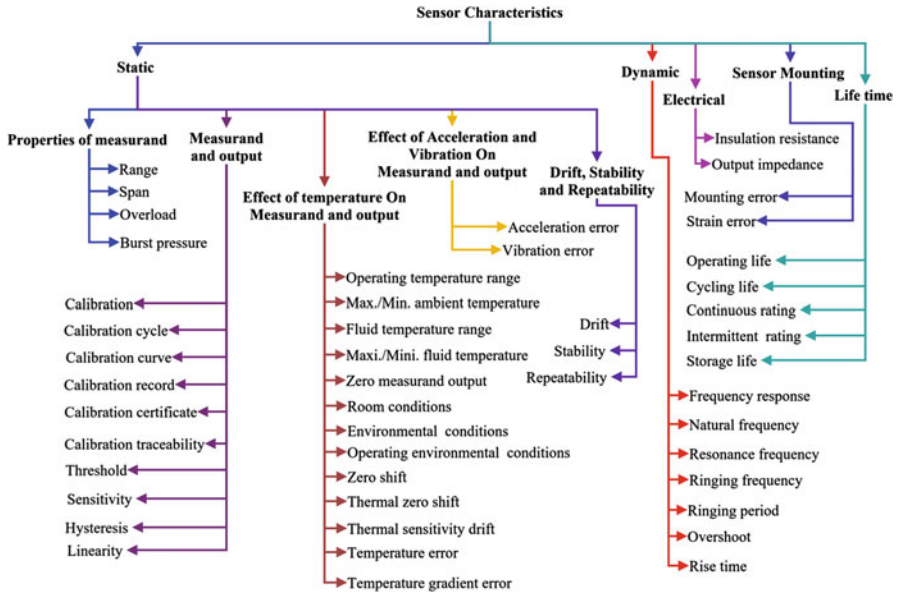
Fig. 2.18 Typical sensor characteristics need to be considered for selecting a piezoelectric sensor (Adapted from [9])

interface can be created by the gas pressure and the thermal stresses due to expansion and contraction. These imposed stresses on the transducer body can have a significant effect on the measured pressure signal. The signal quality of pressure sensor can also be affected by deposits on the transducer face. Carbon deposits can be a problem typically in high soot formation operating conditions depending on the fuel and combustion quality.

Various characteristics of sensors need to be considered for the selection and installation in particular working environment. The properties of sensor govern its effectiveness in generating the desired output signal with respect to working conditions of sensors. Figure 2.18 presents a vast list of sensor characteristics that need to be considered before the selection of transducer including static characteristics, dynamic characteristics, electrical characteristics, and sensor mounting and lifetime-related characteristics. Static properties of sensors are not a function of time, and it can be related to properties of the measurand, measurand and output, the effect of temperature on measurand and output, the effect of acceleration and vibration on measurand and output, drift, stability, and repeatability. Dynamic characteristics of a sensor are related to its response to variations of the measurand with time, which include frequency response, natural frequency, resonance frequency, ringing frequency and period, overshoot, and rise time. All the sensor properties are defined and discussed in the book [9]. However, a brief description of important properties of a piezoelectric pressure sensor for combustion measurement application is provided in this section.
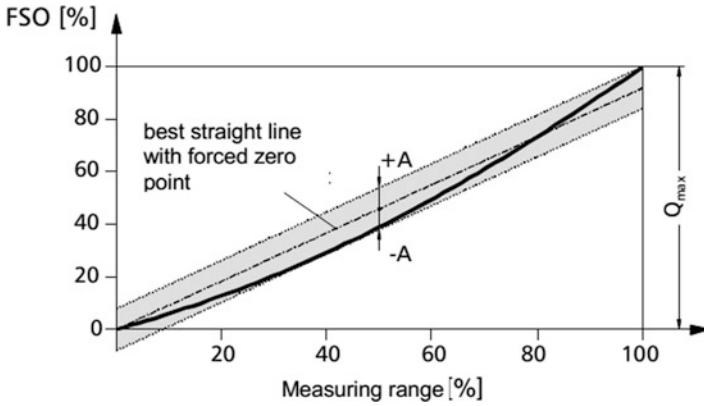
Fig. 2.19 Illustration of sensitivity and linearity of a sensor (Courtesy of AVL)

2.2.4.1 Properties Related to Transmission Performance

The important parameters related to transmission performance of piezoelectric pressure sensor are sensitivity, linearity deviation, natural frequency, insulation resistance, and natural capacitance [8]. The sensitivity of the sensor is defined as the ratio of the change in the output signal (i.e., charge) to the associated change in the measurand quantity (i.e., cylinder pressure). Usually, the manufacturer provides the nominal (or average) sensitivity value of pressure transducer in terms of pC/bar. Typically all the sensors have some amount of sensitivity deviation over the operating range. Figure 2.19 illustrates the sensitivity and linearity of a sensor. Sensitivity and linearity are quantities, which are determined using calibration.

Calibration of the sensor is a test conducted where known values of measurand are acting upon sensor and the associated output signal is recorded in specified operating conditions. In a calibration cycle, measurand values are applied starting from the lowest point of sensor range and increased up to the highest point of the range and back again. The recorded output signal of calibration cycle is processed for estimation of sensitivity, linearity, and hysteresis [9]. The smallest change in measurand which can be measured with the sensor is defined as threshold. The slope of the tangent of the calibration curve is termed as sensitivity. If calibration curve is not a straight line, then the sensitivity of sensor depends on measurand values. The linearity defines the deviation of a calibration curve from a particular straight line. The closeness of calibration curve to the "best straight line with forced zero point" is defined as linearity (Fig. 2.19). The linearity of a sensor is presented as percent of full-scale output (%FSO), which is shown in Eq. (2.6) [8].

$$\text{Linearity}(\%\text{FSO}) = \pm \frac{A}{Q_{\max}} \cdot 100 \tag{2.6}$$

where A is the distance of straight lines enclosing the characteristic from the best line with forced zero point and Q_{max} is the maximum value of output signal (FSO). Piezoelectric sensors (particularly quartz) have a very good linearity and also an exceptionally high ratio of span-to-threshold.

Dynamic characteristics of a sensor are related with its response to variations in the measurand as a function of time. Piezoelectric pressure sensors can be considered as under-damped, spring-mass systems with a signal degree of freedom. This system is modeled by the classical second-order differential equation, whose solution is presented by Eq. (2.7).

$$\frac{a_o}{a_b} \cong \frac{1}{\sqrt{\left[1 - \left(\frac{f}{f_n}\right)^2\right]^2 + \left(\frac{1}{Q^2}\right)\left(\frac{f}{f_n}\right)^2}} \tag{2.7}$$

where f is the frequency at any point of the curve, f_n is the undamped natural frequency, a_o is the output acceleration, a_b is the mounting base or reference acceleration ($f/f_n = 1$), and Q is the factor of amplitude increase at resonance. Quartz sensors have a Q of approximately 10–40.

Figure 2.20 depicts the typical frequency response of piezoelectric pressure sensor (quartz). In a typical frequency response curve (Fig. 2.20), about 5% amplitude rise can be expected at one-fifth of the resonant frequency. Low-pass (LP) filtering can attenuate this effect. The flat response of transducers is seen as a useable range. The defining characteristic of this group is the high resonant frequency leading to a flat response throughout the operating range.

The natural frequency is described as the frequency of free oscillations of the sensing element of a fully assembled transducer, and the resonant frequency is the measurand frequency at which the transducer responds with maximum output signal amplitude. The natural frequency of the pressure transducer must be appropriately

Fig. 2.20 Typical frequency response of piezoelectric pressure sensor (Courtesy of Kistler)

high such that oscillations from the measurand do not excite the transducer into resonance. The excitation of transducers resonance can superimpose false high-frequency components on the measured signal. As a thumb rule, the highest-frequency component expected in the measured pressure signal should not exceed 20% of the resonant frequency of the pressure sensor [15].

Piezoelectric sensors can be described as an electrical device having an active capacitor with a very high insulation resistance. Typically, one electrode of this capacitor is connected to the sensor housing (except ground-isolated transducer). The insulation resistance is the resistance measured between the output signal connector of the sensor and the sensor housing. The insulation resistance should be as high as possible ($>10^{13}$ Ω at room temperature) to keep the influence of the electrical drift as low as possible. Piezoelectric pressure sensors have a natural capacitance, primarily due to the electrodes of the measuring element, and the capacitances of the connector and the line to the measuring element. This natural capacitance can be ignored when a charge amplifier is used [15].

2.2.4.2   Measurement Range and Operating Life

The measurement range of piezoelectric pressure transducer is described as a range of pressure values where it fulfills the defined specifications. This is basically the operational pressure range of the sensor. The algebraic difference between the limits of the range is defined as the span of the sensor. The overload range becomes a concern when the pressure measurement exceeds the normal upper limit. The overload range is defined as the maximum magnitude of a measurand that can be applied to a sensor without causing a change in performance beyond a specified tolerance. Most transducers can withstand some degree of overload without causing any irreversible damage. However, the accuracy of the sensor is not ensured in the overload range. Burst pressure is defined as the pressure which may be applied to sensing element or sensor without rupture. Operating temperature range of pressure transducer is also defined as temperature range in which the defined specifications are fulfilled.

Depending on the quality of installation and operating conditions, the pressure sensor has a finite lifetime. The operating life of pressure sensor is defined as the number of load cycles (or engine combustion cycles) over which the sensor retains its technical performance properties [15]. A generally quoted value is around 10^7 cycles as the projected operating life of a piezoelectric pressure sensor in a typical operating conditions of reciprocating engines. An important means of optimizing the life of the sensor is the use of dummy units when pressure measurement is not required (e.g., warm-up or conditioning of engine).

2.2.4.3   Thermal and Acceleration Influences

Thermal characteristics are important in evaluating a sensor's suitability for accurate measurements of in-cylinder pressure during combustion. Pressure sensors are sensitive to temperature, and any deviations from the calibrated temperature of the sensor may lead to measurement error. The temperature sensitivity of pressure sensor can result into a signal drift. The change in sensitivity of piezoelectric pressure sensor is typically described by the temperature coefficient of the sensitivity, which indicates the actual change in sensitivity as a percentage of the nominal sensitivity per °C within a specific temperature range [8]. The change in sensitivity of pressure sensor is negligible for small change in operating temperature or with cooled pressure sensors.

The pressure transducer is exposed to the non-steady-state heating by the combustion gases on cyclic basis, which results in thermal drift. The amplitude and time characteristic of the temperature-related drift are functions of the type of pressure transducer and heat flow at installation position. Temperature drift in pressure signal is described as the "pressure indicating" that is caused solely by the temperature changes at the pressure sensor and mounting position. Two types of thermal drift phenomena are observed in reciprocating engines, namely, cyclic temperature drift (short-term drift, thermal shock) and the load change drift (long-term drift).

In short-term drift, the measurement error in pressure signal occurs due to cyclic combustion heating of the pressure transducer within a cycle. This cyclic heating problem is more severe at low engine speeds due to the larger duration of combustion time, and relatively more time is available for heat transfer. Figure 2.21 illustrates the cyclic temperature drift in an uncooled pressure sensor. The maximum error in the pressure data within a combustion cycle is related to a point at the start of the heating phase. The figure depicts the temperature distribution and deformation of the transducer at three different points in the cycle (25 °CA before ignition TDC as well as 25 °CA and 180 °CA after intake TDC). Significant deformations in the vicinity of the pressure transducer diaphragm can be clearly seen at the 25 °CA after intake TDC position. The loads on the sensing element due to the deformation lead to cyclic temperature drift (Fig. 2.21).

Thermal shock is one of the major problems limiting the accuracy of piezoelectric transducers for cylinder pressure measurements in reciprocating engines. Thermal shock is generated due to the temperature variation during the engine combustion cycle. The response of a piezoelectric pressure transducer is affected by thermal load variations in two ways: (1) through the corresponding deformation of the transducer/diaphragm and (2) through its effect on the sensitivity of the transducer [20]. A temperature gradient is set up in the transducer material and in the metal surrounding it, when heat is exchanged between the in-cylinder gases and a pressure transducer. The corresponding thermal expansion will deform part of the transducer. Under normal operation, the diaphragm of the piezoelectric transducer deflects toward the piezoelectric crystal of the transducer when the cylinder gas pressure is applied. When the intermittent flame (high thermal load) is exposed to its diaphragm of the transducer, mechanical deformation of the diaphragm occurs due to an abrupt change in temperature on the surface.
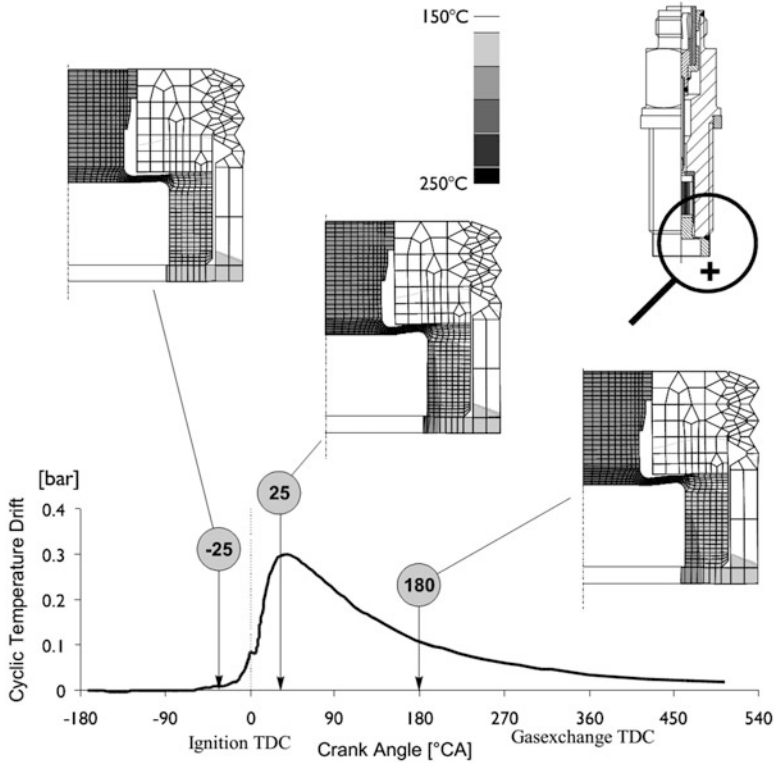
Fig. 2.21 Typical temperature distribution and deformation of a pressure transducer (Courtesy AVL)

Since both sides of the diaphragm are fixed completely, the diaphragm elongates and deflects in the direction of sensing element. To the extent that the piezoelectric crystal is touched by this deformation, this will result in a response of the transducer, even when the pressure remains constant. Therefore, the error in pressure data is strongly influenced by the amount of deflection of the sensor diaphragm due to thermal shock. The temperature variation corresponding to a cyclic thermal loading will penetrate the transducer only to a limited depth, and this depth increases with decreasing cycle frequency. In reciprocating engines, the lowest-frequency components of the thermal load on the transducer are correlated to the changes in engine working condition, and they will penetrate most of the transducer. The highest-frequency components are correlated to the intermittent combustion process, which will affect only the transducer diaphragm (and not the pressure-sensing piezoelectric element because it is located several mm away from the front diaphragm). A cyclic expansion and contraction of the diaphragm occur due to the intermittent combustion process. Transducer sensitivity is affected because thermal load variation influences the stiffness of the pressure-sensing diaphragm. With increasing temperature, the diaphragm weakens and sensitivity of the sensor increases. Of course, the
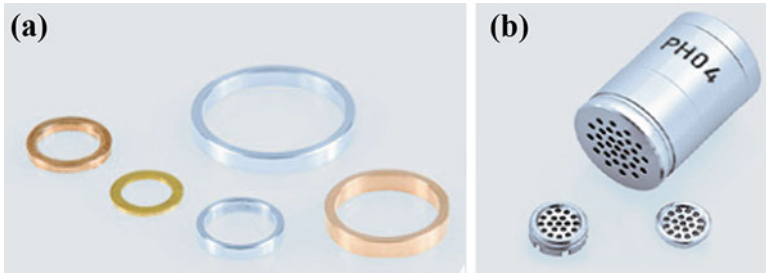
Fig. 2.22 Gaskets and flame arrestors for pressure transducer used in combustion measurements (Courtesy of AVL)

sensitivity of transducer also changes with the operating temperature variation of the piezoelectric crystal [20].

A number of thermal shock reduction methods have been proposed to reduce thermal shock error using mechanical and numerical techniques [21]. The mechanical methods of thermal shock reduction include the water cooling [22], use of heat shields [23], RTV (room temperature vulcanizing) silicones [24], front coating with silicon, and recess mounting [23]. Coating the transducer diaphragm with silicon and water cooling could damp the rapid changes in temperature at the diaphragm. When recess-mounted, the transducer communicates with the cylinder through a single passage or series of passages which quench the flame before its arrival on the transducer surface [23]. Typically, the smaller sensors use the interconnecting passage and face sealing to reduce the thermal load. The larger sensors use heat shield to quench the combustion gases [20, 23]. Figure 2.22 shows the typical gaskets and flame arrestors for the piezoelectric pressure sensors used for cylinder pressure measurement. Gaskets are used as sealing between the sensor and the cylinder head or adaptor. The gasket reduces the additional temperature stress during operation because of the optimized gasket material. During installation of the pressure sensor, the appropriate gasket is used for all sensors with shoulder sealing. The flame arrestors are used as thermo-protection for highly accurate cylinder pressure measurements. During extremely high-temperature operation of the sensor, the use of flame arrestors can result in a significant reduction of the cyclic drift as well as protection of the sensor. However, flame arrestors are not recommended for use in high soot-generating engines due to small holes at the front of flame arrestors.

Thermal shock occurs due to excessive temperatures at low speeds, whereas excessive temperatures at high speeds influence the sensitivity of the transducer, thereby its accuracy [25]. To investigate the thermal effect on the pressure measurement, the temperature of the diaphragm is measured (using fast response thermocouple), and the correlation between surface temperature and thermal shock is derived (Fig. 2.23). Figure 2.23a presents the diaphragm temperatures based upon heat shield design at different engine speeds. The study noted that the diaphragm temperature of all the sensors at idle is approximately the same as the engine coolant temperature, indicating negligible influence from combustion [25]. However, the
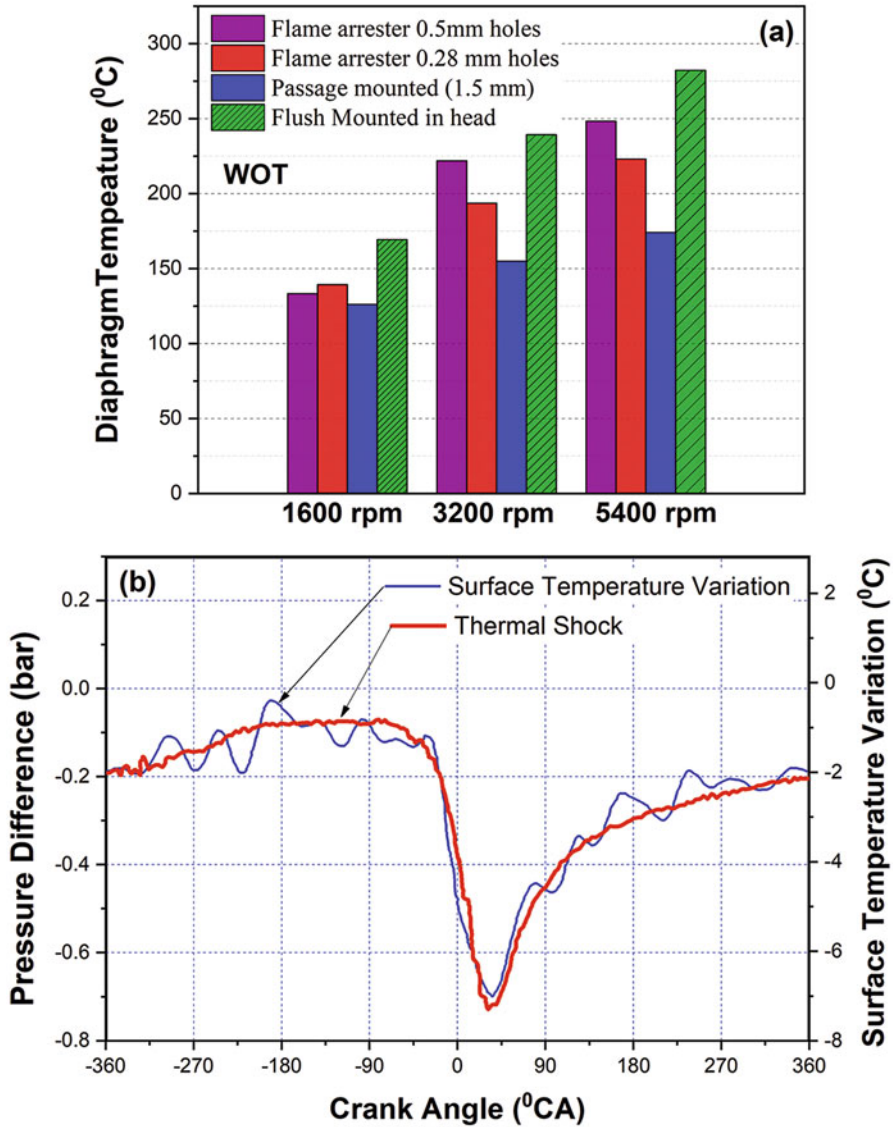
Fig. 2.23 (**a**) Transducer diaphragm temperatures based upon heat shield design (Adapted from [25]) and (**b**) correlation between surface temperature and thermal shock (Adapted from [21])

temperature of a flush-mounted sensor reaches up to 282 °C at higher engine speeds and loads, and this temperature range can influence the sensitivity of the pressure sensor. Figure 2.23a also depicts that the sensors protected by the heat shields have a lower diaphragm temperature. The reduction in passage diameter leads to the reduction in diaphragm temperature. Figure 2.23b shows the correlation between

surface temperature and thermal shock in the diesel engine. The sign of the temperature fluctuation has been changed to allow assessment of the correlation with thermal shock (Fig. 2.23b). The existence of a strong correlation between the pressure error measurements and temperature variations is confirmed by Fig. 2.23b [21]. The location of pressure sensor installation also affects the diaphragm temperature, and thus, thermal shock effect can be reduced by selecting the favorable installation position.

In the published literature, the effect of thermal load on pressure transducer is described in terms of short-term thermal drift (or thermo-shock) and medium (or long)-term thermal drift. Short-term thermal drift is defined as the measurement error within a single cycle due to transducer deformation and sensitivity change caused by the change in thermal load within that cycle. Only the transducer deformation effect can be considered a drift in the strict sense as the effect of a cyclic change in sensitivity is minimal in modern transducers. Medium-term thermal drift is defined as the measurement error related to a change in engine working condition. Finally, long-term drift is caused by the change in sensitivity of the transducer over longer periods (it can be several hours for the good transducers) [20].

There are several methods to evaluate the sensor accuracy during the thermal shock, whether by another sensor or to itself. The methods for evaluating thermal shock include (1) comparing the output signal to a reference sensor, which has a much higher resistance to thermal shocks [15, 26]; (2) using a dedicated heating test rig to measure the response of the transducer to an external heat load [1, 15]; (3) a comparison of the measured signal with a calculated or simulated pressure [21, 27]; (4) a quasi-steady-state test, applying the average cylinder pressure during exhaust stroke as a function of the combustion phase [23, 28]; (5) comparison of pressure signal envelopes [28]; (6) cyclic pressure deviation at specific points in the engine cycle [23, 25]; (7) the relationship of IMEP to the location for 50% mass fraction burned [23, 25]; and (8) the difference between the pressure at 540° ATDC and at −180° BTDC (intake BDC position), called drift, and a value close to zero would be ideal [25, 29].

To evaluate the short-term drift of a sensor by comparison method, a reference sensor known for higher accuracy (typically water cooled) is required. In this method, the absolute value of measured cylinder pressure throughout the entire engine cycle is examined with respect to reference sensor. Figure 2.24 depicts the short-term drift of sensor by presenting the difference in pressure measurements due to the thermal shock effect and reference sensor. Typically, the average of few hundred cycles is computed, and the reference signal is subtracted to highlight the difference. The figure shows that thermal shock occurs during combustion when the flame contacts the diaphragm and persists during the expansion stroke. Effect of thermal shock on reference sensor is minimal and neglected. The difference between the outputs of the two sensors provides an indication of the magnitude of thermal shock. A study defined the thermal shock as the maximum pressure difference after TDC between the test and the reference sensor [26]. It is important to note that the duration of the thermal shock affects IMEP, not just the maximum thermal shock magnitude. This is because the IMEP calculation is an integral of the pressure with
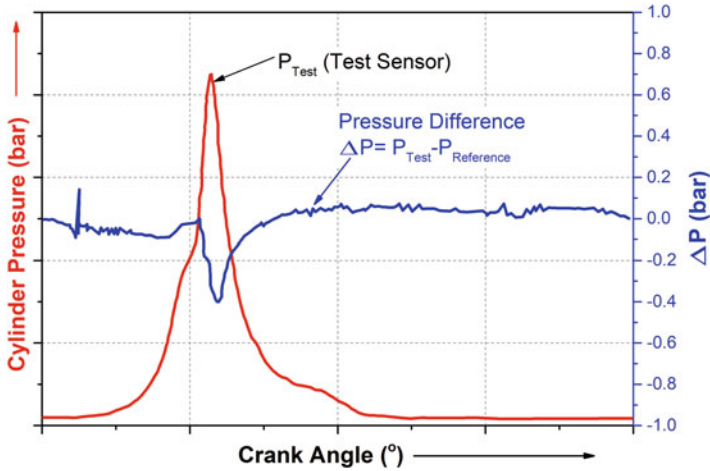
Fig. 2.24 Difference between the reference sensor (water-cooled) and test sensor outputs (Courtesy of Kistler)

respect to the volume change throughout the engine cycle, not just at a single point. The magnitude of thermal shock depends on the (1) duration of high-temperature shock (e.g., flame impingement time), which affected by engine speed, and (2) the peak pressure (or temperature) during engine cycle depending on engine operating conditions. Typically, greatest thermal shock errors occur at low engine speed, high load, advanced ignition timings, slightly rich mixtures, and low EGR operating conditions [26]. As noted, the severity of the thermal shock is controlled by the time history of the instantaneous heat flux into the sensor. The time history of the heat flux varies from cycle to cycle due to normal variations in heat release rates causing the timing and severity of the thermal shock to vary from cycle to cycle as well.

To evaluate the thermal shock on the pressure sensor, the measured signal can be compared with a calculated or simulated pressure data at the same operating conditions. Figure 2.25a presents a comparison between the simulated and experimental pressure data for the blowdown process at two different engine loads. The figure shows that the cylinder pressure level remains relatively constant during the blow-down process irrespective of the engine load in case of modeling data. However, in the case of the experimental data, the cylinder pressure at the higher engine load condition is lower than that at the lower engine load condition. This trend is possible due to the thermal shock which is much higher at high-load condition. Additionally, experimental pressure data should be close to the measured exhaust port pressure during the blowdown process. Once the exhaust valve opens during the exhaust stroke, the pressure in the cylinder should be identical to the pressure in the exhaust port. Any difference between the two can indicate an error with the cylinder pressure sensor. The measured cylinder pressure appears to be lower than the atmospheric pressure for the exhaust process, and it is also lower than the measure of exhaust port pressure (Fig. 2.25a). This can be attributed to thermal shock [21]. Figure 2.25b
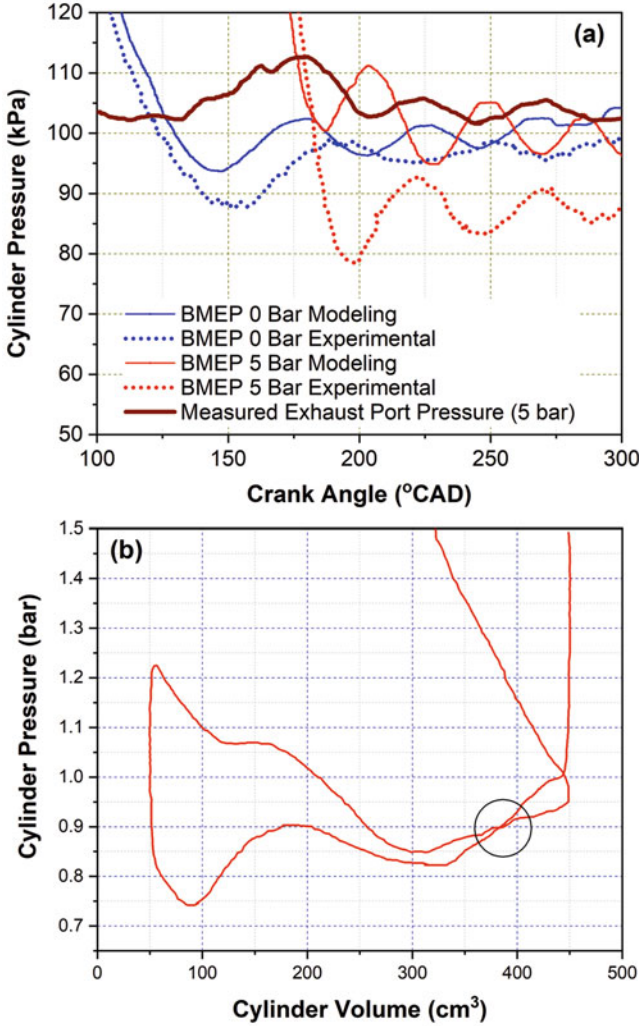
Fig. 2.25 (**a**) Comparison of the modeling and experimental cylinder pressure at the blowdown process at different engine loads (Adapted from [21]), (**b**) effect of thermal shock on *P-V* diagram (Adapted from [30])

illustrates the effect of thermal shock on intake and exhaust stroke on pressure-volume (*P-V*) diagram. The pressure curve of the intake stroke and that of immediately after the blowdown intersect each other (Fig. 2.25b) due to the thermal shock applied to the sensor diaphragm during combustion. The effect of thermal shock appeared after blowdown instead of during combustion period due to the heat capacity of the diaphragm, which causes the time lag of the temperature difference between inside the cylinder and the surface of the diaphragm [30].

The metrics based on analysis of the low pressure or pumping loop can be used to evaluate the effect of thermal shock. The thermal shock causes the transducer output to shift (either high or low) from the actual cylinder pressure depending upon the specific sensor design characteristics. This shift occurs with a relatively fast time constant such that, for typical engine (modern passenger car and light truck engine) speeds, the transducer will generally recover back to its normal state by the end of the intake stroke following the thermal shock event [28]. The average exhaust absolute pressure (AEAP) during exhaust stroke is one of the metrics used to evaluate the thermal shock. The average cylinder pressure during the exhaust stroke is calculated during a portion of the exhaust stroke from about 60° aBDC to about 60° bTDC. The averaging window needs to be selected such that interference from differences in the exhaust blowdown process can be avoided, which may lead to normal cyclic combustion variation. Figure 2.26 demonstrates the effect of thermal shock on AEAP (the average cylinder pressure during the exhaust stroke) as a function of the average CA_{50} (combustion phasing) position. Transducer A has been installed with the proper mounting techniques and in a location within the cylinder so as to minimize the occurrence and severity of thermal shock. The AEAP values during exhaust stroke from transducer "A" do not show any apparent sensitivity to the combustion phasing as expected. Additionally, during the exhaust stroke, the AEAP values from transducer "A" are just slightly higher than the ambient atmospheric pressure of 100 kPa (Fig. 2.26), which is also expected at the relatively low-speed, light load condition (experimental condition). The other transducers experience some level of thermal shock and show pressures either substantially higher than the expected pressure or pressures lower than ambient which is physically not possible. They also show varying amount of the sensitivity of the average cylinder pressure during the exhaust stroke to the combustion phasing [28].

Figure 2.26 also depicts a low value of standard deviation of the average cylinder pressure during the exhaust stroke that is not influenced by the combustion phasing for the transducer A, which is intended to have the least thermal shock. The remaining transducers show a higher standard deviation of the average cylinder pressure during the exhaust stroke and show sensitivity to the combustion phasing. The more advanced combustion phasing leads to the more severe thermal shock and higher standard deviation of the average cylinder pressure during the exhaust stroke (Fig. 2.26).

Thermal shock on transducer during the combustion pressure measurement can be detected by signal envelope method. In this method, three signal envelopes are defined: the average signal envelope (ASE), upper signal envelope (USE), and lower signal envelope (LSE). The ASE is determined by the average pressure recorded at each crank angle increment over the entire set of cycles in the data sample. The USE is calculated by taking the highest pressure recorded at each crank angle increment on any one of the sampled cycles. Similarly, the LSE is calculated by taking the lowest pressure recorded at each crank angle increment on any one of the sampled cycles [28]. It is important to note that USE and LSE traces are composite cycles, which contain the data from many individual cycles at different crank angle positions. Figure 2.27 illustrates the typical USE, ASE, and LSE curves for a transducer
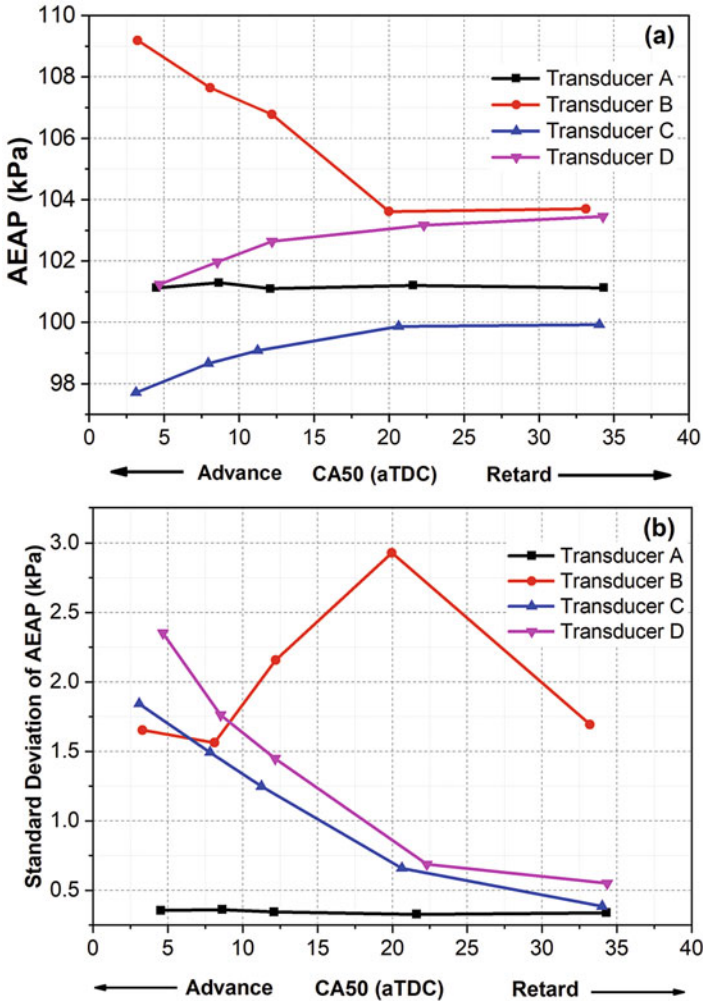
Fig. 2.26 (**a**) Average cylinder pressure and its (**b**) standard deviation during exhaust stroke as a function of combustion phasing (Adapted from [28])

with good (low) thermal shock characteristics and poor (high) thermal shock characteristics. The transducer with low/good thermal shock characteristics can be used as reference pressure sensor. The average spread between the USE and LSE curves at each crankshaft position is small (<3 kPa), which is mainly governed by the digitizer resolution and background noise on the data. Additionally, the comparison of the signal envelopes can also highlight the acceleration sensitivity of the transducer as indicated by the diverging signals during the valve closing events (Fig. 2.27a) [28]. The pressure transducer with poor thermal shock characteristics has the larger average spread between the USE and LSE curves at each crankshaft position, which indicates the presence of thermal shock.
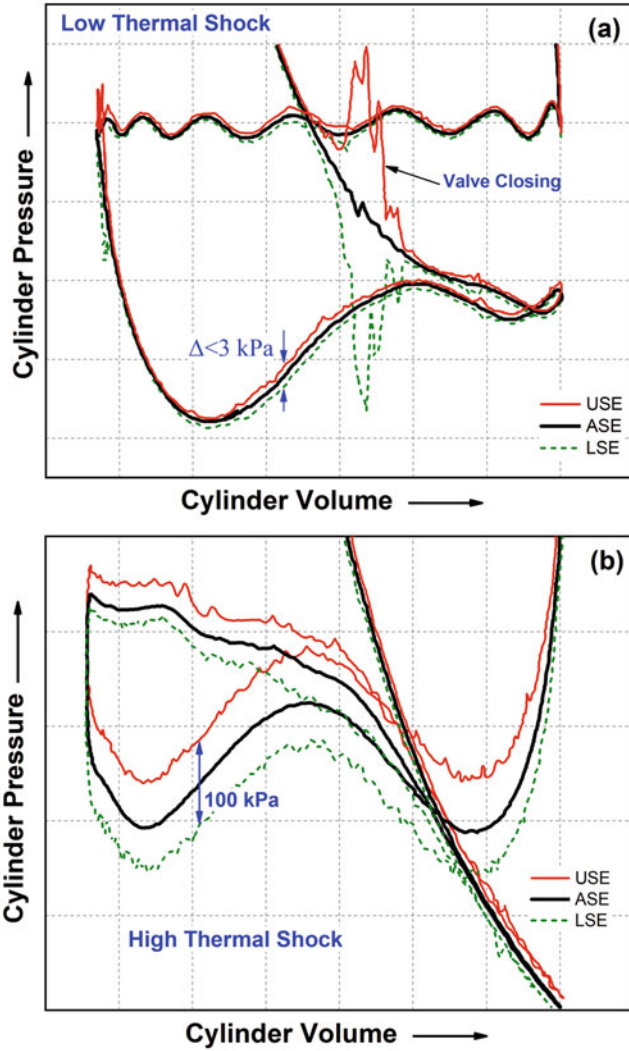
Fig. 2.27 Thermal shock detection with signal envelope method for (**a**) low thermal shock transducer (Adapted from [28]) and (**b**) high thermal shock transducer (Adapted from [27])

Another technique named intra-cycle variability analysis of pressure measurements is used for thermal shock detection, which is also a pressure deviation-based method. Metric in this technique compares the stability of the sensor to itself at specific locations in the engine cycle and shows the relationship of those points during particular sections of the cycle. This helps to show if the sensor is unstable to itself and if it may have recovered before the next portion of the engine cycle. In this method, the cycle-to-cycle variation of the cylinder pressure is compared at specified crankshaft positions (points shown in Fig. 2.28a) along the whole cycle. The cycle-
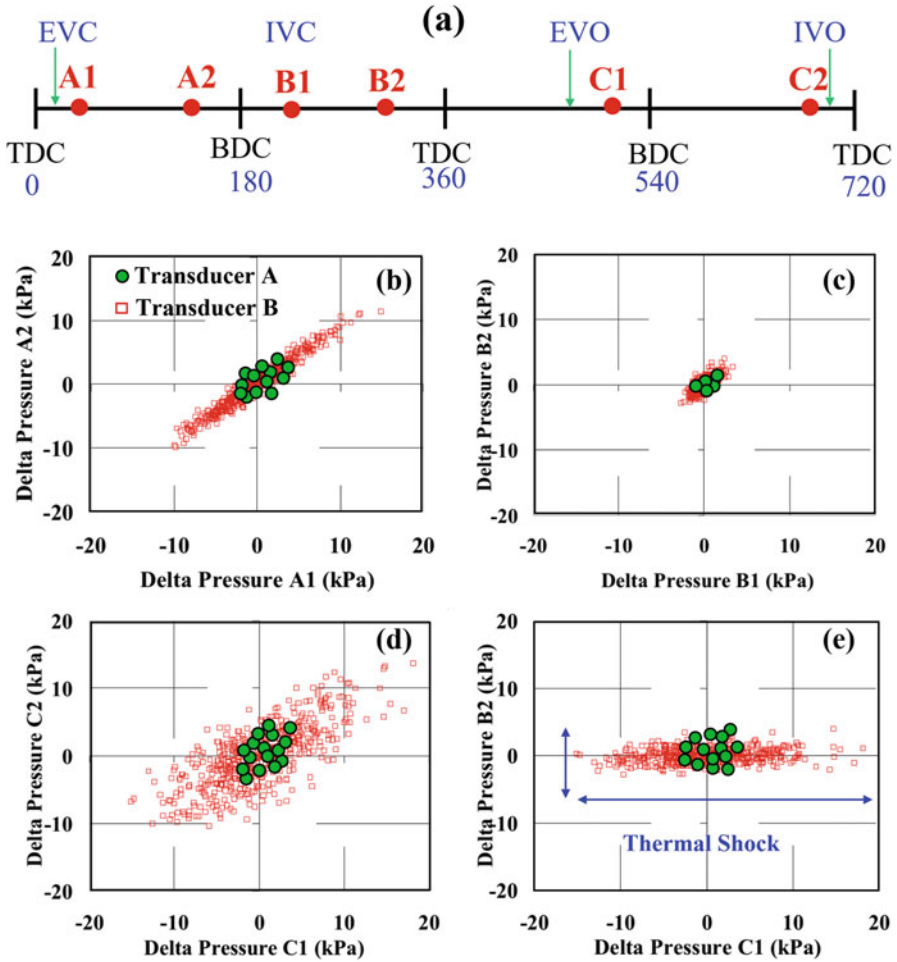
Fig. 2.28 Illustration of intra-cycle variability method for thermal shock detection (Adapted from [25])

to-cycle variability is normal due to the random variations in the combustion process. This variability leads to changes in the pressure transducer thermal load, and when a thermal shock occurs, the sensitivity of the transducer will be changed, and the scattering of pressure measurements will be enlarged. Thus, the pressure variance scattering is used to indicate the presence of a thermal shock [27]. - Figure 2.28 illustrates the intra-cyclic variations in pressure at different defined crank angle positions for two typical pressure transducers. Intra-cycle variability originates during the combustion event and drifts into the exhaust, intake, and compression segments of the pressure curve, while the pressure sensor simultaneously recovers from the thermal shock. With zero intra-cycle variability, all pressure differences would lie at the graph center (origin of the graph). Constant

variability during any segment would cause all the pressure differences to lie along the graph diagonal, while a gradual change of variability during the segment would rotate the line around the graph origin away from the diagonal. The spread of the points along the graph diagonal is a measure of the intra-cycle variability range during the segment, while the spread of the points away from the diagonal quantifies measurement repeatability [31]. A slope of 1 means the sensor's accuracy does not change during the section; instead, the variability is the combustion process. During the intake stroke (Fig. 2.28b), the variability range is larger for transducer B, which suggests the transducer recovers from thermal shock impact as intake proceeds. The variability of the transducers is small in the compression stroke. The maximum amount of intra-cycle variability occurs during the exhaust stroke (Fig. 2.28d). This is expected because this segment of the pressure curve immediately follows the combustion event where the variability is originated. The large change in variability between C1 and B2 crank positions denotes the thermal shock (Fig. 2.28e). Data points are spread along the horizontal axis rather than along the diagonal for transducer B, clearly showing the effect of thermal shock.

Heat shield can avoid the extreme diaphragm temperatures during thermal shock on pressure transducers depending on the design of heat shield. Figure 2.29 depicts the effect of heat shield design on the reduction in AEAP pressure difference and drift as a function of the passage size. The figure shows that as the diameter of the passages decreases, the difference between the two measurements decreases, thereby supporting the flame-quenching process and reduced thermal shock. The drift (pressure difference at intake BDC position of consecutive engine cycles) for the different heat shields is all within the range of 1.6–1.7 kPa indicating sensor distortion is complete by the end of one engine cycle and the start of the next [25]. From an intra-cycle variability perspective, all heat shields reacted about equally.

Fig. 2.29 Drift and AEAP difference in relation to passage sizes (Adapted from [25])
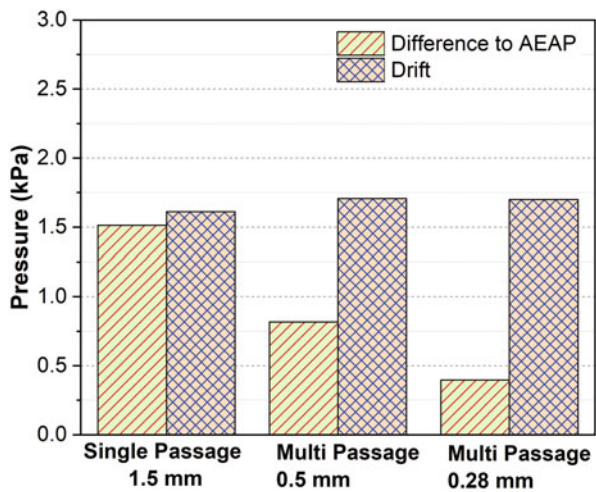
Thermal shock is generally reduced by mechanical methods, such as coating the transducer diaphragm, heat shields, recess mounting of the sensor, water cooling, etc. An empirical equation-based compensation method has also been developed, which provides greatly increased accuracy in the measured IMEP over a wide range of engine speed [21, 30]. From theoretical analysis using actual pressure data, a thermal shock error compensation equation was proposed [30]. The amount of deflection of the diaphragm due to the thermal shock could be expressed as a function of the temperature difference between the temperature of the diaphragm and the minimum temperature of each cycle. It is assumed that the diaphragm deflection is proportional to the additional pressure resulting from thermal shock. The error compensation equation obtained is presented in Eq. (2.8).

$$\Delta p = -\sqrt{A\Delta T^2 + B\Delta T} \qquad (2.8)$$

The constants A and B are experimentally determined.

An IMEP thermal shock error correction equation which has been derived in the study [21] is presented by Eq. (2.9).

$$\text{IMEP}_{\text{corr}} = \text{IMEP}_{\text{meas}} + (F \times P_{\text{max}}) + \text{Offset};$$
$$F = 0.0000834\left(\frac{\text{rpm}}{1000}\right) - 0.00051\left(\frac{\text{rpm}}{1000}\right) + 0.00502 \qquad (2.9)$$
$$\text{Offset} = 0.01534\left(\frac{\text{rpm}}{1000}\right)$$

The numerical approach for correction of IMEP thermal shock errors has a number of advantages: (1) increased measurement accuracy without expensive replacement of existing pressure sensor and extra machining of engine heads; (2) problems created by mechanical, thermal shock reduction techniques can be avoided; (3) the requirement of water-cooled sensor is reduced as it fits with difficulty in modern four-valve heads; and (4) sensors with good characteristics other than thermal shock resistance can also be used [26].

Typically a reciprocating combustion engine operates in transient conditions of speed and load. The variation in engine speed and load conditions affects the temperature as well as heat load experienced by the pressure sensor. The varying thermal conditions of pressure sensor have consequences on the output signal over a number of cycles, after a change in engine operating conditions. The load drift manifests as a slow variation in the pressure signal after a load change due to the altered thermal stresses in the sensor body. This shift in pressure level will only stop when the mean temperature in the pressure sensor no longer changes. Figure 2.30 illustrates the typical load drift on measured pressure signal to a step change in engine load condition. The figure depicts the two characteristics values: (1) maximum zero-line gradient (dp/dt) and (2) permanent zero-line deviation (shown in the bottom half of Fig. 2.30). The maximum zero-line gradient shows the change in pressure level per time unit caused by the heat flow, which will affect the combustion
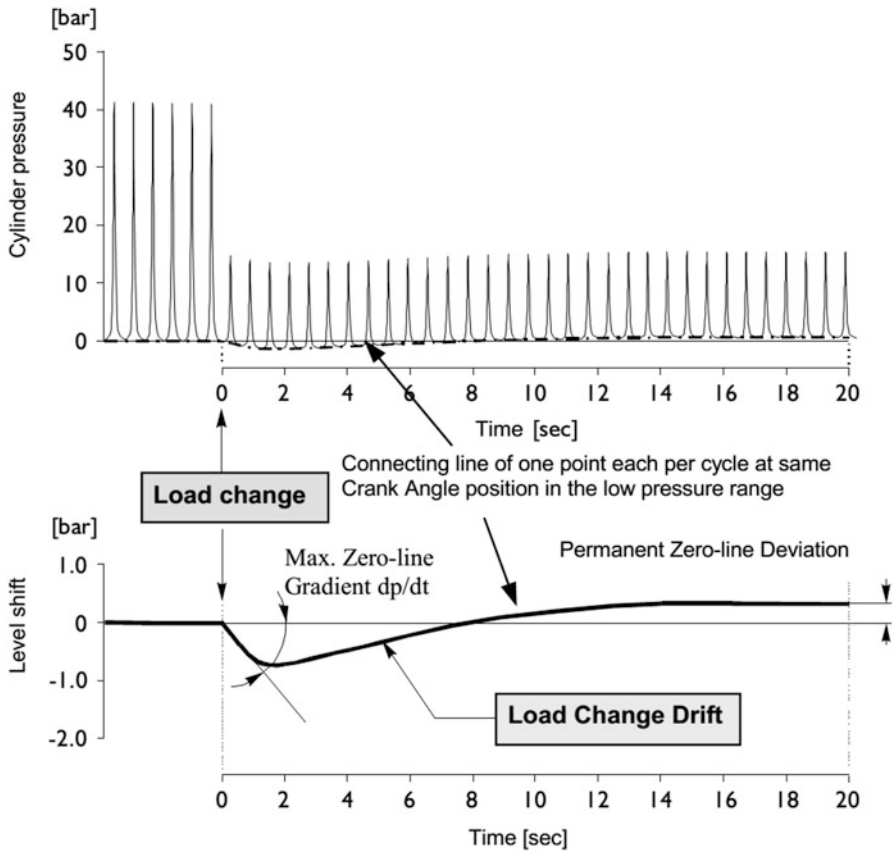
Fig. 2.30 Illustration of load change drifts in the piezoelectric transducer (Courtesy of AVL)

parameter calculation using measured pressure signal. The permanent zero-line deviation is shown as zero point after 20 s of load change (Fig. 2.30). This deviation does not affect measured value because the zero-line determination is always necessary for measurements using piezoelectric pressure sensors [8].

At constant engine working conditions, medium-term drift should not occur. In this case, a measure for long-term drift (LTD) can be obtained from the slope of the signal. To determine the long-term drift, the pressure trace (at a constant crank angle) is fit to a straight line (using the least squares method) as presented in Eq. (2.10) [20].

$$\hat{p}(\alpha)_i = a \cdot i + b$$
$$\text{LTD} = a \tag{2.10}$$

where "i" refers to the cycle number. It can be noted that the LTD errors are compensated if pegging of individual cycles is used.
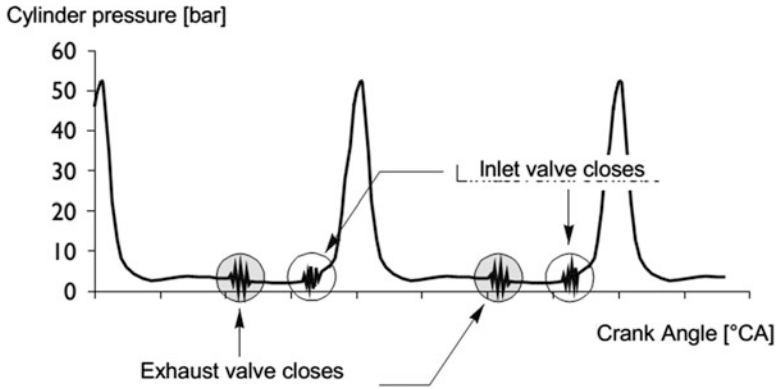
Fig. 2.31 Effect of structure-borne vibration on the measured pressure signal (Courtesy of AVL)

Apart from thermal shock, there are other effects which also lead to drift (error) in the pressure signal also on a short-term basis. The pressure changes during the engine working cycle result in cylinder head deformation which leads to deformation in pressure sensor together with the engine cylinder head [20]. Another major cause is the engine vibration. Acceleration (vibration) causes the quartz element and some of the other components to act as seismic masses leading to measurement error and can also result in a cyclic reduction of transducer cooling for water-cooled transducers.

The sensitivity of the pressure sensor to structure-borne vibrations of the engine can cause false frequency components to be imposed on the measured cylinder pressure signal. Thus, acceleration compensation is provided in pressure sensor by manufactures (illustrated in Fig. 2.15). The extent of the influence of acceleration also depends to a large extent on the installation site, on the direction of the accelerations that occur in relation to the pressure transducer axis, and on the engine speed [8]. Figure 2.31 illustrates the effect of structure-borne vibration/acceleration on the measured pressure signal. The high-frequency oscillations superimposed on the pressure signal are caused in this specific measurement arrangement by the impact of the intake and outlet valves on the valve seat and transmitted by structure-borne noise. Pressure measurements on revving racing engines often reflect a strong influence of structure-borne noise over the entire cycle [8].

2.2.4.4 Chemical Influences and Deposits

The combustion process in reciprocating engines produces hundreds of chemical species (combustion products) depending on the fuel used. Some of the species produced during combustion can lead to corrosive damage to the piezoelectric pressure sensor. Modern sensors use special coatings and corrosion-resistant materials, which makes corrosion effects insignificant [8]. The corrosion effect can be

significant in very unusual conditions such as utilization of fuel with very high sulfur content or other newly developed alternative fuel (with corrosive combustion product).

Typically, deposits build up on the cylinder walls of both petrol and diesel engines. Direct injection diesel engines are well known for the sooting tendency. However, modern gasoline direct injection engines also have the soot formation issues. Soot formed during combustion tends to form deposits on cooler surfaces, and diaphragm of the pressure sensor is a favorable place for building up deposits particularly in cooled pressure sensors. The deposits can have an undesirable effect on measurement signal depending on the type of sensor and engine operating conditions. In extreme conditions, the altered pressure signal due to deposits can lead to more than 10% error in indicated mean effective pressure (IMEP) determination. The IMEP stability is a characteristic value, which provides the information about the sensitivity of pressure sensor to soot deposits. The IMEP stability is defined as the percentage change in IMEP over a defined runtime in relation to values determined with a reference pressure transducer [8].

2.2.5   Transducer Adaptors and Mounting Position

The mounting position of the pressure sensor and the mounting method to access the combustion chamber have a significant effect on the accuracy of measured combustion chamber pressure and the lifetime of the sensor itself. Pressure transducer must be small enough to be accommodated within the cylinder head without affecting the shape of the combustion chamber, and it must be fitted to produce minimal intrusion or disturbance. During installation process, a problem of proper mounting of pressure sensor usually arises, and the optimum is to flush mount the transducer such that it can be directly in contact with the gas. To access the combustion chamber for pressure measurement, there are basically two methods, namely, intrusive mounting (with intervention in test engine) and nonintrusive mounting (without intervention in test engine). Both of these methods have their merits and demerits. Typically, intrusive methods have relatively higher accuracy, and the measuring position can be selected by user. However, higher cost and substantial time and effort is required for intrusive installation of pressure sensor [8]. In nonintrusive mounting of the pressure transducer, installation time and cost is lower as it has to be installed in place of a standard engine component. The intrusive and nonintrusive methods of pressure sensor installation are discussed in the following subsections.

2.2.5.1   Intrusive Mounting

In an intrusive installation of the pressure transducer, intervention via precision modification of the cylinder head is performed in such a way that the transducer and measuring face are suitably positioned for exposure to the cylinder gas pressure.

Fig. 2.32 Illustration of pressure transducer mounting with (**a**) direct installation and (**b**) adapter installation (Courtesy of Kistler)
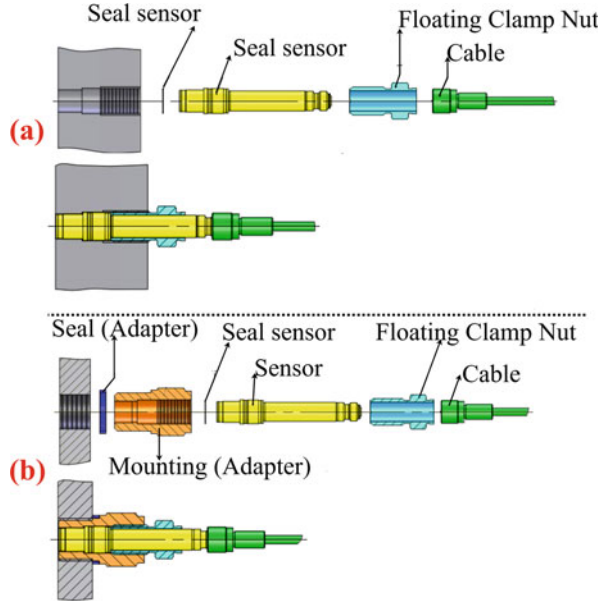
This type of pressure transducer has several variations due to a large number of possibilities with respect to installation position [15]. The intrusive mounting of pressure transducer can be executed with or without an adaptor. Figure 2.32 illustrates the pressure transducer mounting with (a) direct installation and (b) adapter installation. Direct installation method is preferred for small spaces. However, complex drilling with special tools is required for direct installation of the pressure sensor. An adaptor sleeve is required when access to the combustion chamber requires traversing oil or water passages. Installation with adapter is preferred (requires adequate mounting space), and simple tapped hole in the engine head can accept the adapter. Additionally, the adaptor sleeve effectively separates the transducer body from the surrounding cylinder head material (mechanical decoupling), thus isolating the sensor from deformation stresses that could cause a shift in sensitivity during engine operation.

Measuring point accessibility and the measuring task are significant factors determining the position in which sensor is mounted in the engine cylinder head. The position of pressure transducer installation depends on a number of interrelated factors which must be considered judiciously. Pressure sensor installation should not affect the spaces of various engine parts in the combustion chamber such as valves, injectors, and spark plugs. The structural integrity of the engine parts needs to be retained, and the wall thicknesses of engine head casting must be ensured such that it does not lead to failure. The transfer passages for oil or water in the cylinder head should not be blocked by pressure sensor installation. Otherwise thermal conditions of engine head and cylinder can vary drastically. The temperature of the sensor (particularly its diaphragm) depends on the mounting position. Additionally,

measurement errors can also be introduced due to environmental factors, such as heat flow, temperature, and accelerations. Therefore, all these boundary conditions must be considered before choosing the installation site for the in-cylinder pressure sensor of engines.

Mounting positions near the exhaust valves results in increased sensor temperatures due to higher gas temperature and increased flow velocity during the exhaust stroke. Increased sensor temperature can affect the measurement accuracy and sensor service life, and thus, positions near the inlet valve area are preferred [18]. Gas dynamics during intake and exhaust stroke can also affect the measurement and can introduce error in the measured signal. The high flow rates near valves can lead to local pressure differences, which may not be representative of cylinder pressure [15]. The measurement errors due to the design of the measuring position can include dead volume when the transducer is installed in an inclined position or recessed, pipe oscillations for recessed installation, interference to the gas flow, and fuel deposits [8].

The optimal choice of pressure sensor installation is mounting flush with the combustion chamber, perpendicular to the surface, and if possible without the sort of flow pocket produced by inclined mounting. In this mounting, the transducer is recessed just enough to prevent deposit buildup on the piston from damaging the transducer, but not so much as to create a measuring pipe. The recessed installation can produce high-frequency oscillations at resonance or increase cylinder volume, which reduces the engine compression ratio. Figure 2.33 illustrated the flush and recessed mounting installation of the sensor for cylinder pressure measurement. Ideally, for best accuracy, a combustion sensor should be flush-mounted in the combustion chamber (to reduce heat flow load and temperature), but often this is not possible, and sensors are installed recessed. In the recessed installation, the cylinder pressure travels through an indicator passage to reach the sensor, which can lead to signal acoustic oscillations, and signal distortion can occur. Figure 2.34 shows the effect of the length of indicating channel on the measured pressure signal. Five pressure curves (shifted in level) from single cycle measurements are shown for each indicating channel length. The oscillations in pressure signal decrease with reduced length of the channel. The frequency of this interference depends not only on the length of the indicating channel but also on the gas state, which makes the use
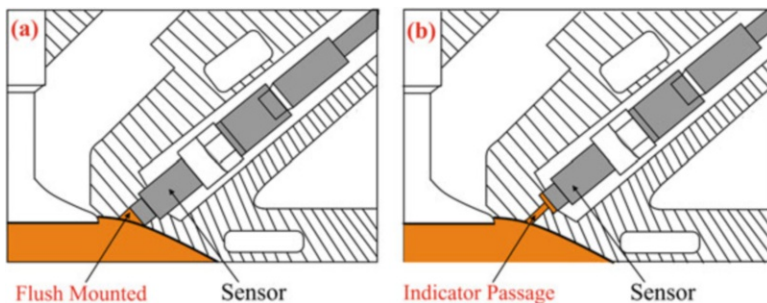
Fig. 2.33 Pressure sensor installation with (**a**) flush mounting and (**b**) recessed mounting
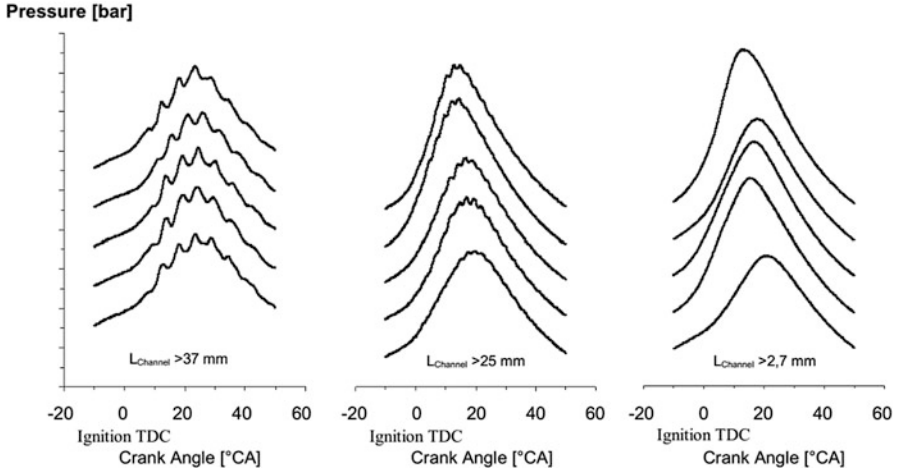
Pressure [bar]

Fig. 2.34 Influence of the length of the recessed channel on the measured pressure signal (Courtesy of AVL)

of frequency filters for eliminating pipe oscillations difficult. Additionally, it is not easy to differentiate the pipe oscillations from actual combustion chamber oscillations [8].

Figure 2.35 presents the two different types (Fig. 2.35a, b) of pressure transducer installation passages. In the first design (Fig. 2.35a), only indicating channel with length (L) is present. However, in the second design (Fig. 2.35b), there is an additional volume (V_{cv}) in front of the pressure transducer with an indicating channel. For the first type of air duct (Fig. 2.35a), the lowest natural frequency of oscillations can be computed using Eq. (2.11) [32].

$$f_n = \frac{a}{4L} \qquad (2.11)$$

where f_n is natural frequency, "a" is local acoustic velocity, and "L" is the length of the air duct.

For the second type of air duct with additional volume (Fig. 2.35b), the natural frequency of oscillations can be computed using Eq. (2.12) [32].

$$f_n = \frac{a}{2\pi L} \left(\sqrt{\frac{A \cdot L}{V_{cv}}} \right) \qquad (2.12)$$

where A is passage cross-sectional area and V_{cv} is the volume of the cavity in front of the pressure sensor.

Figure 2.36 depicts typically achievable natural frequencies as a function of diameter and length of the indicator channel. It is shown that the natural frequency of the passage acoustic oscillation should be above 3 kHz by assuming that the engine has a minimum knock frequency of about 2 kHz. A passage with a diameter

Fig. 2.35 Illustration of installation passage types for piezoelectric pressure sensor (Courtesy of Kistler)
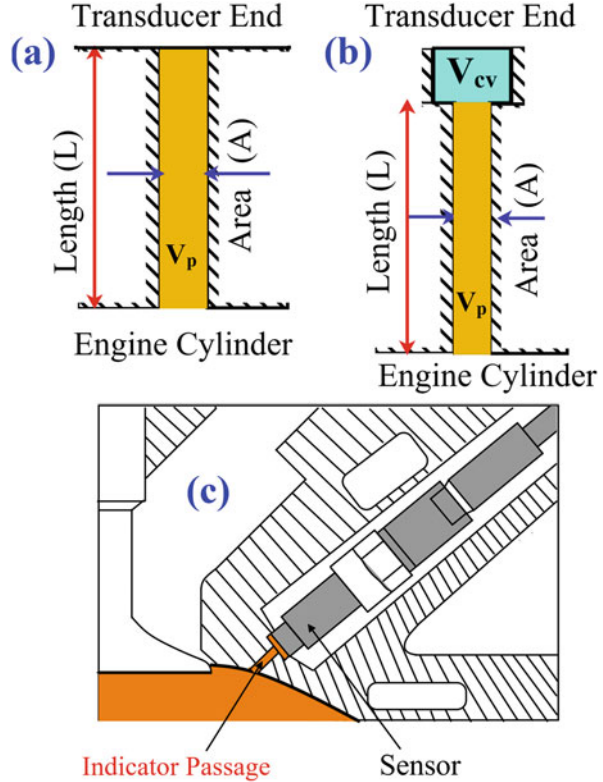
Fig. 2.36 Typical pipe oscillation frequency as a function of indicating channel length and diameter (Adapted from and courtesy of Kistler)
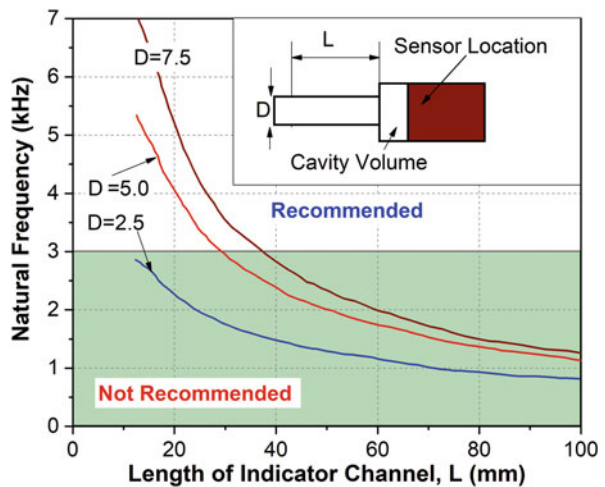
of 2.5 mm (or 5 mm with maximum length 30 mm) will not allow the minimum frequency to be measured (Fig. 2.36). The shorter bores are recommended for monitoring knocking conditions.

In the recessed mounting installation, the thermal shock can be significantly reduced by isolating the transducer tip from the burning and burned gases. Figure 2.37a presents the typical burned and unburned gas temperatures as a function of crank position at wide open throttle (WOT) conditions in spark ignition engine. The figure shows that the burned gases are at a much higher temperature (over 2000 K) than the unburned gases. It is well known that the peak temperatures of the first gases to burn are up to 300 °C hotter than the gases that burn in the middle and toward the end of the combustion event. This results from the fact that as the early gases combust, they expand considerably which effectively removes energy from these burned gases. As additional heat is released from combustion of the remaining charge, energy is added to these initial combustion products, raising their temperature significantly higher than they would have otherwise obtained. The net effect is that the gases that are burned before peak cylinder pressure being reached will achieve a higher peak temperature than the mixture that burns as cylinder pressure is falling. Thus, it is beneficial to mount the transducer away from the ignition source in the end-gas region [33].

Considering the temperature difference of burned and unburned gases, the ability of the connecting passage to quench a propagating flame is not enough to prevent very hot gases from reaching the pressure sensor. The burned gases can be mechanically transported through the passage onto the diaphragm of the sensor because of cylinder pressure rise after passing the flame front from sensor location. To prevent the impingement of hot gases on the transducer face, the connecting passage must have a volume sufficiently large relative to the sensor cavity volume to contain all burned (and burning) gases that are compressed into it after the flame traverses the passage entrance. This critical volume ratio is approximately defined by Eq. (2.13) [33].

$$\left(\frac{V_p}{V_{cv}}\right)_{critical} = \left(\frac{P_{max}}{P_{FA}}\right)^{1/1.32} \tag{2.13}$$

where V_p is the passage volume, V_{cv} is the transducer cavity volume (as shown in Fig. 2.35b), P_{max} is the peak cylinder pressure, and P_{FA} is the in-cylinder pressure at the time the flame front arrives at the passage entrance. The Eq. (2.13) is derived assuming that the volume of gas in the passage at the time of flame arrival must first be completely displaced into the transducer cavity before burned gases can reach the sensor cavity. It can be noted that the Eq. (2.13) is valid only if the cylinder pressure is rising when the flame front arrives at the passage entrance, and it is also assumed that design of passage quenches the flame.

Figure 2.37b presents a typical example of critical volume ratio as a function of transducer radial location and combustion phasing. The critical volume ratio was calculated for a full range of transducer radial locations for a combustion system with
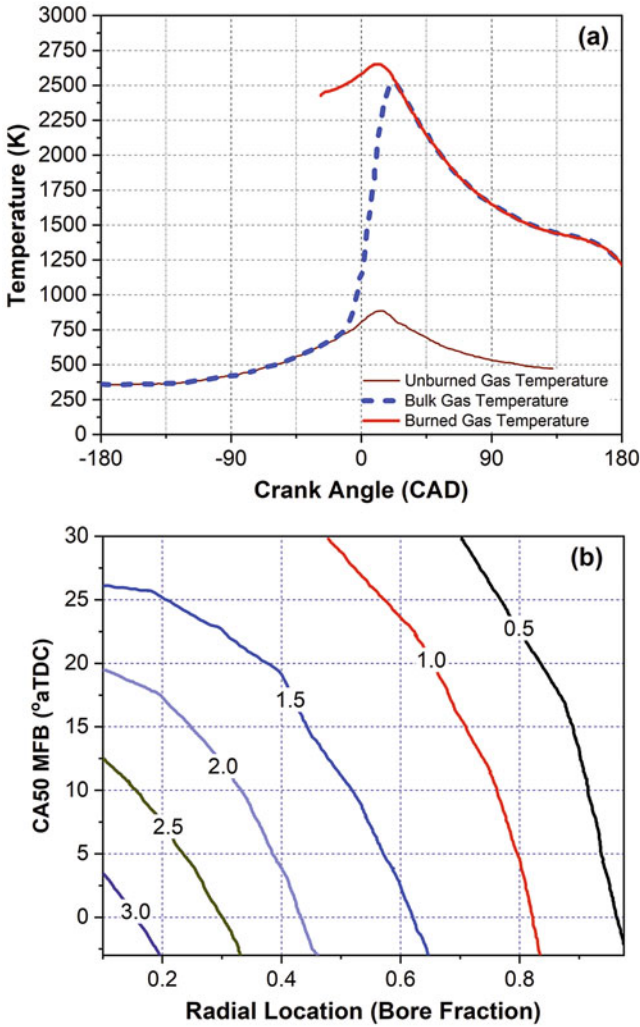
Fig. 2.37 (**a**) Typical burned and unburned gas temperatures as a function of crank position and (**b**) critical volume ratio as a function of transducer radial location and combustion phasing (Adapted from [33])

a centrally located ignition source. The figure depicts that the smaller radial location bore fraction (i.e., sensor is closer to the ignition source) requires the larger critical volume ratio. As the sensor location gets near to the bore wall/end-gas region, the critical volume ratio approaches zero. The critical volume ratio also depends on combustion phasing. A higher critical volume ratio is required for advancing combustion phasing due to higher peak pressure and a larger pressure ratio for a particular radial position of the sensor. A more complete discussion can be found in the original study [33].

Fig. 2.38 Change in compression ratio as a function of the dead volume of measuring bore (Adapted from and courtesy of Kistler)
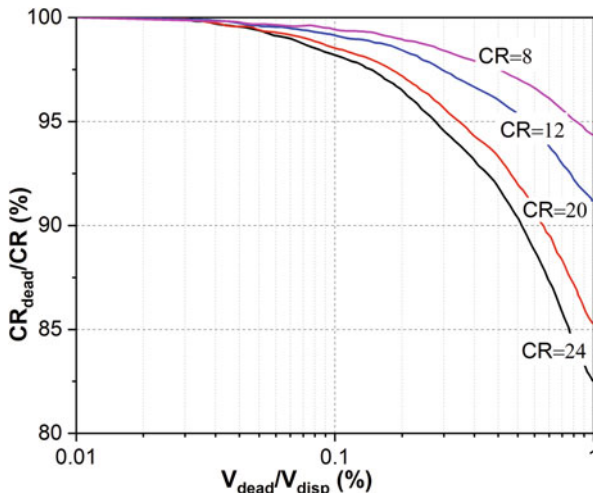
The recessed or inclined mounting of pressure sensor increases the compressed volume of the engine. The dead volume (V_{dead}) of the measuring bore reduces the engine compression ratio (CR). The reduced compression ratio (CR_{dead}) can be calculated by Eq. (2.14) [18].

$$CR_{dead} = \frac{V_c + V_{dead} + V_{disp}}{V_c + V_{dead}} \qquad (2.14)$$

where V_c is clearance volume, V_{disp} is displacement volume, and V_{dead} is the dead volume of measuring bore.

Figure 2.38 depicts the change in engine compression ratio as a function of the dead volume of measuring bore. The change in compression ratio is higher for smaller displacement volume and higher compression ratio engines. For a typical measuring bore (Fig. 2.35c) having a dead volume of 60 mm³, the change in compression ratio is 0.064 for a half liter engine with an original compression ratio of 24. This change can be significant if the cylindrical bore of 8 mm is formed (Fig. 2.35c) and not recessed as original measuring bore. The measuring bore volume is quadrupled and change in compression ratio 0.289. This change in compression ratio is substantial, which need to be taken care off.

There are special criteria for mounting position of pressure sensors in spark ignition and compression ignition engines. In spark ignition engines, the measurement of engine knock modes depends on the position of the pressure sensor. Centrally mounted pressure sensors typically provide the most representative data for knock analysis. Pressure sensor installed near cylinder walls records different knock amplitudes depending on their position relative to exothermic center during knocking. The high-frequency pressure waves reflected from cylinder wall can cause a surge wave, and high amplitude can be recorded by the sensor installed near the cylinder wall [18]. However, depending on the knock detection algorithm, the
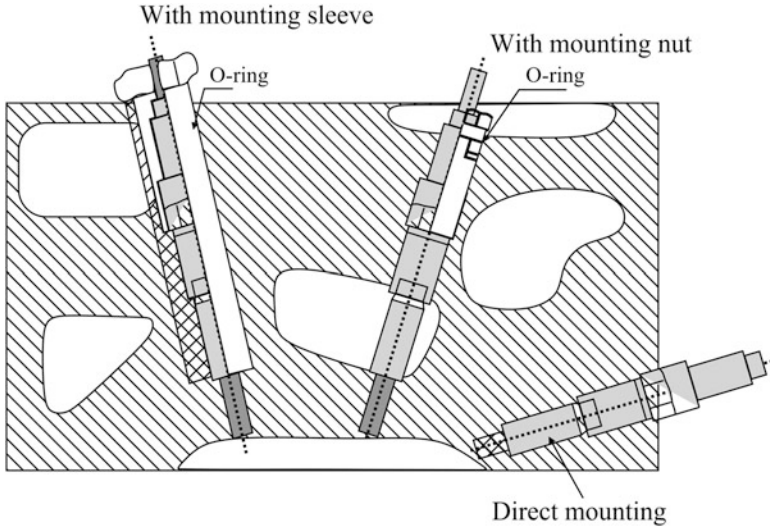
Fig. 2.39 Intrusive pressure sensor mounting examples (Courtesy of Kistler)

central position may not be preferred. Central mounting position may not reliably detect the first fundamental knock oscillation mode depending on combustion chamber shape.

In case of direct injection diesel engines, the sensor can be mounted either in the vicinity of squish clearance or over the piston bowl. Sensors over the bowl indicate the pressure without any delay. In this case, the pressure sensor will also expose to higher thermal load, which can be reduced by recessed mounting. Sensors mounted in the squish area can produce distorted pressure readings due to gas dynamics generated by the motion of the piston around TDC [15, 18]. However, thermal loading is reduced, and for monitoring applications, this position is ideal.

Considering all the factors discussed in this section, different intrusive mounting styles can be selected depending on the mounting location and space available. Figure 2.39 illustrates the different mounting example of an uncooled pressure sensor installed in the engine head. The installation of the pressure sensor can be done by using adapter mounting or direct mounting as illustrated in Fig. 2.39.

2.2.5.2   Nonintrusive Mounting

Cylinder pressure measurement in the modern engine can be possible without intervention (nonintrusive mounting) in the engine head. The nonintrusive mounting of the pressure sensor is possible with existing bores (for a spark plug or glow plug) in the engine head. With the development of piezoelectric crystal technology, it is possible to design miniature uncooled pressure sensor that can be accommodated in adapters which can fit in the space of standard engine components such as glow plug or spark plug. This method of installation of pressure sensor reduces the adaptation

Year	1968	1989	1991	2001	2003
Type	6511	6517	6117	6115	6113
Thread	M14x1,25	M14x1,25	M14x1,25	M12x1,25	M10x1,00
Sensitivity	16 pC/bar	20 pC/bar	15 pC/bar	10 pC/bar	10 pC/bar
Acoust. Reson.	2 kHz	7 kHz	55 kHz	>60 kHz	>60 kHz
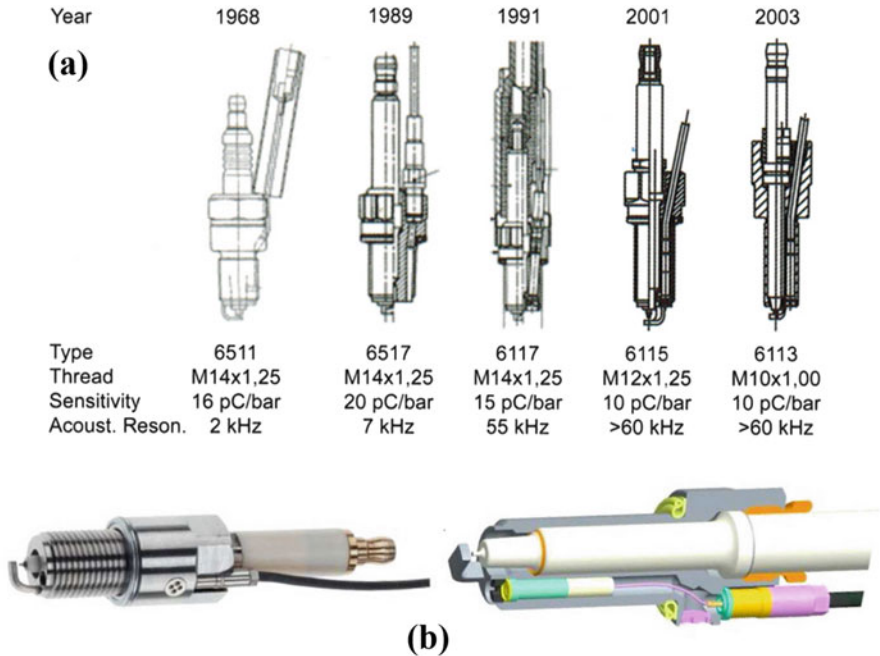
Fig. 2.40 (**a**) Stages of development of measuring spark plug and (**b**) structure of the measuring spark plug (Courtesy of Kistler)

time and cost. However, there is no choice of the installation position of a pressure sensor in the combustion chamber with nonintrusive mounting. The present measuring spark plug is able to match the combustion characteristics identical to the reference sensor (cooled sensor) [34]. The study suggested the following criteria to be considered for measuring spark plug: (1) measuring spark plugs can be installed very easily (i.e., no need of additional measuring bore); (2) turbocharged engines require high ignition voltage up to 40 kV, and thus, the gap of electrodes is very important to avoid misfire; and (3) engines with direct injection are sensitive to the spark position.

Figure 2.40 shows the stages of development of measuring spark plug and a typical structure of modern measuring spark plug. Historically, the measuring spark plugs were conversions of standard spark plugs, and pressure sensors are included using an adapted long and thin passages. This type of conversion required significantly more space in the plug shaft and had the disadvantage of very clear pipe oscillations occurring due to the longer distance between the sensor diaphragm and the combustion chamber. In this arrangement of the pressure sensor, the cyclic thermal drift is very low due to lower thermal load. Additionally, the spark plug remained largely unchanged, and the spark function was thus identical to that of the original spark plug. To prevent the pipe oscillations, there is need to bring the transducer diaphragm close to the combustion chamber. Development of compact

sensors allows flush mounting of the pressure sensor in measuring spark plug (Fig. 2.40b). This arrangement avoids the pipe oscillations with less deterioration in the spark function due to the changed position of the spark distance as well as the maximum possible ignition voltage [34]. The measuring spark plug must be designed to be as close as possible to the original equipment with respect to heat range and position of the electrical arc (spark position is taken to mean the position of the electrode in with respect to the plug face). The displacement of spark position can have a deteriorating effect on the ignition quality particularly in gasoline direct injection (GDI) engines. In GDI engines, the stratified mixture needs to be ignited in the area where the mixture strength is sufficiently rich to initiate combustion. Thus, spark position is more critical in this type of combustion process.

An additional technical requirement related to sensor working environment other than heat range is a separation of high electrical voltage. The spark plug adaptor must separate the high voltage and charge signal, preventing cross-talk and interference of the signals. Additionally, it need to maintain the required level of insulation resistance to ensure no leakage of the high-voltage spark that could cause a misfire, even under the most extreme engine operating conditions [15].

Glow plug adaptors are the nonintrusive access technique for cylinder pressure measurement in compression ignition engines. Typically, most compression ignition engines are equipped with preheating probes (glow plugs) to preheat the cylinder gases, particularly during cold start conditions. For cylinder pressure measurement in diesel engines, glow plug can be removed and replaced with a measuring glow plug (Fig. 2.41) or glow plug adaptor (Fig. 2.42) which contains a suitable, uncooled miniature pressure transducer. The measuring glow plug or glow plug adapters are screwed into the mounting bore of the original glow plug and do not require separate measuring bore. Figure 2.41 presents the section view of measuring glow plug. The figure shows that a measuring probe with particularly small mounting and connection dimensions is screwed in a specially designed glow plug. The heating coil at the end of measuring glow plug necessitates an indication passage between the combustion chamber and measuring probe [18]. The arrangement can result in pipe oscillations, and it limits the frequency range for pressure measurement with good signal quality. The measuring glow plug is suitable for cylinder pressure measurement without dispense with functional glow plugs. The
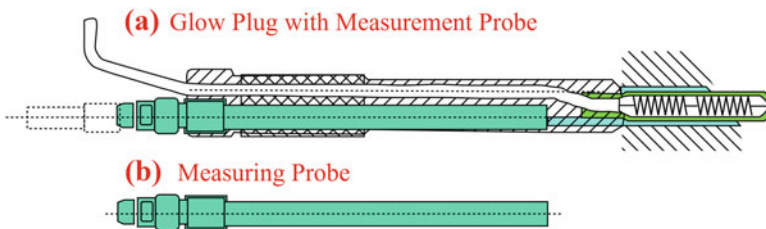
Fig. 2.41 Measuring glow plug with a miniature measuring probe for cylinder pressure measurement (Courtesy of Kistler)
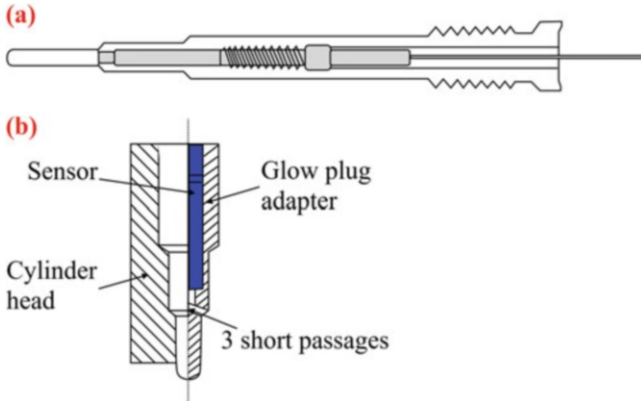
Fig. 2.42 Glow plug adapter with a miniature transducer for cylinder pressure measurement (Adapted from and courtesy of Kistler)

measuring glow plug is beneficial for cold start test without separate indicating bores, on-road measurement applications with glow function, and combustion diagnostics with lower speed and load range (as combustion temperature is lower) with glow function.

Glow plug adapters are also used for the cylinder pressure measurement test, where the engine can be readily started without original glow plugs. Figure 2.42 shows a glow plug adapter for the pressure measurement in a diesel engine. An adapter fitted with a miniature pressure sensor can be mounted on the place of the original glow plug. The cylinder pressure sensor mounted in glow plug adapter is connected to the combustion chamber through several short passages (Fig. 2.42b). The advantages of this arrangement are (1) simplest method of mounting with additional measuring bore in the engine head, (2) design conforming to specified glow plug bore, and (3) high signal quality ensured by measurement close to combustion chamber [18].

Typically different mounting positions are chosen depending on the applications. Some applications (such as engine peak pressure monitoring for continuous operation) requires the selection of the durable measuring system. In such applications, the advantageous mounting position of the sensor (for low thermal load) and high level of robustness of sensor is required. Recessed position of sensor ensures long service life due to lower thermal load exposure with glow plug adapter. Figure 2.43 shows the two different arrangements of pressure sensor mounting in glow plug adapter. The larger recessed position mounting (Fig. 2.43b) has a longer life due to lower thermal load, but it can have the pipe oscillations, which restrict the measurement frequency. Thus, based on the application and measuring requirement, the suitable mounting position of the sensor can be selected in the glow plug adapter.
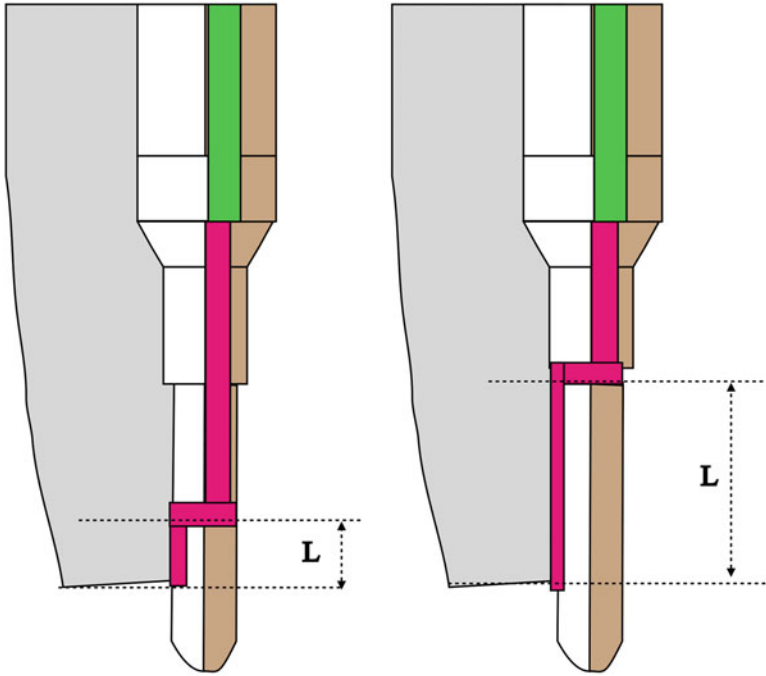
Fig. 2.43 Typical position of a miniature pressure sensor in glow plug adapter for development work

2.2.6 Transducer Selection

The cylinder pressure measurement is used for different tasks such as thermodynamic analysis, noise estimation, calibration, and monitoring of engine. During cylinder pressure measurement, the engine is also operated at different conditions such as knocking, cold start, misfire, etc., which affect the working environment of the pressure sensor. For the particular measurement, the selection of the correct type of transducer and the installation environment is a crucial task for the desired quality of pressure data. Performance of pressure sensor can be maximized with respect to measurement quality and reliability by appropriate selection of sensor and mounting position and type. The final choice will be a compromise among factors and boundary conditions that include (1) measurement task, target, and focus, (2) installation location, (3) installation space, (4) access pathways into the cylinder, (5) cost of sensor and installation, (6) installation effort and time, and (7) permanency of the installation [15]. The measurement task/objective has a significant role on the choice of the transducer. Presently, a wide variety of transducers are available, and many of them can be used for a particular application.

Figure 2.44 shows the relationship between the measuring application, the transducer choice, and the installation method. The measurement task defines the
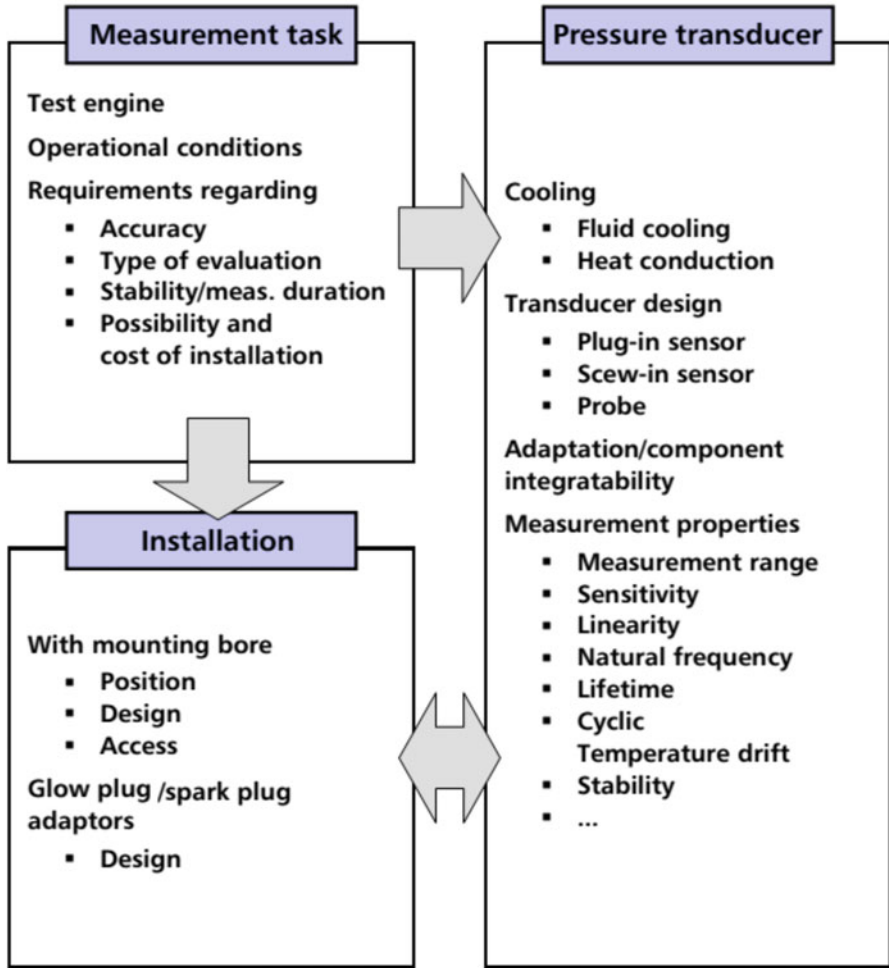
Fig. 2.44 Relationship between measurement tasks, the transducer, and the installation site (Courtesy of AVL)

operational conditions of the engine and the sensor. The measurement application also specifies the requirements regarding accuracy, stability, measurement duration, installation costs, etc., which governs the type/design of sensor to be used and its installation methods (Fig. 2.44). For the maximum accuracy of sensors, specifications of thermal shock value (Δp, ΔIMEP), linearity, and sensitivity are important parameters. The thermal shock specifications are important if the friction loss or gas exchange work is evaluated from firing engine. Pressure sensor must have high sensitivity in order to be able to effectively resolve the relatively small pressure differences (particularly during gas exchange). For the accuracy of data, the sensitivity of sensor needs to be high. The lower-sensitivity sensor requires a higher gain

Type of evaluation (measurement task)

Pressure transducer property	*	**	***	****	*****
Measurement range	W	W	W	W	W
Lifetime (cycles)	W	W	W	W	W
Sensitivity	C	W	C	C	C
Linearity	Significant	W	No effect	Significant	Significant
Natural frequency	W	W	W	Significant	Significant
Acceleration sensitivity	C	W	C	C	Significant
Shock resistance	W	W	W	W	W
Temperature resistance (transducer)	W	W	W	W	W
Change in sensitivity over temperature	C	No effect	C	C	C
Cyclic temperature drift (heat flow pulse)	Significant	W	No effect	Substantial	Significant
Zero-line gradient (Load/Heat flow change)	Significant	W	No effect	Substantial	No effect
Zero point deviation (load change)	No effect	No effect	No effect	No effect	No effect
IMEP stability (in continuous operation)	Significant	No effect	No effect	Significant	Significant
Deformation (Installation)	Significant	No effect	No effect	Significant	Significant
Indicating channel (Installation)	No effect	W	Significant	Significant	Significant
Gas flow (Installation)	Significant	W	W	Significant	Significant

Key

* Maximum, minimum amplitude (cycle)
** Qualitative curve before and after TDC
*** Frequency, amplitude of high frequency oscillation
**** Integral values (energy conversion, mean)
***** Different. Values (heat release, dp/dα)

- No effect
- W Warning!
- C Calculable effect
- Significant effect
- Substantial effect

Fig. 2.45 Effect of transducer installation and properties on the measured signal (Courtesy of AVL)

of the amplifier, where noise will also get amplified. Thus, signal quality gets affected.

For thermodynamic analysis, accurate determination of TDC and specification of thermal shock (Δp, ΔIMEP) are important for the pressure sensor. Recommended limit values are 0.5 bar for Δp and $\pm 2\%$ for ΔIMEP [18]. Figure 2.45 presents the summary of the effect of transducer installation and properties on the measured pressure signal and its analysis. The figure shows an evaluation of the metrological properties of pressure transducers and how their measuring position influences the measurement task, which helps in the selection of pressure sensor by looking at the datasheet of a sensor provided by the manufacturer. Thermal drift (short term and long term) has a substantial effect on the evaluation of combustion parameters that are evaluated by integral of measured pressure signal (Fig. 2.45). The other important variables are linearity, sensitivity, IMEP stability, and installation parameter, which affect the quality of measurement and analysis results.

Figure 2.46 presents a simple flowchart for the selection of pressure transducer to be used for engine combustion measurement. After defining the basic requirement of measurement task such as accuracy, stability, cost, etc., the major decision is required whether sensor installation is intrusive or nonintrusive. In case of
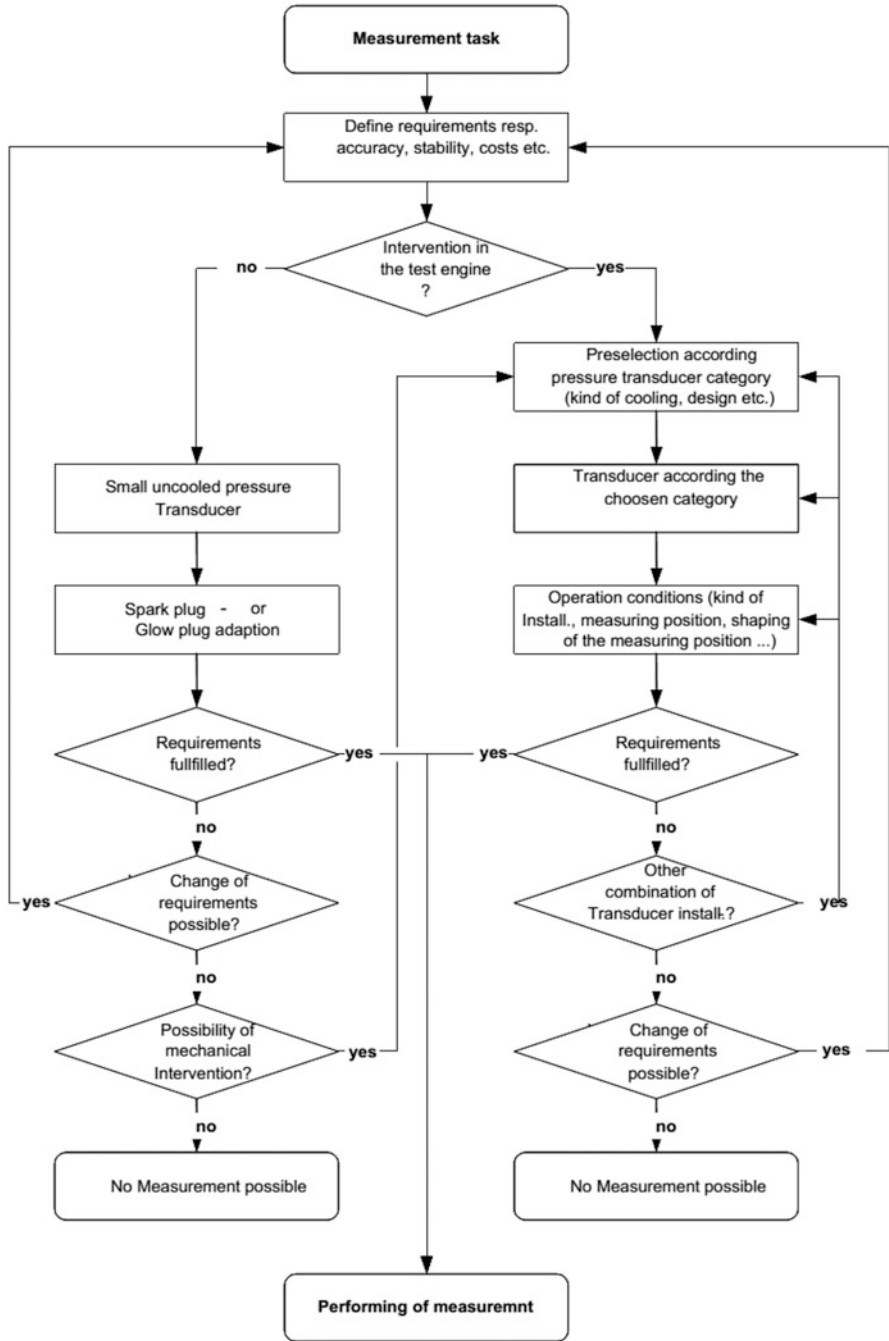
Fig. 2.46 Flowchart for pressure transducer selection for cylinder pressure measurement (Courtesy of AVL)

nonintrusive installation, the miniature uncooled pressure sensor is typically selected and mounted in glow plug or spark plug adapters depending on the engine. With intrusive installation, there is the choice of installation position. The design of pressure sensor is also affected by the available space for mounting and working environment of the sensor during an engine test. The information about the extent of the effects and the metrological properties of the selected transducer should be used to check whether the requirements can be fulfilled and, if so, the measurement can be started.

2.3 Alternatives to Piezoelectric Pressure Transducer

Typically, an ideal transducer for cylinder pressure measurement should have the following features: (1) high sensitivity, accuracy, and linearity; (2) absolute pressure measurement; (3) small size; (4) high natural frequency; (5) stable properties, irrespective of temperature, heat flow, and deformation; and (6) minimal number of components and interfaces in the measurement chain [15]. Presently, there is no single transducer or technology which fulfills all these requirements for all applications. Piezoelectric transducers are most commonly used for combustion pressure measurement in reciprocating engines, which is discussed in Sects. 2.1 and 2.2 in detail. Cost-effectiveness and demand for real-time pressure monitoring on production engines govern the development of alternative sensing technology. Several alternatives of the piezoelectric sensor are investigated over a long period for determination of combustion parameters such as ion current sensor [35–49], optical sensors [49–53], strain gauge-based sensor [54], piezoresistive sensor [17], angular speed [55], etc. Some of the important alternatives are briefly discussed in the following subsections.

2.3.1 Ion Current Sensor

The most practical realization of an ion current sensor is by use of the spark plug particularly in spark ignition (SI) engines. Using the ionization current method in conjunction with the spark plug is an alternative to the cylinder pressure sensor measurement. The ionization current contains information about the combustion process, and it reflects many parameters of the combustion process. The main challenge is to determine the ionization current properties that are useful for electronic engine control and how to extract them [41]. The combustion of fuel inside the engine cylinder produces ions and free electrons. A current can be generated (by applying electric field) and detected by locating two electrodes in the combustion chamber and applying a low DC potential difference between them. The benefit with ionization currents is the possibility of using a conventional spark plug as a sensor. The ignition system must only be slightly modified to allow electrode polarization
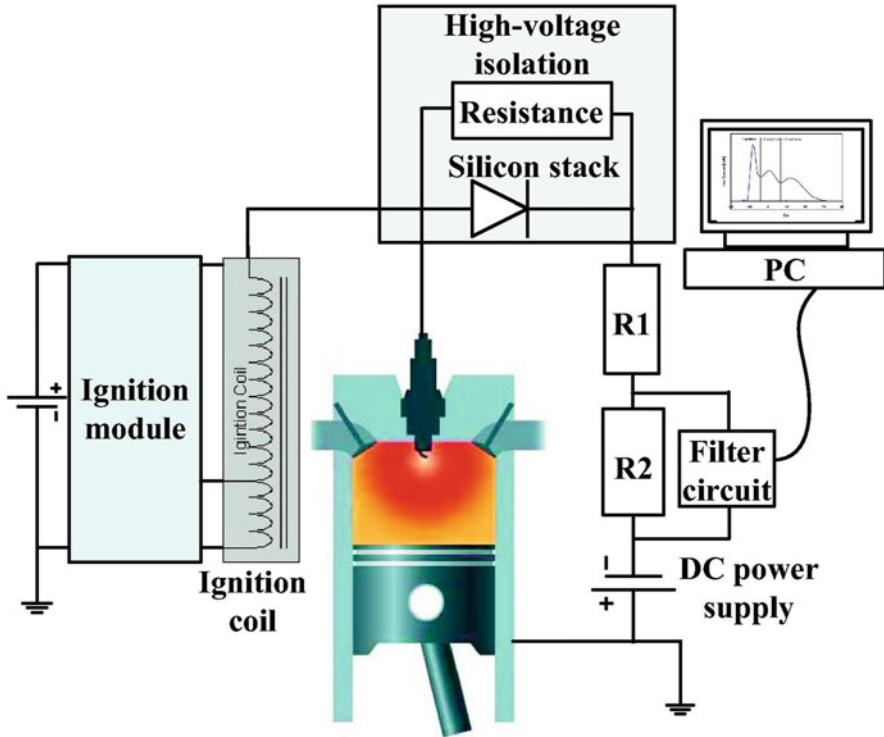
Fig. 2.47 Schematic diagram of ion current measurement setup on a reciprocating engine [35]

and current measurement. Figure 2.47 presents a schematic diagram of typical ion current measurement setup in an engine. In this arrangement, the spark plug acts as an ion current sensor (Fig. 2.47). The central electrode of the spark plug is used as the positive bias for the measurement of the ion signal produced in the cylinder. A bias voltage of 237 V across the spark plug electrode and a resistance of 241 kΩ are applied to obtain high strength ion signals. The ion current signal is acquired by dividing the 241 kΩ into the voltage drop across the resistor [35]. The ion current signal from spark plug has typically three main phases as depicted in Fig. 2.48. The first phase is called ignition phase, which initiates with the coil loading and finishes at the end of the spark. The flame front phase (second phase) appears during the displacement of the flame front in the spark plug electrode, and the post-flame phase (third phase) reveals the burnt gases behind the flame front [36]. The peak of the curve in the flame front phase is related to the combustion process in the flame kernel. It depends on the front flame propagation and ion probe position within the cylinder. The post-flame phase is related to the thermodynamic conditions in the burned gas. The ionization during this phase is due to the high temperature inside the engine combustion chamber. It is generally assumed that the dominating source for the formation of free electrons and the positives ions during post-flame phase is nitric oxide (NO) [39].
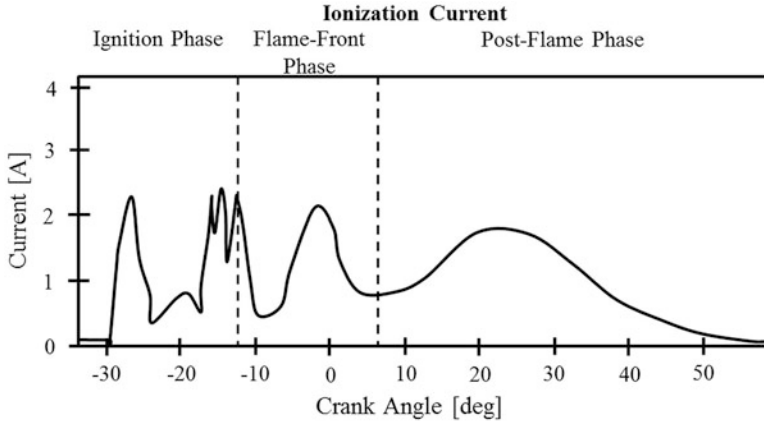
Fig. 2.48 Typical ion current curve with its three characteristic phases [36]

The investigation of ion species responsible for producing the ion current has been conducted [39]. The following chemi-ionization formation and recombination reactions are mainly responsible for ion current during combustion of hydrocarbon fuel. The ion formation reactions are presented as R1 to R3.

$$CH + O \rightarrow CHO^+ + e^- \tag{R1}$$

$$CHO^+ + H_2O \rightarrow CO + H_3O^+ \tag{R2}$$

$$CHO^+ + NO \rightarrow NO^+ + HCO \tag{R3}$$

The initiation of ion formation by CH radical (R1) has been experimentally established on a gasoline engine [42], and no ion current was detected for engine operation on hydrogen. The reaction (R1) is slow compared to the charge transfer reactions (R2) and (R3). The reaction (R2) is dominant in lean and slightly rich hydrocarbon-air flames and produces H_3O^+ ions. In rich and sooty hydrocarbon-air flames, reaction (R4) is dominant and produces $C_3H_3^+$ ions.

$$CH^+ + C_2H_2 \rightarrow C_3H_3^+ + e^- \tag{R4}$$
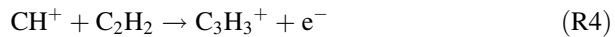
In sooty flames, charge transfer may occur between small ions such as $C_3H_3^+$ and H_3O^+ and large polynuclear aromatic hydrocarbons. The ionization potential of these large molecules is small enough so that the charge transfer is thermodynamically favorable [39]. In another study, the reactions of formation of positive ions of $C_2H_3O^+$, CH_3^+, and $C_3H_3^+$ are found in hydrocarbon flames along with H_3O^+ and CHO^+ [43]. By comparing the concentration and the mobility of these ions, the hydronium ion (H_3O^+) is recognized as the main source for producing the ion current signal during combustion measurement [37]. In addition, negative ions can be

formed and contribute to the ion current. The ion recombination reactions are presented by reaction (R5).

$$H_3O^+ + e \rightarrow 2H + OH \tag{R5}$$

During post-flame period, thermal ionization takes places. The formation of ions at high temperatures in close to stoichiometric hydrocarbon-air flames is mainly by the reaction (R6). The destruction of NO$^+$ ions is by reaction (R7). In fuel-rich hydrocarbon-air flames, a fraction of the large hydrocarbon molecules and soot particles, both presented by R, can be ionized directly by reaction (R8) [39].

$$NO + M \rightarrow NO^+ + e + M \tag{R6}$$

$$NO^+ + e \rightarrow N + O \tag{R7}$$

$$R \rightarrow R^+ + e \tag{R8}$$

The fuel properties and engine operating conditions also affect the ion current signal. Typically, local information is obtained using the ion current method, but local measurement can be sufficient when the charge is homogeneous [10]. - Figure 2.49 depicts the numerically predicted distribution of hydronium (H_3O^+) ion in homogeneous charge compression ignition (HCCI) combustion chamber. In this case, the charge is prepared using double fuel injection, and injection ratio (Inj_{ratio}) of fuel injected in both injection events is varied. The figure shows the ion distribution for two injection ratios, and in the injection ratio 0.2, higher quantity fuel is injected during the compression stroke. For CA10 (crank angle corresponding to 10% heat release) position, the ion concentration is more heterogeneous for injection

Fig. 2.49 In-cylinder H_3O^+ ion distribution under different injection ratio conditions in HCCI combustion [37]
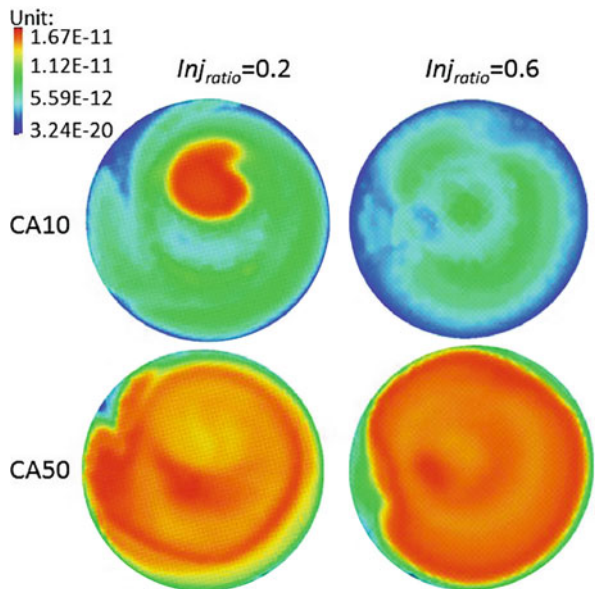
ratio 0.2 in comparison to injection ratio 0.6 (more premixed case). At the CA50 position, the ion concentration is distributed significantly for both operating conditions (Fig. 2.49). The numerically obtained data are in good agreement with the signal amplitude variation experimental engines. Therefore, ion-sensing system can be optimized by this tool [37] for better prediction of combustion parameters for effective combustion control and diagnostics of the engine.

The often cited advantages of ion sensing are that no additional sensor and no additional bore are required on engine head. No additional sensor requirement advantages are negated to some extent by the practical difficulty of packaging the current sensing registers since the ignition system itself has to be modified. The main disadvantage of the ion current sensor is that it measures local properties of the combustion products, rather than the global properties of the combustion gases in the entire cylinder [39, 41]. Additionally, both the ion current shape and magnitude depend on the (1) design of the sensor, (2) its location in the combustion chamber, and many (3) engine operating parameters such as A/F ratio, speed, load, and EGR. Since these parameters vary from one engine to another, strategies developed for one engine cannot be used for other engines particularly if the strategies are based on absolute values [41]. Another demerit of the ion current sensors is their inability to detect small cylinder-to-cylinder variations in multicylinder engines (particularly when the engine is operated with EGR) [39].

Ion current sensors appear to be quite resilient to electrode soiling. However, caution should be exercised since any electrically conducting deposits will permit current leakage. Operation of the spark plug is, on occasion, also compromised by fouling. Current leakage measurement shows that plug fouling by soot and/or water condensation takes place following a cold start [7]. The ion current signal typically appears in three parts (the interference of the ignition energy of the charge, interference of the spark plug ignition energy release, and combustion-related ion current) due to the inability to isolate the signal interference caused by ignition (Fig. 2.50). Sometimes a third peak also appears (Fig. 2.50), which is also created by spark plug ignition energy release. This is discovered by the nonidealities of components in the circuit that can be optimized by using more ideal components. The effective ion current signal from the combustion-related part can be used for combustion analysis. Figure 2.50 also depicts that the ion current signal strength is quite low during misfire condition relative to normal combustion conditions. However, the signal can be used for determination of engine combustion by careful calibration and validation [38].

The ion current sensing spark plug frequently serves as both sensor and igniter; this double duty is purely for convenience. It is not essential, and, where appropriate, the igniter function can be discarded, or an additional electrode can be provided in spark plug purely for ion sensing. Figure 2.51 shows the different methods for ion current sensing in reciprocating engines. The figure shows that ion current can be measured either by stand-alone ionization sensor or use the standard spark plugs. The spark plug can either have the dual function of sensor and igniter or additional electrode for ion current sensing. Using spark plug as a sensor, the position of sensing is fixed, while with stand-alone ionization sensor, the sensing position in the combustion chamber can be selected/defined by the user.
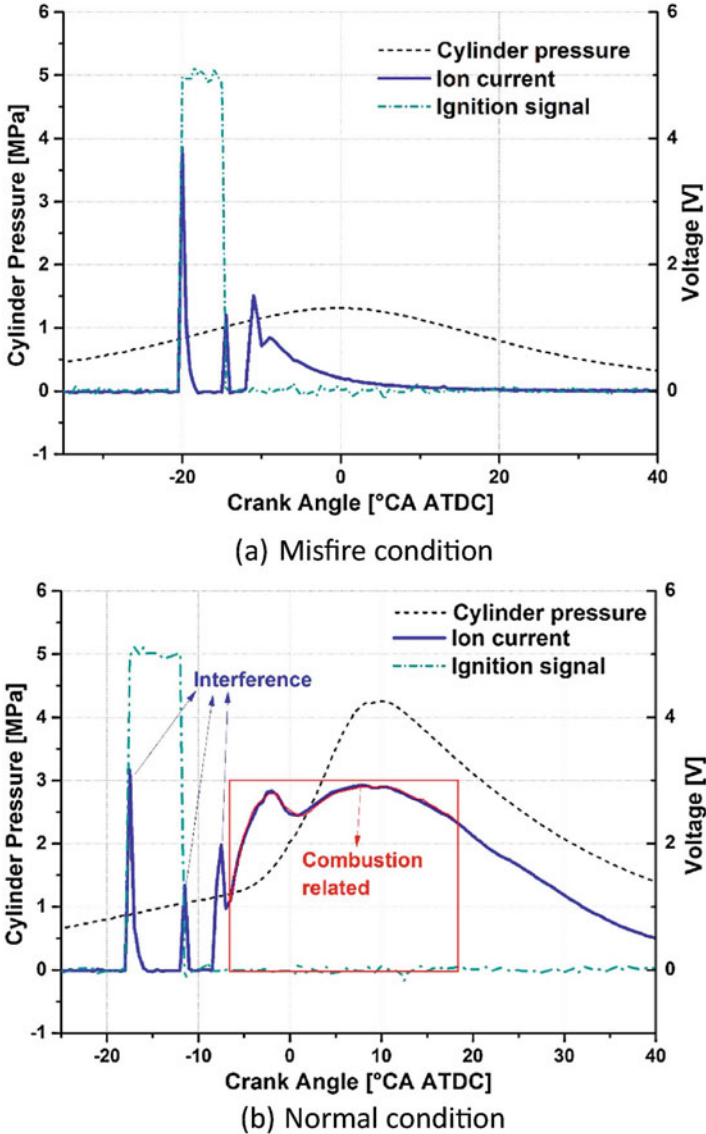
Fig. 2.50 Typical ion current signal in misfire and normal operating conditions in spark ignition engine [38]

Ion current sensing based on the conventional spark plug has certain additional limitations. For example, the electrode is optimized for spark discharge, rather than ion current measurement. The ion current measurement is limited to a single spatial location unless more sensors are installed. Moreover, the ion current signal is affected by the spark current during the sparking event. Use of a multielectrode spark plug which has three independent central electrodes is proposed to address
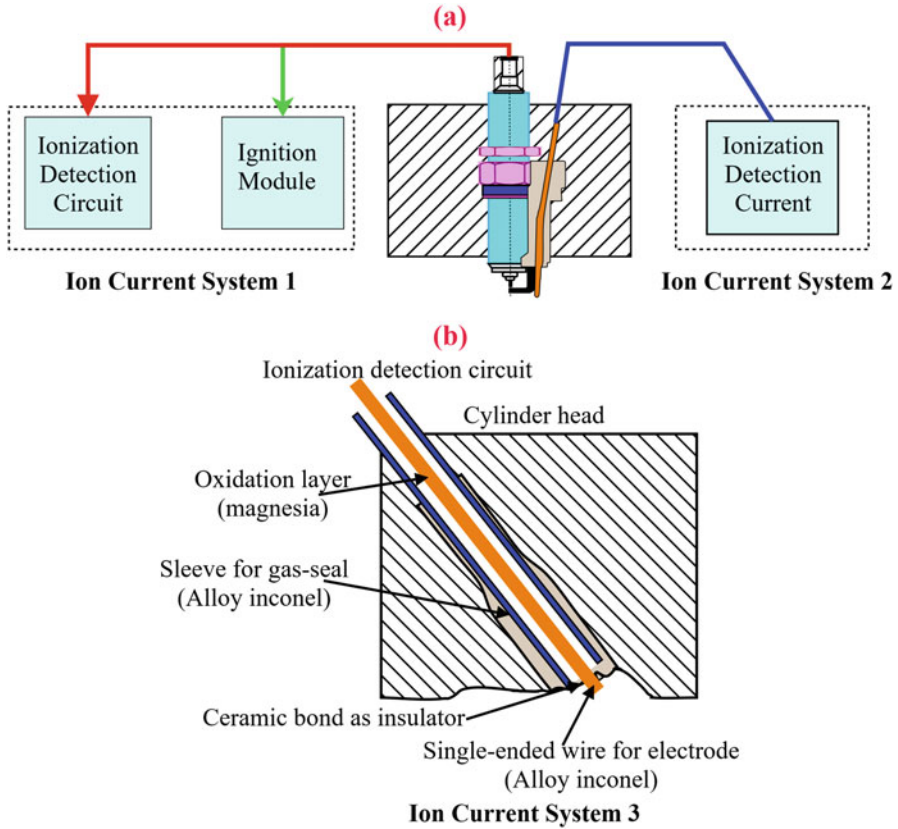
Fig. 2.51 Different methods of ion current sensing (Adapted from [41, 44])

some of the limitations of conventional spark plug [40]. Two of the electrodes are dedicated for ion current measurement, while the third electrode is used for spark discharge. Compared to the conventional spark plug, the ion signal COV of CA5 and CA50 for the multielectrode plug is a closer match to the overall trend and magnitude determined from the cylinder pressure signal. For measuring the combustion quality in the production SI engine, ring shaped gasket ion sensor are also proposed [45].

The ion current signal is normally too weak particularly at low engine speed and lower engine load. The stability of ion current signal under a wide range of engine speed and load should be solved before its industrial application. The ion current signal shape is also dependent on the location of ion current sensor because it provides the local information. Figure 2.52 illustrates the effect of ion current sensor location on the shape of the signal in SI engine. In the ion current measurement with a spark plug or its surrounding, there are two peaks in the signal waveform. It is also reported by several studies that the ion current traces in the gasoline engine have two peaks, under most operating conditions. It is well accepted that the first ion peak is
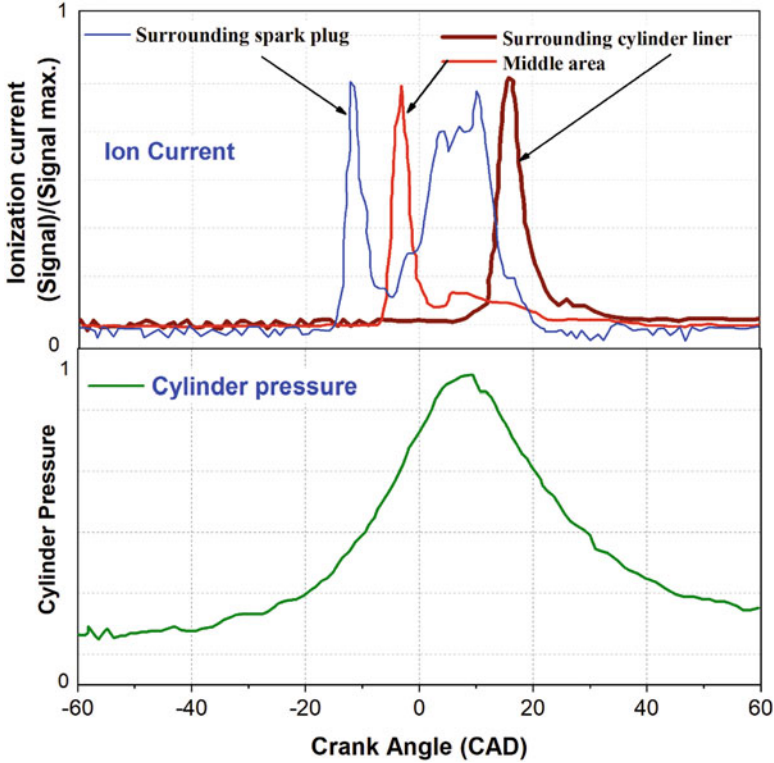
Fig. 2.52 Typical ionization current signal with the location of the sensor (Adapted from [44])

the result of chemi-ionization produced in the reaction zone of the flame kernel that is present in and around the electrode gap at that time. The amplitude of the first peak depends mainly on the equivalence ratio (Φ) of the mixture, which affects the concentration of the ion-producing species (CH and O) and the temperature of the combustion products. The gas temperature also depends on the thermal capacity of the charge immediately after the discharge of the electric spark in addition to Φ. The thermal capacity of the charge depends on its density, composition, and specific heat of its components, all of which depend on the operating variable of the engine, such as throttle valve opening, engine speed, and EGR rate [39]. As the flame front moves away from the spark plug zone, the combination reactions cause the ion current to drop and reach a minimum, after which it increases again toward the second peak. The second peak (post-flame zone) is due to thermal ionization (breaking of N_2) caused by the increase in the temperature of the gases around the spark plug.

In the ion-sensing position away from the spark plug, the two ionization timings (flame front and post-flame zones) are superimposed on each other and not separable (Fig. 2.52). This superimposition is due to the delay added by the front flame propagation. The second peak, mainly related to the cylinder pressure, is unchanged, while the first peak, related to the presence of the flame, is shifted toward the second peak [41]. The remote sensing plug detects the flame front as ion current, caused by

ionization within the gap of its electrodes, yielding this single sharp spike. Under light loads, the second ion current peak disappears, because of low NO^+ concentration. The first ion peak is much higher than the second ion peak and is most suitable for the feedback control of the engine [39].

Figure 2.53 illustrates the ion current traces in HCCI and CI engines. Figure 2.53a shows that the ion current in HCCI engine has only one peak, due to the homogeneity of the charge. It can be used to detect the start of combustion under the different
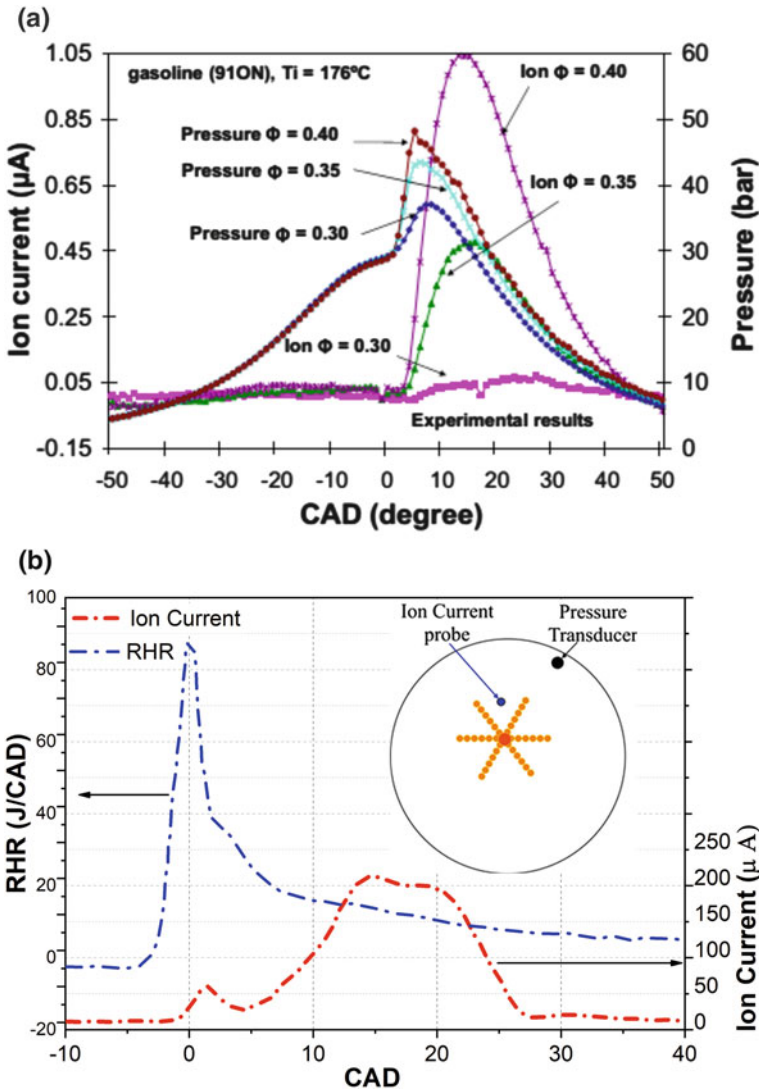
Fig. 2.53 (**a**) Ion current traces in HCCI engine at three equivalence ratios [46] and (**b**) heat release rate and ion current traces in compression ignition engine (Adapted from [39])

engine operating conditions. The strength of ion current also decreases as charge becomes leaner (Fig. 2.53a). Another study [47] also showed that the ion current amplitude is affected by both equivalence ratio and combustion phasing, but the ion current timing is only affected by the combustion phasing in HCCI engine.

Figure 2.53b shows the ion current trace in a diesel engine, which showed four peaks under medium and heavy loads. The possible sources of ionization are explained by considering the shape of the ion current trace, the location of the ion current probe relative to the fuel sprays, and the effect of the swirling motion in the original study [39] that is as follows. The first ion peak follows the peak of the premixed combustion fraction under different speeds and loads. The phase shift between the two peaks depends on the geometry of the ion current probe, its location in the combustion chamber particularly relative to the closest fuel spray, and the spray characteristics. The second ion current peak is caused by the turbulent premixed and diffusion flames carried to the probe by the swirling motion. In addition to gaseous components, these flames carry soot particles that contribute to the ion current. The third peak is due to flames and combustion products reflected on the combustion chamber walls. The fourth peak appears only under heavy loads and is considered to be caused by the third-in-line fuel spray that reaches the ion probe by the swirling motion. The ion current peaks in diesel engines may merge and produce one or more peaks under different probe locations and engine design and operating conditions. A more complete detail can be found in the original study [39].

Ion current sensors have been widely used in SI engines for in-cylinder combustion diagnostics; to determine the flame speed, A/F ratio, and mass fraction burned; to detect knocking, misfire, and partial burn; and to control the combustion stability. The use of ion current sensors in diesel engines has been limited compared to their use in spark ignition and HCCI engines [39]. Ion current sensors are found to be prone to soot deposition in diesel engines, where conducting tracks introduce offset to the signal [48]. The conductivity of soot deposits is not constant and changes during the engine cycle. This may be due to compression of soot by overlying gas. The short circuit can appear and then disappear as soot is re-entrained [7]. Soot particles can themselves carry charge [49], although the implications of this phenomenon for ion current sensing need more investigation.

2.3.2   Optical Sensors

For the study of engine combustion, optical methods are used in two ways. In the first way, luminosity-based sensors are used [50], while in the second way, optical techniques are used for pressure measurement [51]. The present section is focused on measurement of cylinder pressure by optical methods. Optical sensors were developed as an alternative to a piezoelectric sensor for combustion pressure measurement. Figure 2.54 illustrates the typical construction of optic-based pressure sensor. In this technique, the deflection (due to combustion pressure) of a measuring diaphragm is measured using a fiber optic-based method. A light source is used to
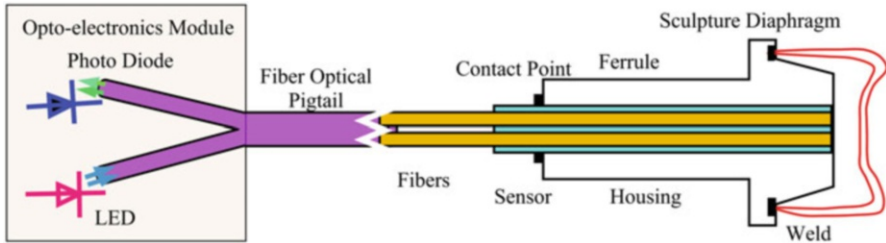
Fig. 2.54   Optical pressure sensor illustration (Adapted from [51])

send light to the metallic diaphragm. The light reflected from the deflected diaphragm is captured via an electronic optical receiver. The optical fiber system is completely enclosed within the transducer body. The output from the transducer is an electrical signal whose magnitude varies as a function of the change in cylinder pressure. For a given diaphragm displacement caused by a pressure change, the sensor response, i.e., sensitivity and linearity, can be adjusted by appropriate selection of optical fiber core diameters and layout [15]. The signal is nonmonotonic since the deflection in the diaphragm changes, not just the total distance traveled by light but also the area of intersection between the incident and received light as projected onto the diaphragm [7]. The optical pressure sensors are reported in various designs [52, 53], measuring the light reflected from a flexing hat-shaped metal diaphragm.

To meet the requirements of high strength at combustion temperatures, the diaphragm shape and material are selected having low creep and fatigue life of well over a hundred million pressure cycles. To minimize the mounting space, the measuring diaphragm should be as small as possible. The smallest sensor available has a diaphragm diameter of approximately 1.7 mm [15]. The full-scale deflection of the diaphragm is 10–15 μm. A critical aspect of the design is the hermetic seal since the reflective properties of diaphragm surface are modified by oxidation [7]. The advantage of the optical pressure-sensing technology is its compact size, which permits easy integration into existing engine installations. Additionally, these sensors are highly immune to the effects of electromagnetic interference produced by the engine's ignition and electrical systems.

2.3.3   Strain Gauges and Indirect Methods

Over the last few decades, advanced engine control systems have been developed that use cylinder pressure signal as the primary feedback variable for closed-loop combustion control. The cylinder pressure sensors have high degrees of accuracy due to direct access to the combustion chamber. However, application of pressure sensor on production vehicle is limited by cost, reliability, and packaging challenges associated with the intrusive mounting of the sensor. The cylinder pressure sensors

operate in the harsh conditions (high temperature and pressure in the cylinder), which strongly limit the lifetime of the sensor. Several alternative sensor types have been proposed to address the cost, durability, and mounting issues of direct access pressure transducers through an indirect cylinder pressure estimation. No access to the combustion chamber is necessary along with the benefit of reduced engine machinery in the indirect cylinder pressure estimation methods. Additionally, cheaper measurement devices can be used, as they do not operate in high pressure and temperature environment. However, numerical modeling is necessary to correlate the measured quantity to the cylinder pressure trend [56]. The alternative indirect sensing-based method includes washer-based load cells under the head bolts, spark plugs, injectors, and head (head gasket or boss), crank angle velocity or torque changes, engine vibration, and acoustic emissions [56, 57]. Among these methods, the crankshaft speed fluctuations can be directly correlated to the in-cylinder pressure by a mathematical relation. This relation is achieved by calculating the equilibrium of the forces acting on the crank mechanism [58]. The other methods (vibrations, acoustic emissions, and forces acting on the head's components) are indeed related to the in-cylinder pressure, but it is very difficult to define a mathematical relation that expresses a direct relationship. In such cases, the pressure trend can be evaluated by using different approaches as frequency response functions (FRF), autoregressive moving average techniques (ARMA), and artificial neural networks (ANN) [56].

A study proposed a system for measuring the in-cylinder pressure using strain gauges by mounting strain gauges on external walls of the cylinder [54]. This strategy takes advantage of the fact that the cylinder block is usually made of aluminum or cast iron, hence metallic materials showing an elastic behavior. Unlike viscoelastic materials, such metallic materials are characterized by a linear relationship between stress and strain that does not depend on time; for this reason, any change in the in-cylinder pressure will cause an instantaneous change in the deformation of the cylinder wall which is not influenced by the time history of the deformation. Thus, by installing the strain gauges on cylinder wall at an appropriate position, combustion pressure information can be obtained. The strain gauge must be positioned near the combustion chamber, in correspondence of TDC. At TDC position of the piston, the component of the inertia forces acting perpendicularly on the internal surface of the cylinder is null because the piston roll is parallel to the cylinder axis. Consequently, the mechanical deformation of the cylinder surface is due only to the combustion pressure and is not influenced by the inertia forces when the piston is at TDC. Considering the high sensitivity of strain gauge to temperature variations, the researchers selected the placement of the sensor on the part of the cylinder wall that is in contact with the coolant flowing in the block. The study showed that it is possible to retrieve both the instant of time in which the maximum pressure occurs and the magnitude of the maximum pressure with high precision from the measurement of the maximum deformation of a strain gauge positioned along the circumferential direction in correspondence of TDC [54].

Another study used a strain washer placed on an engine stud for estimation of cylinder pressure [56]. It was possible to measure the stress due to the pressure

variation into the engine cylinder during the combustion process. To correlate the in-cylinder pressure and the stress signal, a numerical model based on the neural network was developed. The results showed the good agreement between the direct and indirect pressure measurements [56].

The cylinder pressure can also be estimated back by measuring the engine vibrations with an accelerometer placed on the cylinder head or the engine block. The rapid pressure variations in the cylinder transfer part of the combustion energy to the engine block in the form of mechanical vibrations. This strategy of pressure estimation is intrinsically unable to reconstruct low amplitude stresses such as in the compression phase. Additionally, besides to the combustion information, the vibration signal contains also the effects of unwanted vibration sources as piston slap, mechanical unbalances, valves impacts, gear transmissions, and other stochastic forces. However, important excitation forces have their characteristic frequency. Therefore, it can be isolated by curtailing and filtering the signals, and several models are demonstrated to reconstruct the cylinder pressure by vibration measurements such as inverse filtering, time series model, and neural networks [59].

The acoustic emissions produced during the combustion phase can be used to reconstruct the pressure trend. Typically, a microphone is mounted on top of the cylinder block to acquire the acoustic data. During the engine operation, a wide range of noise sources is possible such as combustion, valve clatter, piston slap, turbulent gas flow, and many other fluids and mechanical events. Therefore, it is necessary to isolate the significant features and remove the events not related to the combustion for cylinder pressure estimation. The pressure signal reconstructed from the acoustic emissions is generally more accurate than that obtained from the vibrations because of high signal-to-noise ratio [60].

In-cylinder pressure can also be reconstructed from measured instantaneous crankshaft speed [55]. During engine combustion cycle, the crankshaft speed varies due to the variation of cylinder pressure, which varies the torque acting on the crankshaft and, thus, leads to acceleration. Therefore, it is possible to trace back the in-cylinder pressure by measuring the instantaneous crankshaft speed by phonic wheel or an optical encoder. The instantaneous variation in crankshaft speed depends on a number of cylinders and mean engine operating speed. The instantaneous variations in crankshaft speed decreases with the higher number of cylinders and higher mean engine speed, which limits this strategy of pressure estimation. However, it can be overcome by accurate modeling of the vehicle and the engine mechanism [55, 58].

2.4   Crank Angle Encoder

In modern engines, the cylinder pressure data is recorded using the high-speed data acquisition system. Any signal can be recorded with either internal time clock or external time clock (trigger). The internal time clock of data acquisition system can record the data at a fixed set time interval, which is defined by sampling frequency

provided by the user. However, in external trigger mode, the user defines the points (instants) where data needs to be recorded by giving an external clock pulse. For the cylinder pressure measurement in reciprocating engines, typically external crank angle clock is used. The events occurring in the reciprocating engine are dependent on the crankshaft rotation, which governs the motion of piston and valves, fuel injection timings, spark timings, etc. It should be noted that these events are not dependent on time but depend on the angular position of crankshaft relative to a reference position (TDC or BDC). Since the instantaneous crankshaft speed varies with crank angle position, the time interval for traveling same crank angle duration varies depending on the position of the piston, even in one rotation of the crankshaft. Therefore, it is important to record the data on crank angle basis.

For thermodynamic analysis, precise cylinder volume as a function of crankshaft position is calculated from engine geometry. There is a high requirement for precise crank angle measurement along with obtaining high accuracy cylinder pressure data for combustion analysis. Two commonly used methods for the crank angle measurement are (1) a crank angle encoder and (2) a teethed/slotted wheel. The most accurate method is to use a crank angle encoder as a trigger source to guarantee that each pressure data is recorded at a predefined crank angle position. Although this solution shows high angular accuracy, it cannot be applied in production engine due to the practical and price restrictions and reliability reasons. Therefore, wheel-based solutions are commonly used in production applications [27].

2.4.1 Working Principle and Output Signal

The encoder senses mechanical motion of the shaft and translates this information (position) into useful electrical signals. Shaft encoders are used to determine the location of movable machine members such as crankshaft in the engine for accurate positioning. A rotary encoder is a transducer used for converting rotary motion or position into a series of electronic pulses. Figure 2.55 illustrates the different types of
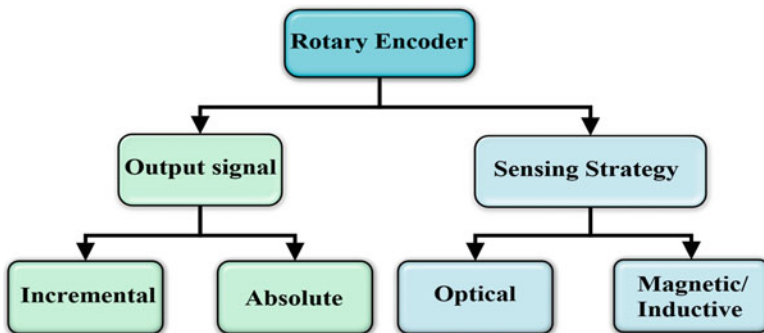
Fig. 2.55 Types of rotary shaft encoders

the rotary encoder based on their output signal and sensing strategy. Based on the output signal, the rotary encoders are of two types, namely, incremental encoders and absolute encoders. The incremental encoder has output as a series of square pulses, from which absolute position cannot be marked. On the basis of sensing strategy, rotary encoders can be divided as an optical encoder and magnetic/inductive encoders. Mostly, an incremental rotary encoder with optical sensing strategy is used for cylinder pressure measurement in reciprocating engines during laboratory tests. However, on production engines, inductive crank angle encoders are typically used.

Figure 2.56 shows the basic principle of incremental optical encoder along with its output signal. The basic components of a rotary encoder consist of light-emitting diodes (LED), a coded disk, and light detectors on the opposite side of the disk as illustrated in Fig. 2.56. The disk is mounted on the rotating crankshaft. Patterns of opaque and transparent sectors are coded into the disk. Incremental encoders work by rotating the coded disk in the path of a light source with the coded disk acting as a shutter to alternately shut off or transmit the light to a photodetector. This generates square wave pulses, which can then be interpreted into position or motion. The resolution of the encoder is same as the number of lines on the coded disk. Since the resolution is "hard coded" on the coded disk, optical encoders are inherently very repeatable and very accurate. There are two main signal outputs from encoder: the
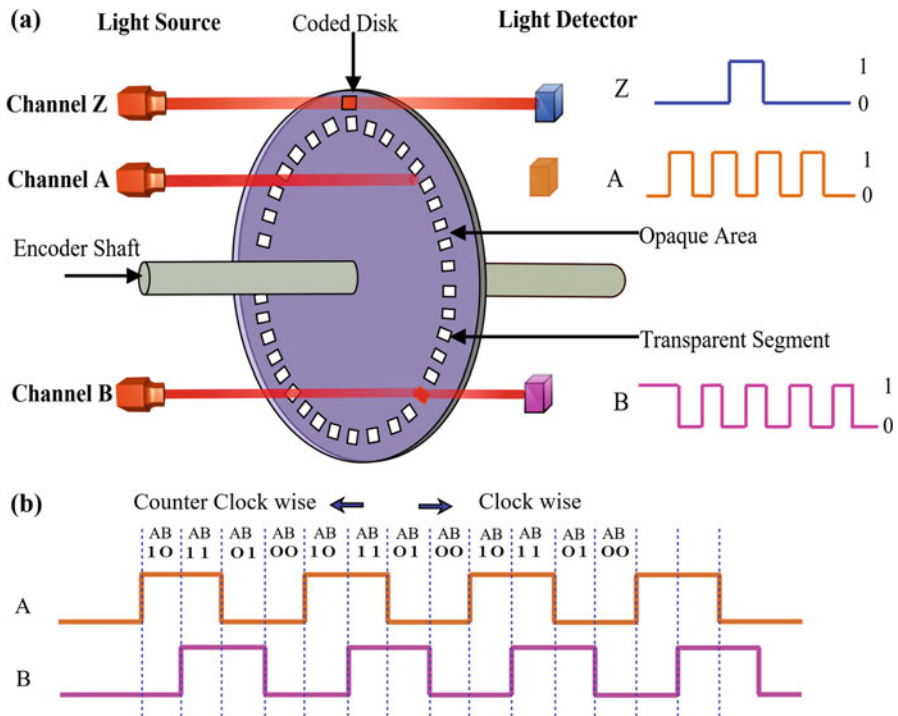
Fig. 2.56 (a) Optical shaft encoder principle and (b) quadrature output signal
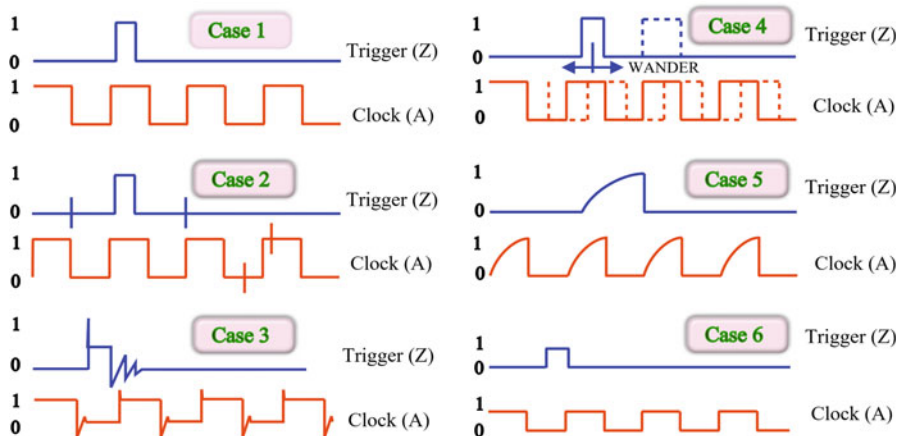
Fig. 2.57 Practically possible encoder signals during measurement (Adapted from [61])

first comprises a train of clock pulses (A or B); the second comprises just a single pulse (Z) per revolution of the crankshaft (Fig. 2.56a). An incremental rotary encoder, also known as a quadrature encoder, has two outputs called quadrature outputs. It consists of two tracks and two sensors whose outputs are called channels A and B. The signals from the A and B channels are a 1/4 cycle out of phase with each other (Fig. 2.56b). As the shaft rotates, pulse trains are generated on these channels at a frequency proportional to the shaft speed, and the phase relationship between the signals yields the direction of rotation. By counting the number of pulses and knowing the resolution of the disk, angular motion can be measured. The A and B channels are used to determine the direction of engine shaft rotation by assessing which channels "leads" the other. Third output channel, known as index (or reference) signal, yields one pulse per revolution, which is used in counting full revolutions and as a reference to define the zero position.

Figure 2.57 shows the different types of encoder signal encountered during cylinder pressure measurement [61]. The encoder signal presented in case 1 is the ideal situation for a good signal. The encoder signal can have noise spikes (case 2 in Fig. 2.57) due to poor signal connections and ground loop noise. The noise spikes can cause a false trigger, or poorly clocked data can be achieved. Ringing in the signal (case 3) can be due to high system inductance. This type of signal can also lead to false clocked data. As presented in case 4, wandering trigger and clock can be obtained due to loose encoder disk or faulty shaft coupling and encoder electrics. Rounding can also appear in signal (case 5) due to excessive system capacitance, which leads to inaccurate trigger and poor repeatability. The lower amplitude of trigger and clock signal (case 6) is typically achieved due to the poor power supply, bad connection, and lower impedance input device. This type of signal also results in improper triggering and clocking [61].

The data acquisition system must always record an engine cycle reference signal along with input from various engine sensors. This signal allows the transducer

voltage to be related to the position of mechanical components of the engine. The cycle reference signal must be obtained from an engine crankshaft sensor. Typically, crank angle encoder produces one pulse (Z signal) in every rotation of encoder disk. However, in a four-stroke engine, the combustion cycle completes in two rotation of the crankshaft. Thus, the distinction is required for reference signal that in which stroke it occurs. Figure 2.58 presents different ways to generate the reference signal for four-stroke cycle. The first method (Fig. 2.58a) is to skip one of the two reference signals using a simple toggle-type flip-flop circuit. The reset switch is operated momentarily to select the desired output while observing the cylinder gas pressure [50].

The second approach (Fig. 2.58b) involves the cylinder gas pressure signal being supplied to a threshold detecting circuit which produces a digital "high" output when
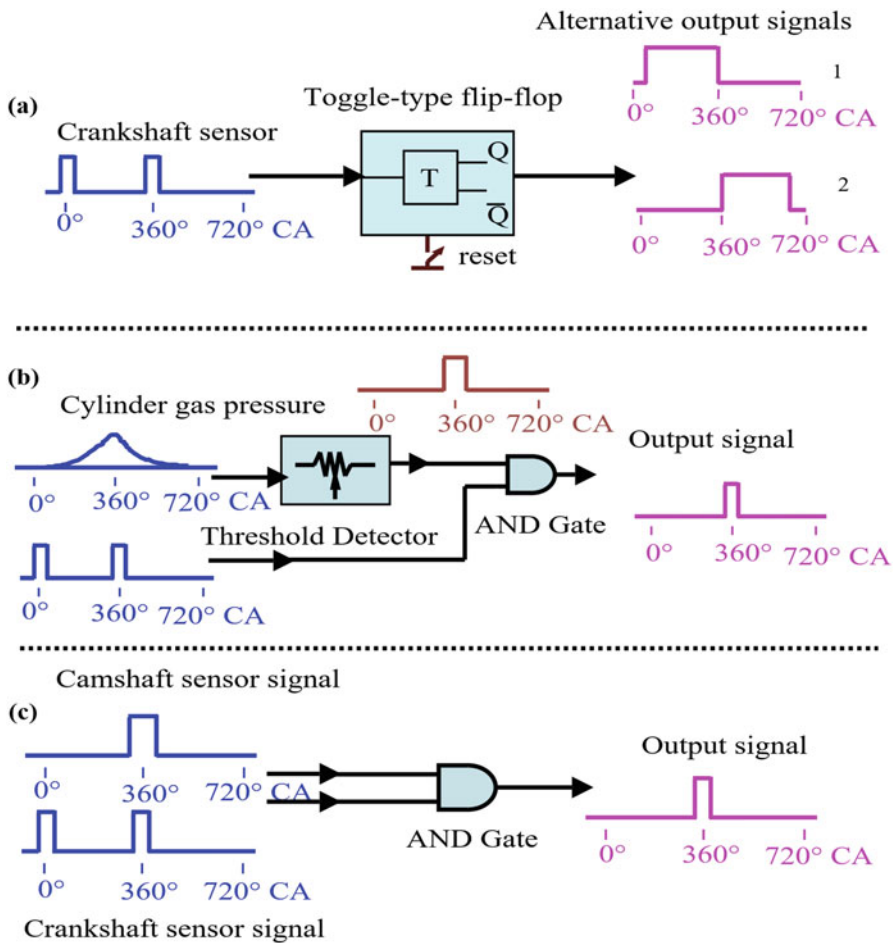
Fig. 2.58 Different methods for creating cycle reference signal (Adapted from [50])

gas pressure exceeds the threshold. The reference signal together with threshold detector output can then form the input of AND gate. This generates a "high" output at the TDC of the engine power revolution only. The third approach (Fig. 2.58c) is a similar strategy, where instead of threshold detector signal, camshaft sensor signal is provided. The cycle reference signal must be set accurately with respect to the position of the piston. The reference signal can also be dynamically set by using a proximity sensor [50].

Several automotive engines use 60-1 or 60-2 encoder wheels (60 teeth but missing 1 or 2 in a row) to create a reference position and control timing events. The signal is typically picked up by Hall effect sensor. Reference position can be determined by observing if the time from the last tooth is more than twice the time of the previous tooth. The wheel having the 60 teeth provides a resolution of 6 crank angle degree, and between the teeth, interpolation is used to find the exact position. Inductive crank angle measurement is one of the most common solutions for production applications because of its reliability, durability, and cost-effectiveness [27]. An inductive sensor consists of a permanent magnet with a ferromagnetic core surrounded by a coil, and it is usually mounted with an air gap to the ferromagnetic teethed or slotted flywheel. When teeth or slots pass through the sensor's magnetic source, the magnetic flow is changed, and an electric analog signal is generated. However, in practice, this system always produces considerable deviation from the actual crank angle position caused by mechanical and operating sources [27].

2.4.2 Resolution Requirement

For combustion pressure measurement and analysis, the crank angle resolution is one of the most important variables that needs to be adequately selected for better estimation of combustion parameter. The crank angle resolution is defined as the crank angle interval at which the pressure data are measured. Increasing the crank angle resolution (short CA interval) has three main advantages: (1) the bandwidth is increased allowing higher cylinder pressure variations to be detected and analyzed; (2) it increases the accuracy of identifying the crank angle position at which a certain absolute, or rate of change of parameter value occurs; and (3) the accuracy of the crank angle phasing (between pressure and volume curve) may be improved (if TDC determination using encoder), depending on the type of data acquisition and analysis system being used [62]. Figure 2.59 illustrates the effect of crank angle resolution on the measured cylinder pressure curve. The figure shows that the higher variations in pressure signal (also in terms of frequency response) can be detected by using higher-resolution crank angle encoder. Thus, higher resolution is preferred for frequency-based combustion analysis, and for lower encoder resolution, some of the frequencies present may not be detected in the pressure signal.

Typically, one of the two (A or B) clock signals from crank angle encoder are used for cylinder pressure measurement. The crank angle resolution defines the clock of data acquisition system. To increase the resolution of measurement, either

Fig. 2.59 Effect of crank
angle encoder resolution on
measured cylinder pressure
(Adapted from [63])
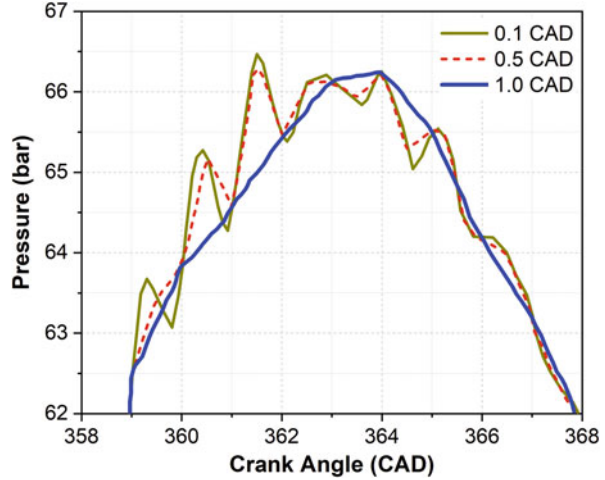
both the clock signals can be used, or angle encoder of higher resolution needs to be selected/used. Figure 2.60 shows the method to increase the resolution of data acquisition system. Three different resolutions of the clock signal (R, 2R, and 4R) can be produced by decoding transitions of A and B by using sequential logic circuits. During acquisition of shaft encoder pulse used as an external trigger, the data can be acquired at different resolutions by selecting the position of data acquisition. When data acquisition is at rising or falling edge of the clock, then it is equal to the original resolution. The resolution of data acquisition is double with the acquisition at both rising and falling edges of the clock. Resolution can be further doubled (4R) by using both A and B signals and data acquisition at both the edges (Fig. 2.60). Higher resolution is required for the engine test conditions such as knocking, where higher data acquisition rate is required to understand the engine combustion phenomenon.

In contrast, increasing the crank angle resolution has a number of disadvantages: (1) it reduces the upper limit of the maximum engine speed and/or number of data channels due to sampling rate limit of data acquisition system, (2) it reduces the number of consecutive engine cycles that can be acquired due to system memory capacity limitations, (3) it reduces the speed of data handling and processing due to the increased volume of data, (4) it increases the data storage requirements, and (5) it increases the sensitivity to noise in some of the derived variable data [62]. A major problem with very high crank angle resolution is noise in some of the derived parameter data. This noise can be reduced by filtering, mathematical smoothing, and using a coarser calculation crank angle resolution. Additionally, there are certain calculations or applications that do not require such high crank angle resolution. Thus, adequate selection of crank angle resolution can be made based on application and measurement task. Typically, for IMEP calculation, friction measurement, heat release calculation, calculation of polytropic exponent, and direct analysis of pressure curve, the resolution of one crank angle degree (CAD) is suggested and
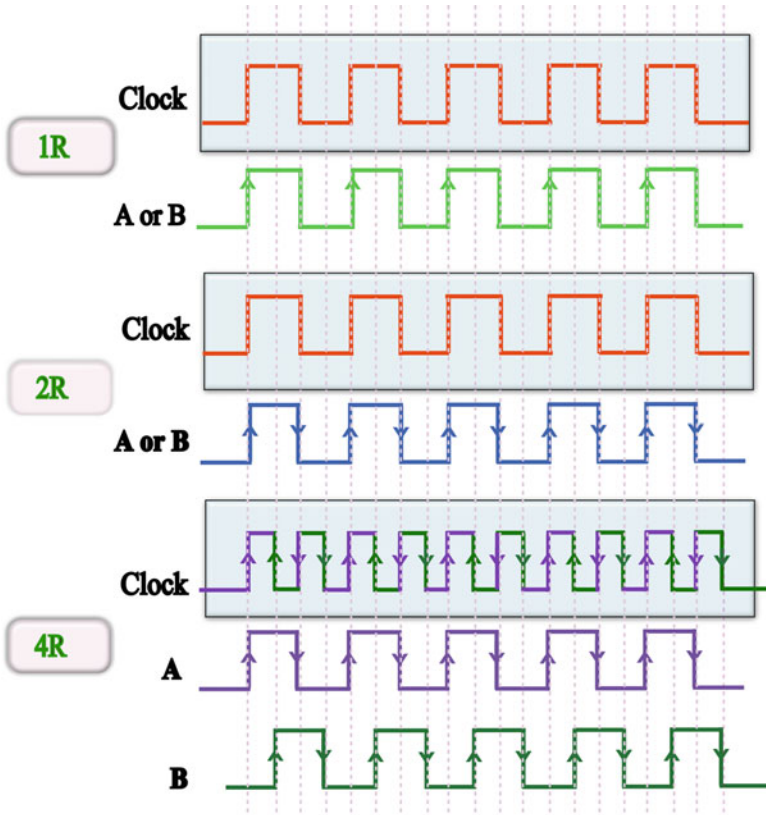
Fig. 2.60 Method for creating higher-resolution external clock using encoder signals

appropriate. However, crank angle resolution less than 0.2 CAD is suggested for knocking and combustion noise analysis [15]. A variable crank angle resolution technique which dynamically adjusts the crank angle interval over which the calculation is performed has been demonstrated to have good results [62].

Discussion/Investigation Questions

1. Discuss the applications where high accuracy and/or high repeatability of cylinder pressure measurement is required during engine development and testing process. Also, list the applications with moderate requirements on accuracy or repeatability for cylinder pressure measurement.
2. Discuss and list the design issues related to combustion sensors (piezoelectric pressure sensor, ion current sensors, and optical sensors) on automotive engine installed in laboratory test cell or a production vehicle.

3. Discuss the main advantages and disadvantages of piezoelectric sensors. List and explain the properties required of materials suitable for transduction elements in sensors. Fill the table showing the basic characteristics of sensing materials with notations low, very low, high, very high, and normal.

Transduction principle	Strain sensitivity	Threshold	Span-to-threshold ratio
Piezoelectric			
Piezoresistive			
Inductive			
Capacitive			

4. Discuss the advantages of direct pressure derivative measurement using current-to-voltage converter over charge amplifier-based measurement for cylinder pressure indicating by the piezoelectric transducer. Justify your answers.

5. Differentiate between piezoelectric and piezoresistive sensors. Explain why piezoelectric sensors are used for in-cylinder pressure measurement and piezoresistive sensors are used for manifold pressure and fuel line pressure measurement. Complete the following table showing different criteria for which a measurement technology is preferable to the others. Use the notation "↑" for preferred and "↓" for not preferred.

Criteria	Static measurement	Quasi-static measurement	Dynamic measurement	Pressure pulsation	Small sensor dimension	Wide temperature range
Piezoelectric						
Piezoresistive						

6. Explain the longitudinal, transverse, and shear cuts in piezoelectric elements and how it affects the charge output of the sensor.

7. Draw a typical cross-sectional diagram of a piezoelectric pressure transducer, and discuss all the major elements along with their functions. The piezoelectric sensor can be divided into two categories based on the output signal. Pressure sensors are available as charge output (PE) and voltage output (IEPE). Discuss the merits and demerits of PE and IEPE sensors.

8. Discuss the merits and demerits of pressure sensor mounting on engine cylinder head using direct installation and installation using adapters/sleeves.

9. Define the thermal drift during cylinder pressure measurement and write its causes. Discuss at least three methods to characterize the short-term thermal drift in measured in-cylinder pressure signal.

10. Discuss the methods for mitigating the short-term thermal drift from pressure sensors during in-cylinder pressure measurements in reciprocating engines.

11. Discuss the advantages of cooled pressure sensor over uncooled pressure sensor and uncooled pressure sensor over cooled pressure sensor designs. Write the applications when you will prefer cooled pressure sensor and applications when uncooled pressure sensor will be preferred.

12. Four possible positions (A, B, C, and D) for intrusive pressure sensor installation (red circle) are shown in Fig. P2.1 for a two-valve spark ignition engine with homogeneous combustion. Arrange four configurations (A, B, C, and D) in ascending order of preference for pressure sensor installation based on thermal as well as gas dynamics considerations. Justify your answer by discussing the merits and demerits of each sensor installation position.

Fig. P2.1 Engine head cross section with transducer installation at different locations
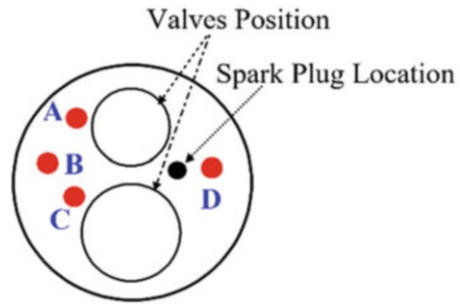
13. Two possible mounting positions (A & B) for intrusive pressure sensor installation (red circle) is shown in Fig. P2.2 for a two valve diesel engine with piston bowl combustion chamber. Write the preferred method for pressure sensor installation in this case and justify your answer by discussing the merits and demerits of both the positions. Discuss the effect of both measuring position by drawing a typical graph of the measured pressure signal.

Fig. P2.2 Engine head cross section with transducer installation at different locations along with piston bowl (Courtesy of Kistler)
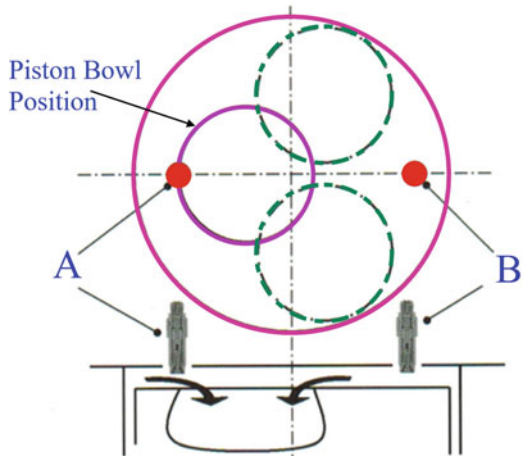
14. Figure P2.3 shows the typical variations of pressure difference due to thermal shock as a function of crankshaft position for different spark timings, engine loads (BMEP), engine speeds, and operating air-fuel ratios. Discuss the effect of

thermal shock on pressure measurement by explaining the trend observed with different engine operating parameters. Explain the reasons why maximum thermal shock occurs at 2000 engine speed instead of 1000 rpm (Fig. P2.3c). Thermal shock is also highest for stoichiometric ($\lambda = 1$) engine operations (Fig. P2.3d). Justify this observation with the explanation of combustion process.
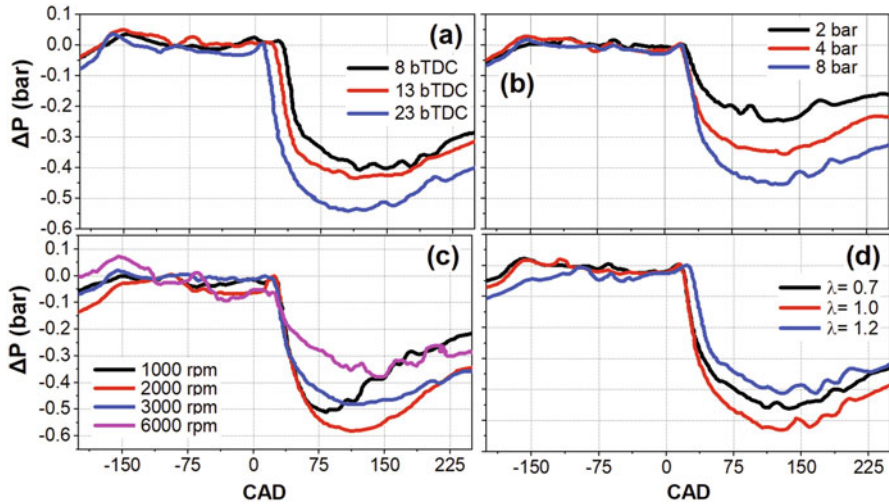
Fig. P2.3 Variation of pressure difference due to thermal shock at different engine operating conditions (adapted from [26])

15. Assume a recessed installation of the miniature pressure transducer on engine head (Fig. 2.35b). Calculate and plot the frequency of pipe oscillations in measured pressure signal for cylinder gas temperature of 500, 1000, and 2000 K as a function of measuring channel length. Measuring channel radius can be considered as 1.5 mm, and cavity volume (V_{cv}) ahead of the pressure transducer is 12 mm^3. Discuss the effect of gas temperature on the frequency of oscillations at particular channel length.

16. Explain the trend in variation of the pipe oscillation frequency of the measured signal with advanced spark timing in a recessed installation of the pressure sensor. Explain how you will choose the channel length for pressure sensor mounting during knocking operating conditions.

17. Explain the working principle of ion current sensor. Write the merits and limitations of using the ion current sensor for combustion diagnostics and engine control. Discuss the advantages of using multielectrode spark plug over signal electrode spark plug for ion current sensing.

18. What are the typical ions formed during combustion, which are mainly responsible for ion current signal? Discuss the effect of air-fuel ratio, EGR, and

combustion temperature on the signal strength of ion current sensor in spark ignition engine.

19. Draw the typical shape of the ion current signal as a function of crank angle position for spark ignition (SI), compression ignition (CI), and homogeneous charge compression ignition (HCCI) engines. Justify the different peaks observed in the curve for different combustion modes.

20. Discuss the sources of error during cylinder pressure measurements. Specifically list the possible error sources at the level of the pressure sensor, crank angle encoders, TDC determination, transmission cables, signal conditioning, data acquisition, and data processing.

21. Discuss the reasons why crank angle encoders (not time-based signal recording) are used for cylinder pressure measurement in reciprocating engines. Define the resolution of crank angle encoder. Write the effect of crank angle resolution on cylinder pressure measurement and its further analysis for different combustion parameters.

22. Discuss the difference between the optical encoder and inductive-type encoder. In terms of accuracy, which one is preferred for cylinder pressure measurement? Write the sources of error in inductive crank angle measurement system.

23. Calculate the obtained sampling frequency for a four-stroke spark ignition engine that is running at 5000 rpm and uses the incremental crank angle encoder of two pulses per degree. Assume that you are using only "A" pulse of the encoder. Comment on whether this resolution is sufficient for knocking combustion analysis. Discuss the ways to increase the sampling frequency of the measurement.

References

1. Teichmann, R., Wimmer, A., Schwarz, C., & Winklhofer, E. (2012). Combustion diagnostics. In *Combustion engines development* (pp. 39–117). Berlin, Heidelberg: Springer.
2. Van Basshuysen, R., & Schäfer, F. (2016). *Internal combustion engine handbook-basics, components, systems and perspectives* (2nd ed.). Warrendale: SAE International. ISBN: 978-0-7680-8024-7.
3. Obert, E. F. (1968). *Internal combustion engines* (3rd ed.). Scranton, PA: International Textbook Co.
4. Amann, C. A. (1985). *Classical combustion diagnostics for engine research* (No. 850395). SAE Technical Paper.
5. Bueno, A. V., Velásquez, J. A., & Milanez, L. F. (2012). Internal combustion engine indicating measurements. In *Applied measurement systems*. London: InTech.
6. Bueno, A. V., Velásquez, J. A., & Milanez, L. F. (2009). A new engine indicating measurement procedure for combustion heat release analysis. *Applied Thermal Engineering, 29*(8–9), 1657–1675.
7. Eastwood, P. (2009). Combustion sensors. In *Automotive sensors* (pp. 115–157). New Jersey: Momentum Press.
8. Pischinger, R. (2002). *Engine indicating user handbook*. Graz: AVL List GmbH.
9. Gautschi, G. (2002). *Piezoelectric sensorics: Force, strain, pressure, acceleration and acoustic emission sensors, materials and amplifiers*. Berlin, Heidelberg: Springer.

10. Maurya, R. K. (2018). *Characteristics and control of low temperature combustion engines: Employing gasoline, ethanol and methanol*. Cham: Springer.
11. Luján, J. M., Bermúdez, V., Guardiola, C., & Abbad, A. (2010). A methodology for combustion detection in diesel engines through in-cylinder pressure derivative signal. *Mechanical Systems and Signal Processing, 24*(7), 2261–2275.
12. Shimasaki, Y., Kobayashi, M., Sakamoto, H., Ueno, M., Hasegawa, M., Yamaguchi, S., & Suzuki, T. (2004). *Study on engine management system using in-cylinder pressure sensor integrated with spark plug* (No. 2004-01-0519). SAE Technical Paper.
13. Maurya, R. K., Pal, D. D., & Agarwal, A. K. (2013). Digital signal processing of cylinder pressure data for combustion diagnostics of HCCI engine. *Mechanical Systems and Signal Processing, 36*(1), 95–109.
14. Kusakabe, H., Okauchi, T., & Takigawa, M. (1992). *A cylinder pressure sensor for internal combustion engine* (No. 920701). SAE Technical Paper.
15. Rogers, D. R. (2010). *Engine combustion: Pressure measurement and analysis*. Warrendale: Society of Automotive Engineers.
16. Claudio Cavalloni, C., & Sommer, R. (2003). *PiezoStar® crystals: A new dimension in sensor technology*. Winterthur: Kistler Instrumente AG.
17. Takeuchi, M., Tsukada, K., Nonomura, Y., Omura, Y., & Chujou, Y. (1993). *A combustion pressure sensor utilizing silicon piezoresistive effect* (No. 930351). SAE Technical Paper.
18. Gossweiler, C., Sailer, W., & Cater, C. (2006). *Sensors and amplifiers for combustion analysis, a guide for the user 100-403e-10.06*. © Kistler Instrumente AG, CH-8408 Winterthur, Okt.
19. Donovan, J. E. (1970). Triboelectric noise generation in some cables commonly used with underwater electroacoustic transducers. *The Journal of the Acoustical Society of America, 48* (3B), 714–724.
20. Rosseel, E., Sierens, R., & Baert, R. S. G. (1999). *Evaluating piezo-electric transducer response to thermal shock from in-cylinder pressure data* (No. 1999-01-0935). SAE Technical Paper.
21. Lee, S., Bae, C., Prucka, R., Fernandes, G., Filipi, Z., & Assanis, D. N. (2005). *Quantification of thermal shock in a piezoelectric pressure transducer* (No. 2005-01-2092). SAE Technical Paper.
22. Kuratle, R. H., & Märki, B. (1992). Influencing parameters and error sources during indication on internal combustion engines. *SAE Transactions, 101*, 295–303. Paper No-920233.
23. Randolph, A. L. (1990). *Cylinder-pressure-transducer mounting techniques to maximize data accuracy* (No. 900171). SAE Technical Paper.
24. Stein, R. A., Mencik, D. Z., & Warren, C. C. (1987). Effect of thermal strain on measurement of cylinder pressure. *SAE Transactions, 96*, 442–449. Paper No-870455.
25. Soltis, D. A. (2005). *Evaluation of cylinder pressure transducer accuracy based upon mounting style, heat shields, and water cooling* (No. 2005-01-3750). SAE Technical Paper.
26. Rai, H. S., Brunt, M. F., & Loader, C. P. (1999). *Quantification and reduction of IMEP errors resulting from pressure transducer thermal shock in an SI engine* (No. 1999-01-1329). SAE Technical Paper.
27. Storm, X., Salminen, H. J., Virrankoski, R., Niemi, S., & Hyvonen, J. (2017). *Analysis of cylinder pressure measurement accuracy for internal combustion engine control* (No. 2017-01-1067). SAE Technical Paper.
28. Davis, R. S., & Patterson, G. J. (2006). *Cylinder pressure data quality checks and procedures to maximize data accuracy* (No. 2006-01-1346). SAE Technical Paper.
29. Randolph, A. L. (1990). *Methods of processing cylinder-pressure transducer signals to maximize data accuracy* (No. 900170). SAE Technical Paper.
30. Higuma, A., Suzuki, T., Yoshida, M., Oguri, Y., & Minoyama, T. (1999). *Improvement of error in piezoelectric pressure transducer* (No. 1999-01-0207). SAE Technical Paper.
31. Roth, K. J., Sobiesiak, A., Robertson, L., & Yates, S. (2002). *In-cylinder pressure measurements with optical fiber and piezoelectric pressure transducers* (No. 2002-01-0745). SAE Technical Paper.

32. Hsu, B. D. (2002). *Practical diesel-engine combustion analysis*. Warrendale, PA: Society of Automotive Engineers.

33. Patterson, G. J., & Davis, R. S. (2009). Geometric and topological considerations to maximize remotely mounted cylinder pressure transducer data quality. *SAE International Journal of Engines, 2*(1), 414–420. https://doi.org/10.4271/2009-01-0644

34. Bertola, A., Dolt, R., & Höwing, J. (2015). *The use of spark plug pressure transducers for engine indication measurements-possibilities and limits* (No. 2015-26-0041). SAE Technical Paper.

35. Chen, Y., Dong, G., Mack, J. H., Butt, R. H., Chen, J. Y., & Dibble, R. W. (2016). Cyclic variations and prior-cycle effects of ion current sensing in an HCCI engine: A time-series analysis. *Applied Energy, 168*, 628–635.

36. Laganá, A. A., Lima, L. L., Justo, J. F., Arruda, B. A., & Santos, M. M. (2018). Identification of combustion and detonation in spark ignition engines using ion current signal. *Fuel, 227*, 469–477.

37. Dong, G., Chen, Y., Li, L., Wu, Z., & Dibble, R. (2017). A skeletal gasoline flame ionization mechanism for combustion timing prediction on HCCI engines. *Proceedings of the Combustion Institute, 36*(3), 3669–3676.

38. Chao, Y., Chen, X., Deng, J., Hu, Z., Wu, Z., & Li, L. (2018). Additional injection timing effects on first cycle during gasoline engine cold start based on ion current detection system. *Applied Energy, 221*, 55–66.

39. Henein, N. A., Bryzik, W., Abdel-Rehim, A., & Gupta, A. (2010). Characteristics of ion current signals in compression ignition and spark ignition engines. *SAE International Journal of Engines, 3*(1), 260–281. https://doi.org/10.4271/2010-01-0567

40. Dev, S., Sandhu, N. S., Ives, M., Yu, S., Zheng, M., & Tjong, J. (2018). *Ion current measurement of diluted combustion using a multi-electrode spark plug* (No. 2018-01-1134). SAE Technical Paper.

41. Peron, L., Charlet, A., Higelin, P., Moreau, B., & Burq, J. F. (2000). *Limitations of ionization current sensors and comparison with cylinder pressure sensors* (No. 2000-01-2830). SAE Technical Paper.

42. Reinmann, R., Saitzkoff, A., & Mauss, F. (1997). *Local air-fuel ratio measurements using the spark plug as an ionization sensor* (No. 970856). SAE Technical Paper.

43. Starik, A. M., & Titova, N. S. (2002). Kinetics of ion formation in the volumetric reaction of methane with air. *Combustion, Explosion and Shock Waves, 38*(3), 253–268.

44. Kato, T., Akiyama, K., Nakashima, T., & Shimizu, R. (2007). *Development of combustion behavior analysis techniques in the ultra high engine speed range* (No. 2007-01-0643). SAE Technical Paper.

45. Yoshiyama, S. (2010). *Detection of combustion quality in a production SI engine using ion sensor* (No. 2010-01-2255). SAE Technical Paper.

46. Bogin, G., Jr., Chen, J. Y., & Dibble, R. W. (2009). The effects of intake pressure, fuel concentration, and bias voltage on the detection of ions in a Homogeneous Charge Compression Ignition (HCCI) engine. *Proceedings of the Combustion Institute, 32*(2), 2877–2884.

47. Vressner, A., Hultqvist, A., Tunestål, P., Johansson, B., & Hasegawa, R. (2005). *Fuel effects on ion current in an HCCI engine* (No. 2005-01-2093). SAE Technical Paper.

48. Kubach, H., Velji, A., Spicher, U., & Fischer, W. (2004). *Ion current measurement in diesel engines* (No. 2004-01-2922). SAE Technical Paper.

49. Kittelson, D. B., & Collings, N. (1987). Origin of the response of electrostatic particle probes. *SAE Transactions, 96*, 353–363. Paper No 870476.

50. Zhao, H., & Ladommatos, N. (2001). *Engine combustion instrumentation and diagnostics*. Warrendale, PA: Society of Automotive Engineers. ISBN: 978-0768006650.

51. Ulrich, O., Wlodarczyk, R., & Wlodarczyk, M. T. (2001). *High-accuracy low-cost cylinder pressure sensor for advanced engine controls* (No. 2001-01-0991). SAE Technical Paper.

52. He, G., & Wlodarczyk, M. T. (1994). Evaluation of a spark-plug-integrated fiber-optic combustion pressure sensor. *SAE Transactions, 103*, 498–505. Paper No-940381.

53. Poorman, T. J., Xia, L., & Wlodarczyk, M. T. (1997). *Ignition system-embedded fiber-optic combustion pressure sensor for engine control and monitoring* (No. 970845). SAE Technical Paper.

54. Amirante, R., Casavola, C., Distaso, E., & Tamburrano, P. (2015). *Towards the development of the in-cylinder pressure measurement based on the strain gauge technique for internal combustion engines* (No. 2015-24-2419). SAE Technical Paper.

55. Moro, D., Cavina, N., & Ponti, F. (2002). In-cylinder pressure reconstruction based on instantaneous engine speed signal. *Journal of Engineering for Gas Turbines and Power, 124* (1), 220–225.

56. Romani, L., Lenzi, G., Ferrari, L., & Ferrara, G. (2016). *Indirect estimation of in-cylinder pressure through the stress analysis of an engine stud* (No. 2016-01-0814). SAE Technical Paper.

57. Andrie, M. J. (2009). *Non-intrusive low cost cylinder pressure transducer for internal combustion engine monitoring and control* (No. 2009-01-0245). SAE Technical Paper.

58. Liu, F., Amaratunga, G. A., Collings, N., & Soliman, A. (2012). *An experimental study on engine dynamics model based in-cylinder pressure estimation* (No. 2012-01-0896). SAE Technical Paper.

59. Jia, L., Naber, J., Blough, J., & Zekavat, S. A. (2014). Accelerometer-based combustion metrics reconstruction with radial basis function neural network for a 9 L diesel engine. *Journal of Engineering for Gas Turbines and Power, 136*(3), 031507.

60. El-Ghamry, M., Steel, J. A., Reuben, R. L., & Fog, T. L. (2005). Indirect measurement of cylinder pressure from diesel engines using acoustic emission. *Mechanical Systems and Signal Processing, 19*(4), 751–765.

61. Atkins, R. D. (2009). *An introduction to engine testing and development*. Warrendale: SAE International. ISBN 978-0-7680-2099-1.

62. Brunt, M. F., & Lucas, G. G. (1991). *The effect of crank angle resolution on cylinder pressure analysis* (No. 910041). SAE Technical Paper.

63. Katrašnik, T., Trenc, F., & Oprešnik, S. R. (2006). A new criterion to determine the start of combustion in diesel engines. *Journal of Engineering for Gas Turbines and Power, 128*(4), 928–933.